Study of acute liver failure in children using next generation sequencing technology

Hegarty, Rob

Awarding institution:
King's College London

Study of acute liver failure in children using next generation sequencing technology

Robert Hegarty

A thesis submitted for the degree of Doctor of Medicine (Research) in Molecular Genetics

School of Immunology and Microbial Science Research
Faculty of Life Sciences and Medicine, Immunology and Microbial Sciences

Student number 1833679
September 2023
King's College London

DECLARATION

I declare that the work presented in this thesis is original and was carried out by myself. Where information was derived from other sources, I confirm that this has been indicated in the thesis. The publications related to this work (APPENDIX D) were written by me and may, therefore, partly overlap with my thesis.

Robert Hegarty

ACKNOWLEDGEMENTS

I am very grateful to my supervisor, Prof Richard Thompson for giving me the opportunity to carry out this work. It has been a great privilege to learn from his scientific expertise, scrutiny, and guidance. His support allowed me to acquire new skills and knowledge to carry out further work related to genetics of liver disease in children. The members of the Liver Molecular Genetics Laboratory have also been invaluable in providing support and welcoming me in their lab.

I am also extremely thankful to my second supervisor, Dr Tassos Grammatikopoulos for his support and guidance. He has been a mentoring figure providing enthusiasm, expert knowledge and timely advice.

I would also like to express my gratitude to Prof Anil Dhawan and members of his team. Prof Dhawan and his team not only provided scholarly advice but an incentive to complete this work.

Finally, I would like to give a very special thanks to my wife, Lindsay, who has been truly supportive and accommodating. It is through her dedication that I managed to complete this work with William and Felicity growing up.

ABSTRACT

Acute liver failure (ALF) in children is a rare but potentially fatal condition without treatment. Diagnosis can be difficult and remains indeterminate in up to approximately half of cases. The study's aim was to identify undiagnosed, monogenic causes of ALF using targeted next generation sequencing (NGS).

A capture library designed to target 64 genes known to cause ALF and / or a liver based metabolic disorder was constructed. Sequencing was carried out in 41 children who previously suffered from ALF without an identifiable aetiology.

Biallelic variants were identified in 8 patients which may have been the cause of ALF or contributed to the clinical phenotype. Variants in *NBAS* and genes encoding mitochondrial proteins were the most common findings.

Biallelic variants in *NBAS* is a cause of recurrent ALF triggered by fever. The pathobiology has been described to be due to disrupted retrograde transport between the Golgi and endoplasmic reticulum. However, it has also been suggested that disruption in nonsense mediated decay (NMD) may be involved.

Skin fibroblasts from 4 children with biallelic variants in *NBAS* were used for the functional analyses including assessment of cell viability and protein expression. The gene expressions of *GADD45A* and *GADD45B*, endogenous NMD targets, were measured to assess whether NMD was disrupted.

Cell viability was impaired in isolated cell culture conditions when placed under stress by glucose deprivation or incubation at 40°C. However, this was not consistent across all culture conditions. Western blot demonstrated reduced protein expression in 2 patients with two in-frame insertions. *GADD45A* and *GADD45B* gene expressions were not elevated in patient samples compared to controls suggesting that NMD is intact in these patients although disruption to a more localised NMD pathway remains a possibility.

Next generation sequencing will be essential in improving diagnostic yield in future children with ALF. Using NBAS deficiency as an archetypal example of a monogenic cause of ALF insight was provided into its pathobiology. Progress is still required for the clinical application of NGS in children with ALF and future efforts should focus on overcoming the practical challenges.

Table of Contents

LIST OF FIGURES

LIST OF TABLES

ABBREVIATIONS

A	
Acyl-coA	Acetyl-coenzyme A
ACMG	American College of Medical Genetics and Genomics
ALF	Acute liver failure
ALT	Alanine aminotransferase
ARS	Aminoacyl-tRNA synthetase
AST	Aspartate aminotransferase
ATP	Adenosine triphosphate
B	
BCL	Binary base call
BLAST	Basic local alignment search tool
BSEP	Bile salt export pump
BSA	Bovine serum albumin
C	
CADD	Combined Annotation Dependent Depletion
CASAVA	Consensus Assessment of Sequence and Variation
CDG	Congenital disorder of glycosylation
CNV	Copy number variant
COP1	Coat protein complex 1
C_T	Cycle threshold
D	
dbSNP	Database of single nucleotide polymorphisms
DILI	Drug induced liver injury
DLD	Dihydrolipoamide dehydrogenase
DMEM	Dulbecco's Modified Eagle Medium
DMSO	Dimethylsulphoxide
DNA	Deoxyribonucleic acid
dNTPs	Deoxyribonucleotide triphosphates
dsDNA	Double stranded DNA
E	
EDTA	Ethylenediaminetetraacetic acid
EGF	Epidermal growth factor
EJC	Exon junction complex
ER	Endoplasmic reticulum
ExAC	Exome Aggregation Consortium
F	
$FADH_2$	Dihydroflavine-adenine dinucleotide
FAM	Fluorescein amidites
FBS	Foetal bovine serum

G

G1 phase	Growth 1 phase
GADD45	*Growth arrest and DNA damage-inducible 45*
GAPDH	*Glyceraldehyde 3-phosphate dehydrogenase*
GI	Gastrointestinal
GLI1	Glioma-Associated Oncogene Family Zinc Finger 1

H

HE	Hepatic encephalopathy
HFF1	Human foreskin fibroblast 1
HGF	Hepatocyte growth factor
HHH syndrome	Hyperammonaemia, hyperornithinaemia, homocitrullinuria syndrome
HNF	Hepatocyte nuclear factor
HPLC	High performance liquid chromatography
HRP	Horseradish peroxidase
H&E	Haematoxylin and eosin

I

IL-6	Interleukin-6IMD
IMD	Inherited metabolic disorders
INR	International normalised ratio
iPSC	Induced pluripotent stem
IVA	Ingenuity Variant Analysis

K

KCH	King's College Hospital
kD	Kilodalton

L

LNA	Locked nucleic acids
LT	Liver transplantation

M

M	Molar
MET	Mesenchymal Epithelial Transition
mRNA	Messenger RNA
MiRNA	MicroRNA
MtARS	Mitochondrial ARS
MtDNA	Mitochondrial DNA
MDS	Mitochondrial DNA depletion syndromes

N

NADH	Nicotinamide adenine dinucleotide
NAG	*Neuroblastoma amplified gene*
NBAS	*Neuroblastoma amplified sequence*
NF-κB	Nuclear factor-κB

NGS	Next generation sequencing
NMD	Nonsense mediated decay
O	
OTC	Ornithine transcarbamylase
P	
PAGE	Polyacrylamide gel electrophoresis
PALF	Paediatric acute liver failure
PBS	Phosphate-buffered saline
PCR	Polymerase chain reaction
PDH	Pyruvate dehydrogenase
Pen-strep	Penicillin-streptomycin
PolyPhen	Polymorphism Phenotyping
PTC	Premature truncation codon
Q	
q-PCR	Quantitative-polymerase chain reaction
QS	Quantity sufficient
R	
RFU	Relative fluorescence units
RIN	RNA integrity number
RINT-1	RAD50-interacting protein 1
ROI	Regions of interest
RPM	Revolutions per minute
RNA	Ribonucleic acid
RT	Reverse transcription
S	
S phase	(DNA) synthesis phase
SDS	Sodium dodecyl sulphate
SiRNA	Small interfering RNA
SNP	Single nucleotide polymorphism
SNAP	Soluble NSF attachment protein
SNARES	Soluble NSF Attachment Protein (SNAP) receptors
SIFT	Sorting intolerant from tolerant
STAT3	Signal transducer and activator of transcription 3
T	
TAE	Tris-acetate-EDTA
Tris-HCl	Tris(hydoxymethyl)aminomethane-hydrochloric acid
TBS	Tris-buffered saline
TBST	TBS and Tween 20
TEAD domain	Transcriptional enhancer-associated domain factor
TNF	Tumour necrosis factor
TRIUMPH	TReatment for ImmUne Mediated PathopHysiology

TRNA	Transfer RNA
U	
UK	United Kingdom
UNG	Uracil N-glycosylase
UPL	Universal ProbeLibrary
UV	Ultraviolet
V	
V	Volts
VCF	Variant call file
W	
WNT	Wingless-INT

1 INTRODUCTION

The liver is the largest internal organ and contributes to numerous physiological functions including metabolism, detoxification, synthesis and storage. It is anatomically situated in such way that nutrient as well as toxin-rich blood is continually received from the gut. It is also unique in that it is one of few organs that have the capacity to grow. The principal cell type of the liver is the hepatocyte and occupy approximately 80% of the hepatic mass (Michalopoulos, 2007).

1.1 General introduction

1.1.1 Hepatocytes: embryogenesis and at steady state

Hepatocytes are derived embryologically from the endoderm. The hepatic endodermal cells, or hepatoblasts, are bi-potential with the ability to differentiate into hepatocytes and cholangiocytes (Tanimizu and Mitaka, 2014). This differentiation occurs in relation to the portal vein: those that are in contact with the portal vein become cholangiocytes whilst those that are not, in the parenchyma, gradually differentiate into mature hepatocytes. This process of differentiation is mediated by a complex interplay of cytokines, growth factors and hormones (Zorn, 2008). The developing liver with differentiated hepatocytes has a dramatic capacity to grow as demonstrated in mice where a 500-fold increase in size is observed between the embryonic and postnatal liver (Rollins et al., 2010). The final maturation of the liver continues postnatally (Zorn, 2008).

In adulthood, the liver must continue to maintain homeostasis as it exposed to the toxins from the circulation of the intestines, spleen and pancreas through the portal vein. Any insult resulting in loss of cell mass is compensated by the liver's capacity to regenerate. This is mainly carried out by the proliferation of mature adult hepatocytes and the other hepatic cell types (Michalopoulos, 2007). However, it has been demonstrated that hepatic stem cells also play important roles in the growth, maintenance and repair of normal liver (Iverson et al., 2011).

1.1.2 Liver necrosis in acute liver failure

Acute liver failure (ALF) is a clinical syndrome characterised by a sudden and severe hepatic injury resulting from a wide range of causes (Bernal et al., 2010). It is primarily a clinical description and explored in more detail in section 1.2. At a cellular level, ALF occurs when hepatocyte death exceeds the regenerative capacity of the liver (Bantel and Schulze-Osthoff, 2012).

Histologically, ALF is characterised by marked loss of hepatocytes and proliferation of bile ductular structures (ductular reaction) around the portal area (Lefkowitch, 2016). The liver may be reduced in weight by one half to two thirds due to massive parenchymal loss (Lefkowitch, 2016). A regenerative response may be seen in a matter of days in the form of nodules that are visible macro- and microscopically (Figure 1-1). This response is due to contributions both from residual hepatocytes as well as liver progenitor cells located in the periportal canal of Hering (Weng et al., 2015). In a histopathological study after auxiliary liver transplantation (LT), brisk proliferation of residual hepatocytes was the initial regenerative mechanism and the contribution from liver progenitor cells were secondary in areas of total hepatocyte loss (Quaglia et al., 2008).

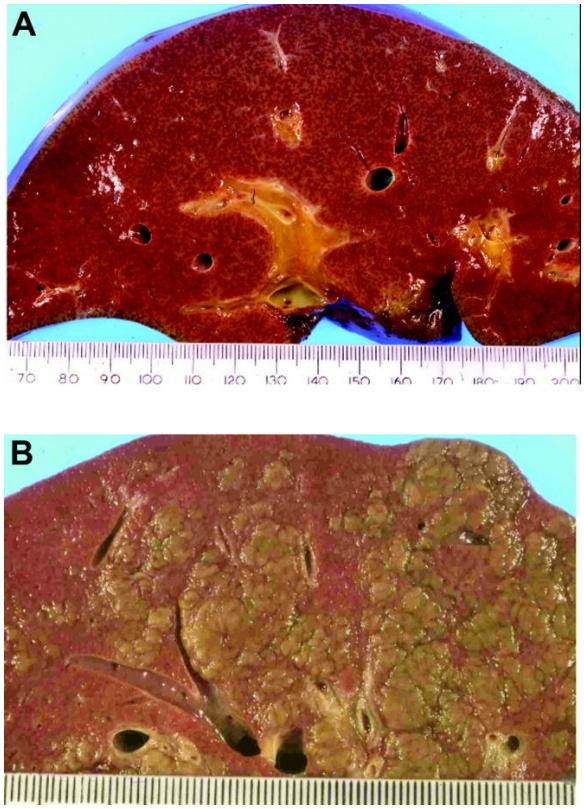

Figure 1-1 A regenerative response is seen after acute liver failure.
A, there is no evidence of nodularity in a diffuse pattern of liver injury and parenchymal collapse. B, greenish nodules are demonstrated in a regenerating liver (Quaglia et al., 2008).

Cell death in ALF classically occur by either apoptosis (programmed cell death) or necrosis (uncontrolled cell death) although there is growing evidence of other modalities such as necroptosis, pyroptosis and autophagic cell death (Table 1-1) (Eguchi et al., 2014). Apoptotic cell death is a highly organised and genetically controlled process that is initiated by either membrane receptors (extrinsic pathway) or intracellular stimuli (intrinsic pathway) (Eguchi et al., 2014). Both of these pathways converge to activate proteolytic caspase enzymes (effector caspases 3 and 7) which result in apoptosis (Riedl and Shi, 2004). It is an active process that requires adenosine triphosphate (ATP). On the other hand, necrosis is a passive process that is caspase independent. During necrosis, there is reactive oxygen species build up, mitochondrial dysfunction and ATP depletion. This results in oncosis or cellular swelling and subsequently, membrane rupture.

Mechanism of cell death	Definition
Apoptosis	ATP-dependent, programmed cell death.
Necrosis	Unprogrammed, premature cell death by autolysis due to ATP depletion.
Necroptosis	A programmed form of necrosis.
Pyroptosis	An inflammatory, lytic, programmed cell death that occurs most frequently upon infection with intracellular pathogens and is likely to form part of the antimicrobial response.
Autophagic cell death	Cell death characterised by autophagy - a process that delivers cytoplasmic material of endogenous or exogenous origin to the lysosome for degradation.

Table 1-1 Mechanisms of hepatocellular death are implicated in ALF.
Apoptosis and necrosis are the main causes of cell death in ALF although other modalities such as necroptosis, pyroptosis and autophagic cell death have been described.

1.1.3 Regenerative capacity of the liver

Hepatocytes are one of few differentiated cell types that can replicate deoxyribonucleic acid (DNA) and proliferate to regenerate (Iverson et al., 2011). Much work has been carried out on liver regeneration given its direct therapeutic relevance when considering procedures such as hepatectomies and living-donor LT that rely on the liver's ability to regenerate to achieve recovery. Hepatectomy animal models have formed the basis for elucidating the underlying mechanisms. An archetypal example of this is the rodent, two-thirds hepatectomy model where the original mass of the liver is recovered in approximately, 10 days following hepatectomy (Gilgenkrantz and Collin de l'Hortet, 2018).

Liver regeneration takes place by one of three processes: hyperplasia, an increased rate of hepatocyte proliferation; hypertrophy, an increase in cell size; redifferentiation, when liver progenitor cells are repopulated and differentiate into hepatocytes. The rodent model has demonstrated that the type of regeneration is dependent upon the type of resection: hypertrophy is the principal response after one-third partial hepatectomy; hyperplasia after two-thirds hepatectomy; redifferentiation takes place when 80 to 90% of the liver is resected

(Figure 1-2) (Gilgenkrantz and Collin de l'Hortet, 2018). Therefore, the regenerative response is dependent upon the stimulus.

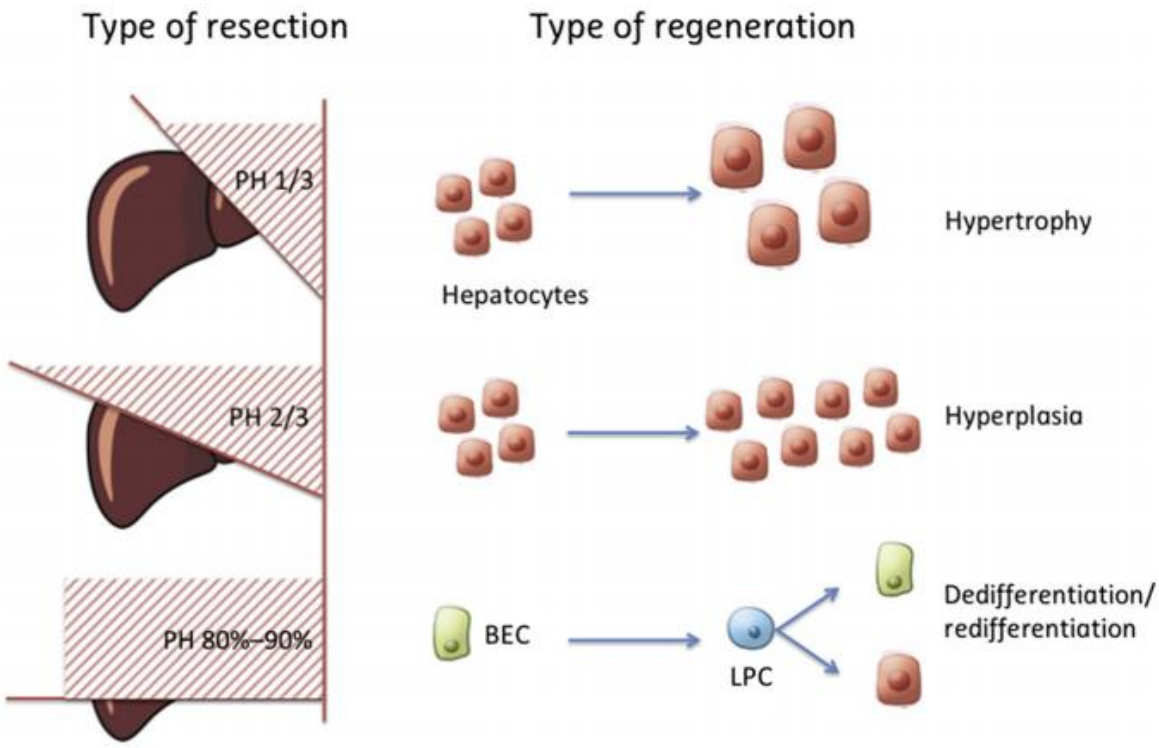

Figure 1-2 The partial hepatectomy model.
The regenerative response is dependent upon the volume of liver resected. BEC, biliary epithelial cell; LPC, liver progenitor cell; PH, partial hepatectomy. The figure was adapted from (Gilgenkrantz and Collin de l'Hortet, 2018).

There are multiple intracellular, extracellular and auxiliary pathways that are triggered when liver regeneration takes. The key components of these signals are listed below (Figure 1-3).

Intracellular signals

- The transcription factors signal transducer and activator of transcription 3 (STAT3) regulated by interleukin-6 (IL-6) (Taub, 2004) and nuclear factor-κB (NF-κB) regulated by tumour necrosis factor (TNF) (Fausto et al., 2006) are the principal intracellular signals. The kinases cyclins D1 and D2 regulated by β-catenin are required to signal hepatocytes to progress from G1 to S phase (Mullany et al., 2008).

Extracellular signals

- Hepatocyte growth factor (HGF) and its receptor, mesenchymal epithelial transition (MET), and epidermal growth factor receptor (EGF) work extracellularly and are regarded as complete mitogens. Mitogens can directly induce hepatocyte replication by stimulating DNA synthesis and liver enlargement. Without them liver regeneration is abolished (Paranjpe et al., 2016).

Complex signalling pathways with intra and extracellular components

- β-catenin is a multifunctional protein involved in gene transcription and cell-cell adhesions. When the Wingless-INT (WNT)/ β-catenin pathway is activated, β-catenin translocates to the hepatocyte nucleus and induces proliferative genes such as cyclin D1 (Gilgenkrantz and Collin de l'Hortet, 2018). The growth factor receptors EGFR and MET are closely linked to this pathway as they phosphorylate β-catenin before it enters the nucleus.
- Hedgehog is a signalling pathway that is activated in embryonic cells for cell differentiation that is usually turned off later in life. It has been shown that the messengers related to the pathway are increased during liver regeneration (Bhave et al., 2013) and liver regeneration is delayed when inhibitors of the pathway are administered (Ochoa et al., 2010). The transcription factor GLI1 is the end messenger of the Hedgehog pathway.
- The Hippo pathway and Yes-associated protein (YAP) orchestrate liver homeostasis and hepatocytes' fate (Yimlamai et al., 2014). The Hippo pathway converges on YAP which translocate into the nucleus and binds to transcriptional enhancer-associated domain (TEAD) factor which, in turn, activates proliferative genes. It has been shown that interference with YAP affects cell proliferation as well as organ size (Septer et al., 2012). The Hippo-YAP pathway closely interacts with the Hedgehog pathway.

Auxiliary signals

- Auxiliary signals have the effect of delaying but not fully inhibiting hepatocyte proliferation when eliminated. TNF, vascular endothelial growth factor (VEGF), noradrenaline and bile acids are such examples.

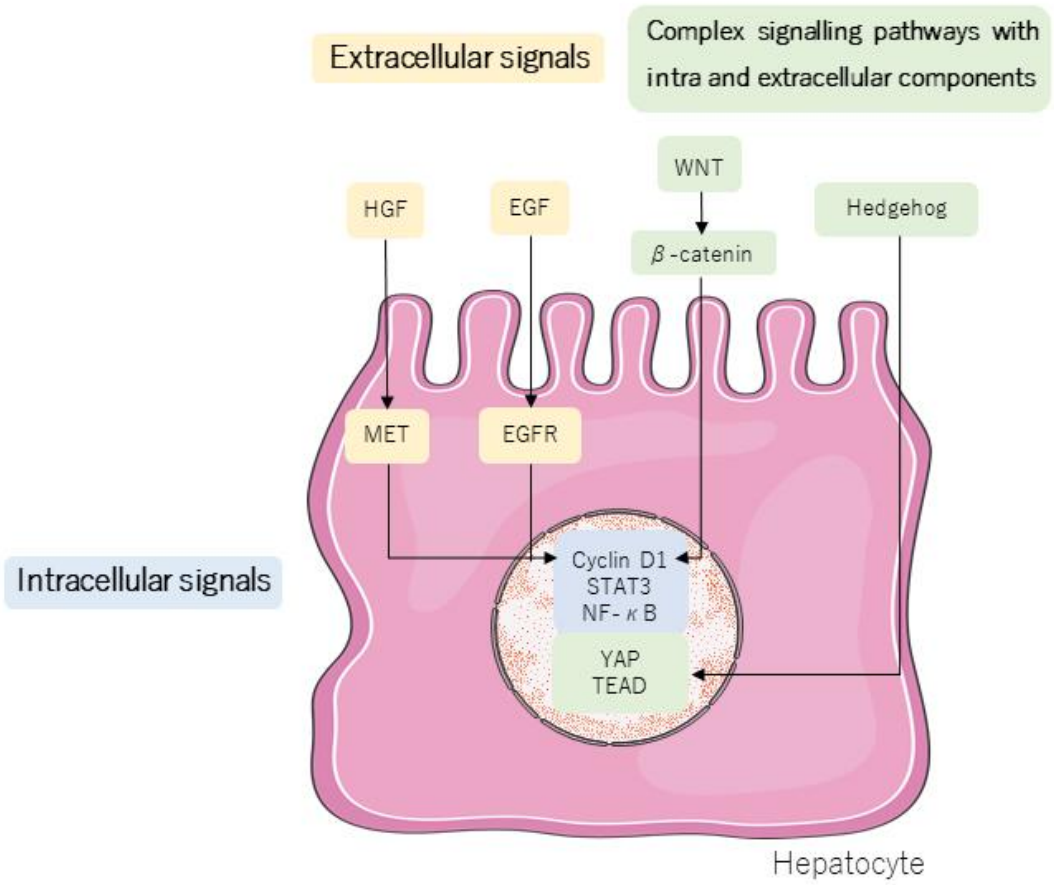

Figure 1-3 Illustration showing a simplified representation of the key pathways involved in liver regeneration.
Activation of multiple intracellular, extracellular and auxiliary pathway together lead to hepatocyte proliferation.

The interactions of these stimuli are complex but orchestrated to some extent in timing. Traditionally, liver regeneration has been described as occurring in three phases. The first phase is the priming phase and prepares hepatocytes to respond to growth factors. β-catenin translocates to the nucleus within 5 minutes on partial hepatectomy in rats (Gilgenkrantz and Collin de l'Hortet, 2018). The second phase involves the activation of growth factors including HGF and EGF. MET (the HGF receptor) and EGF are activated within 30 minutes (Stolz et al., 1999) and large amounts of HGF are detectable within an hour of partial hepatectomy (Lindroos et al., 1991). The third is the termination phase where inhibitors of liver regeneration such as transforming growth factor-β and integrin signalling become activated.

1.1.4 Genetic alterations in liver cell death

Liver regeneration following insult is accompanied by a significant change in gene expression by hepatocytes. It has been demonstrated that following hepatectomy more than 100 genes are upregulated within hours (Taub, 1996, Apte et al., 2009). This is accompanied by five to seven consecutive cell doublings resulting in a 30- to 100- fold increase in the number of hepatocyte genomes occurs during hepatocyte proliferation in a growing liver (Rollins et al., 2010). The immediately upregulated genes include some of the transcription factors mentioned above, growth factors and signal transduction regulators. Their transcription occurs within minutes of hepatectomy independent of any protein synthesis (Taub, 1996). This results in a further cascade of transcription factors at the G1 phase of the hepatocyte cell cycle.

The upregulation of these genes lasts up to 14 days when termination of the regenerative process takes place so that the liver grows back to its original mass without exceeding it. On the other hand, when termination of liver regeneration is experimentally abolished continued expression of genes that were upregulated immediately following hepatectomy is seen (Apte et al., 2009). This includes a 5-fold higher expression of HGF, an overall increase in cell cycle genes such as c-Myc and genes involved in hepatocyte differentiation.

MicroRNAs (miRNAs) are small, non-coding ribonucleic acids (RNA) about 22 nucleotides in length which are involved in the post transcriptional regulation of gene expression by degrading their target mRNAs and/or inhibiting their translation (Espinoza-Lewis and Wang, 2012). They are involved in many biological processes including cell proliferation, differentiation and apoptosis as well as disease processes, particularly, cancer. Within the liver, miR-122 and miR-199 are enriched and serve to regulate liver-specific transcription factors hepatocyte nuclear factor (HNF) 1α, HNF3α, and HNF3β) and have been studied as potential biomarkers of acute liver injury (Eguchi et al., 2014). In murine models of paracetamol toxicity, miR-122 and miR-199 were upregulated in a dose-dependent manner and preceded the rise in plasma aminotransferase levels as well as the histopathologic changes (Wang et al., 2009). In humans with paracetamol toxicity, miR-122 correlated with

peak alanine aminotransferase (ALT) levels although not with prothrombin time (Starkey Lewis et al., 2011).

1.2 Genetics of acute liver failure in children

Acute liver failure is a clinical syndrome characterised by a sudden and severe hepatic injury resulting from a wide range of causes (Bernal et al., 2010). These patients develop jaundice, coagulopathy and hepatic encephalopathy (HE) and in many cases multiorgan failure ensues. In adults, the term *fulminant hepatic failure* as opposed to *fulminant hepatitis* was first coined in 1970. The authors described a potentially reversible condition with an onset of encephalopathy within 8 weeks of the appearance of the first symptoms in the absence of pre-existing liver disease (Trey and Davidson, 1970). In 1993, the definition was refined to subcategorise the syndrome into hyperacute, acute and subacute arms according to the time interval between the onset of jaundice to HE (O'Grady et al., 1993). The purpose of this was to highlight the important aetiological and prognostic differences that were noted between these groups to, ultimately, help make important treatment decisions such as listing a patient for LT.

The definition of ALF in children was adapted from these evolving observations in adults. However, due to the difficulty in identifying HE in children, the designation adopted in paediatrics was that of a *rare multisystem disorder in which there is severe impairment of liver function, with or without encephalopathy, that occurs in association with hepatocellular necrosis in a patient with no recognised underlying chronic liver disease* (Bernal et al., 2010, Bhaduri and Mieli-Vergani, 1996).

1.2.1 Causes of acute liver failure: known and unknown

Acute liver failure is a rare condition with an incidence in adults between 1.4 and 6.2 cases per year per million in Western countries (Bretherick et al., 2011, Bower et al., 2007, Escorsell et al., 2007). The incidence in children is thought to be even less but there is no quoted figure.

There is much geographical variation in aetiology such that, in adults, drug induced liver injury (DILI) is the most common cause in the West in comparison to infection due to hepatitis A, E and B in developing countries (Blackmore and Bernal, 2015). However, the incidence has reduced and aetiologies changed over the last three decades accounted for by public health policies aimed at reducing viral hepatitis transmission or legislation to discourage the purchase of large quantities of paracetamol (Blackmore and Bernal, 2015). However, on the other hand, ALF due to an indeterminate aetiology (cause not discernible after extensive evaluation) continues to be a sizeable group (Bernal et al., 2015).

The aetiology of ALF in children demonstrates a different picture to that seen in adults. The largest study to date has been that carried out by the Pediatric Acute Liver Failure (PALF) Study Group - a prospective, international, multi-centre study initiated in 1999. The rate of indeterminate cases of ALF was 49% in 2006 and 30% in 2017 whilst paracetamol toxicity and metabolic disease were 14% and 10%, respectively (Squires et al., 2006, Alonso et al., 2017). The reason for such high rates of indeterminate cases has been attributed to the complex and rapidly progressive nature of the disease where investigations were hampered by: the large volume of blood required for some tests, a short time interval between presentation and outcome such as LT or death, an incomplete differential diagnosis, the lack of consensus on an age-appropriate evaluation or clinical improvement mitigating further work up (Narkewicz et al., 2009). Standardisation of investigations such as by use of an electronic order set was shown to be effective in reducing the rate of indeterminate cases (Narkewicz et al., 2018). However, even with such interventions, pitfalls within the laboratory investigations can be encountered during acute decompensation of a patient. Biochemical and histological investigations may be unfeasible or ineffective due to the numerous confounders produced by severe organ injury (Nicastro and D'Antiga, 2018, Odaib et al., 1998). For instance, in the evaluation of a patient with a suspected mitochondrial DNA depletion syndrome (MDS), respiratory chain enzyme activity in the liver may be secondarily reduced risking a false positive diagnosis.

1.2.2 Monogenic causes of acute liver failure

A large proportion of liver diseases in children, both acute and chronic, are of genetic aetiology with Mendelian inheritance. For instance, monogenic diseases affecting the liver are thought to contribute to 20% of cases of LT (Nicastro and D'Antiga, 2018); when biliary atresia and autoimmune liver disease are excluded most of the remaining serious causes of liver disease are monogenic (Nicastro and D'Antiga, 2018). The suspicion of a monogenic aetiology is further strengthened the younger the affected individual is or if the individual is born to consanguineous parents (Hegarty et al., 2015, Sze et al., 2009). Figure 1-4 summarises 6 single and multiple centre studies of ALF aetiologies in children. Most monogenic causes of ALF are inherited metabolic disorders (IMD) further explained in section 1.2.3.

Study characteristics	Total	Monogenic (% of total)	Mitochondrial	FAOD	Tyrosinemia	UCD	Galactosemia	NPC	WD	Other monogenic	Indeterminate (% of total)
London, 2001-11 Retrospective, < 5 years	127	36 (28)	7	0	4	4	17	3	0	1	32 (25)
USA, 1999-2012 Prospective, multicentre, < 18 years	348	35 (10)	11	4	4	2	2	1	9	2	169 (49)
Paris, 1986-2000 18 Retrospective, < 1year	80	34 (43)	17	0	12	2	2	0	0	1	13 (16)
Coimbra, 1989-2015 Retrospective, < 2 years	34	18 (53)	4	1	1	3	4	0	0	4	Not stated
New Delhi, 2011-2016 Retrospective, < 18 years	109	14 (13)	2	2	2	2	4	0	0	0	16 (15)
Bergamo, 1996-2012 Retrospective < 15 years	55	9 (16)	2	0	0	2	1	0	3	1	26 (47)
Madrid, 2008-2013 Retrospective, < 15 years	23	2 (9)	2	0	0	0	0	0	0	0	5 (25)
Essen, 2010-2013 Retrospective, < 18 years	5	5 (100)	3	0	0	0	0	0	1	1	16 (43)
Birmingham, 2009-2011 Retrospective, < 2 years	39	9 (23)	5	0	0	1	2	0	0	1	12 (31)
Brisbane, 1991-2011 Retrospective, < 16 years	54	10 (19)	5	0	0	0	0	0	5	0	17 (31)

Other monogenic = 3 HFI, 1 MMA, 1 CDG II, 1 citrullinemia, 1 GSD IV, 1 ASL def, 1 A1AT deficiency

A1AT: alaph-1 antitrypsin; ASL: arginosuccinate lyase deficiency; CDG: congenital disorder of glycosylation; FAOD: fatty acid oxidation disorder; HFI: hereditary fructose intolerance; LCHAD: long chain acyl CoA dehydrogenase deficiency; NPC: niemann pick type C; UCD: urea cycle disorder; WD: wilson disease

Figure 1-4 Select 10 single and multiple centre studies of ALF aetiologies in children.
The proportion of children admitted with indeterminate ALF range from 16 to 49% according to the institution. Mitochondrial disorders account for the most common cause of monogenic ALF.

1.2.3 Inherited metabolic disorders

The classical IMD are a group of conditions in which there is a defect in the enzymatic metabolism of carbohydrates, proteins, lipids or in mitochondrial metabolism of energy. It has grown from a group of limited, rare disorders with no treatment to a complex set of disorders for which there may be specific treatment or its complications mitigated by being increasingly picked up on Newborn Screening (Trust, 2019). As a major organ carrying out the body's metabolic function, liver disease is a common and important sequelae of IMD.

More recently, attempts to update the classification of IMD have been made in view of the increasing complexity and growing number of IMD that are being picked up by NGS. One oversimplified way of classification proposed by Saudubray et al aims to move away from the organelle-centric approach that splits arbitrarily metabolic pathways but provide basic and practical rules to orientate clinical thinking (Saudubray et al., 2019). Under this simplified classification, disorders are classed under 1) accumulation or deficiency of *small molecules*, 2) accumulation, deficiency or abnormal trafficking of *complex molecules* or 3) *energy metabolism* disorders. Another proposal with a wider, international endorsement was published in 2021 - the International Classification of Inherited Metabolic Disorders (Ferreira et al., 2021). Under this nosology, almost 1500 monogenic diseases are grouped into a hierarchical structure to provide a system for understanding and remembering individual conditions. Its use can be extended for teaching and clinical decision making in IMD. The categories under this classification are as follows, expanded where there are known causes of ALF:

1) Disorders of amino acid metabolism

   Disorders of protein and amino acid metabolism result in accumulation of toxins that frequently lead to organ damage including the liver. Amongst this group, known causes of ALF include the urea cycle disorders ornithine transcarbamylase deficiency (*OTC*), rarely, HHH (hyperammonaemia, hyperornithinaemia, homocitrullinuria) syndrome (*SLC25A15*) and argininosuccinate lyase deficiency (*ASL*). Tyrosinemia type

I due to fumarylacetoacetase deficiency (*FAH*) and defective tyrosine metabolism is another relatively common cause of ALF.

2) Disorders of peptide and amine metabolism

3) Disorders of carbohydrate metabolism

Carbohydrates are an important, rapid source of energy. Once broken down from their complex form, glucose, galactose and fructose undergo glycolysis to be catabolised to pyruvate before entering the mitochondria and Krebs cycle. Disorders of galactose and fructose metabolism are known causes of ALF such as galactosemia, hereditary fructose intolerance due to galactose-1-phosphate uridylyltransferase (*GALT*) (Anvret et al.) and aldolase B (*ALDOB*) deficiencies, respectively. Similarly, disorders of pentose metabolism (*TALDO1*) can lead to ALF (Verhoeven et al., 2005, Balasubramaniam et al., 2011).

4) Disorders of fatty acid and ketone body metabolism

Mitochondrial β-oxidation of fatty acids is the main source of cellular energy generating acetyl-coenzyme A (acyl-coA), $NADH^+$ (nicotinamide adenine dinucleotide) and dihydroflavin-adenine dinucleotide ($FADH_2$). The β-oxidation reaction consists of four biochemical reactions: oxidation, hydration, second oxidation, and thiolysis taking place on the β-carbon of the fatty acyl-coA ester (Adeva-Andany et al., 2019). This is in contrast to α-oxidation of branched-chain fatty acids (e.g. phytanic acid) in peroxisomes which cannot undergo β-oxidation until removal of the methyl group from the β-carbon. In the fed state fatty acid synthesis occurs primarily in the liver whilst during fasting fatty acid degradation occurs in the muscle and liver. Disorders of fatty acid metabolism can cause liver dysfunction often with neurological and muscular systems involvement (Olpin, 2013, Alonso, 2005). This could be suggested by lack of ketone production during fasting (non-ketotic hypoglycaemia) in fatty acid oxidation or carnitine transporter defects due to the lack of acyl-coA required for ketogenesis. In long-chain fatty acid oxidation disorders there is elevation of fatty

acids of 14-20 carbons indicated by prominence of C14, C14:1 and hydroxy-C18:1 on plasma acylcarnitine profile. Their toxic accumulation leads to neonatal lactic acidosis, cardiomyopathy and liver failure (Odaib et al., 1998, Alonso, 2005).

5) Disorders of energy substrate metabolism

Pyruvate is the product of glycolysis and enters the Krebs cycle after being converted to acetyl-CoA by pyruvate dehydrogenase (PDH). PDH is a multi-subunit enzyme complex and deficiency of any of its components causes a phenotype characterised by neurodevelopmental problems often of poor prognosis. The *E3* complex known as dihydrolipoamide dehydrogenase (*DLD*), when deficient, causes recurrent ALF both in children and adults with or without neurological involvement (Brassier et al., 2013, Barak et al., 1998, Aptowitzer et al., 1997).

6) Mitochondrial DNA-related disorders

7) Nuclear-encoded disorders of oxidative phosphorylation

Around 1500 mitochondrial proteins are encoded by mostly nuclear but also mitochondrial genes which can give rise to primary mitochondrial diseases (Davison and Rahman, 2017) leading to disordered respiratory chain function and ATP synthesis. Mutations in nuclear genes encoding assembly factors of the respiratory chain enzyme complex subunits are a recognised cause of infantile ALF. *BCS1L* and *SCO1* which encode for complex III and IV subunits assembly factors, respectively, are such examples (Gil-Borlado et al., 2009, Olahova et al., 2019).

8) Disorders of mitochondrial cofactor biosynthesis

Synthesis of mitochondrial cofactors including coenzyme Q10 (ubiquinone), lipoic acid, iron-sulphur clusters and cytochrome c are included under this category. *BOLA3* encodes for a protein involved in the formation of iron-sulfur clusters required

Multiple mitochondrial dysfunction syndrome caused by mutations in *BOLA3* results in multi-organ failure including liver with early death (Akiyama et al., 2021).

9) Disorders of mitochondrial DNA maintenance and replication

Mutations in nuclear genes causing mitochondrial DNA depletion (*DGUOK*, *MPV17*, *SUCLG1*, *POLG* and *TWNK*) are some of the classic forms of mitochondrial hepatopathies and ALF.

10) Disorders of mitochondrial gene expression

Mitochondrial elongation factor G1 is encoded by the nuclear gene *GFM1* and its role is to translocate ribosome as each new codon is recognised during mitochondrial translation. Mitochondrial DNA is depleted and respiratory chain enzyme activity of complex I and IV is reduced on biochemical examination of cultured fibroblasts from affected patients (Balasubramaniam et al., 2012). Liver disease in *GFM1* deficiency is rapidly progressive and fatal (Molina-Berenguer et al., 2022). Similarly, mutations in *TUFM* and *TSFM* which encode for enzymes involved in the elongation step of mitochondrial protein translation cause ALF associated with mitochondrial DNA depletion and reduced respiratory chain activity (Vedrenne et al., 2012).

11) Other disorders of mitochondrial function

12) Disorders of metabolite repair/proofreading

13) Miscellaneous disorders of intermediary metabolism

14) Disorders of lipid metabolism

Acute liver failure secondary to fatty acid oxidation disorders is a rare but recognised problem (Alonso, 2005). These include disorders of long chain fatty acid which are

predominantly oxidised in the mitochondria (*HADHA*)(Odaib et al., 1998, Baruteau et al., 2014).

15) Disorders of lipoprotein metabolism

16) Disorders of nucleobase, nucleotide and nucleic acid metabolism

Mutations in nuclear translation factor genes of the respiratory chain enzyme complexes (*TRMU)* are a known cause of ALF. In most patients, ALF is transient Loss-of-function TRMU variants were associated with poor survival (Vogel et al., 2022). Additionally, there is an emerging group of disorders involving aminoacyl-transfer RNA (tRNA) synthetases (ARSs), that lead to childhood liver disease including ALF. The role of ARSs is to covalently attach amino acids to their cognate transfer RNA for delivery to the ribosome for protein translation. The genetic nomenclature of cytosolic ARSs are denoted without a number whilst mitochondrial ARSs (mtARSs) are denoted with a number *2* for example, *LARS* and *LARS2*, respectively, for leucyl-tRNA synthetase. To date, mutations in *LARS* (Casey et al., 2012, Peroutka et al., 2019) and isoleucyl-tRNA (*IARS*) (Kopajtich et al., 2016) have been described to cause ALF in infants and children whilst derangement in liver function tests is commonly reported in the remaining ARS disorders.

17) Disorders of tetrapyrrole metabolism

18) Congenital disorders of glycosylation

Congenital disorders of glycosylation (CDG) is a group of heterogeneous disorders characterised by abnormal glycosylation of lipids and proteins with over 100 subtypes described so far (Marques-da-Silva et al., 2017). The phenotypic spectrum is varied making disease classification difficult. Broadly speaking, however, type 1 CDGs are due to abnormal glycan assembly at the endoplasmic reticulum (ER); type 2 due to abnormal glycan modification at the Golgi. CDG1b results from mannose phosphate isomerase deficiency and is the prototype of hepatic CDG with approximately 25 cases

described so far with most patients presenting in the first few months of life (Marques-da-Silva et al., 2017). Liver dysfunction is also encountered in phosphomannomutase deficiency (Sparks and Krasnewich, 1993). Liver transplantation have been performed for defects in *CCDC115*, a type 2 CDG, in children with gross hepatosplenomegaly resembling a storage disorder (Jansen et al., 2016).

19) Disorders of organelle biogenesis, dynamics and interactions

20) Disorders of complex molecule degradation

21) Disorders of vitamin and cofactor metabolism

22) Disorders of trace elements and metals

23) Neurotransmitter disorders

24) Endocrine metabolic disorders

1.2.4 Activated T-cell hepatitis

The immune system and its aberrant activation are pathobiological drivers of ALF. From a clinical perspective, this concept underpins the basis of the treatment strategies aimed at inhibiting the inflammatory reaction in the use of corticosteroids or equine anti-thymocyte globulin (Karkhanis et al., 2014) including the TReatment for ImmUne Mediated PathopHysiology (TRIUMPH) trial (https://classic.clinicaltrials.gov/ct2/show/NCT04862221).More recently, a distinct phenotype involving hepatic infiltrates of CD8+ T-cells has emerged. In a study examining explant liver specimens following ALF, 27 (82%) cases of indeterminate ALF compared to 1 (7%) in the group with a known diagnosis were found to have immunohistochemical evidence of dense cytotoxic T-cell infiltration. (Chapin et al., 2018). In these patients, peripheral blood T-cell phenotype also demonstrated a unique pattern of increased percentage of effector memory CD8+ CD103+ T-cells (Chapin et al., 2023). A similar immune phenotype has been

described in a child with severe, acute hepatitis following severe acute respiratory syndrome coronavirus 2 infection alluding to the theory that a dysregulated immune response is the common underlying pathobiology (Morita et al., 2022).

1.2.5 Other novel causes of ALF

Neuroblastoma amplified sequence (*NBAS*) deficiency was first reported to be associated with human disease in 2010 following a description of a cohort from the Yakut population isolated in the northeastern region of Siberia (Maksimova et al., 2010). Homozygosity mapping revealed 33 patients with the substitution c.5741G>A, p.Arg1914His in patients with short stature, optic nerve atrophy and Pelger-Huët anomaly characterised by abnormal nuclear shape in neutrophil's granulocytes (SOPH syndrome; MIM 169400). In 2015, *NBAS* was described for the first time in fever-triggered, recurrent, ALF patients using whole genome sequencing (Haack et al., 2015). It was highlighted to be a relatively common cause of ALF given the frequency of the finding in a small cohort of patients (Staufner et al., 2016). Since then, over 110 patients have been described (Staufner et al., 2016, Segarra et al., 2015, Rius et al., 2019, Regateiro et al., 2017, Park and Lee, 2017, Ono et al., 2019, Li et al., 2017, Capo-Chichi et al., 2015, Balasubramanian et al., 2017, Calvo et al., 2017). The disease has become known as *NBAS deficiency* given the reduced level of NBAS protein detected in patients' fibroblasts (Haack et al., 2015).

Other "newer" monogenic causes of ALF include defects in *SCYL1*. Disruptive *SCYL1* mutations have been described in patients with early onset recurrent acute liver failure, peripheral neuropathy, cerebellar vermis atrophy and ataxia. This "hepatocerebellar neuropathy syndrome" has been described in 10 patients (Shohet et al., 2019, Li et al., 2019, Lenz et al., 2018).

1.3 Neuroblastoma amplified sequence

1.3.1 NBAS deficiency and acute liver failure

Acute liver failure secondary to NBAS deficiency has been described world-wide in children and adults from Europe (Haack et al., 2015), Australasia, (Ono et al., 2019, Rius et al., 2019) and North America (Staufner et al., 2020). It is an autosomal recessive disease observeded in families of consanguineous (Ricci et al., 2019) as well as non-consanguineous descent. Presentation of the disease is typically in the first two years of life with ALF usually in a child without any significant, prior, health or developmental problems (Chavany et al., 2020, Staufner et al., 2016). However, further history may reveal fetal growth retardation and / or short stature (Ricci et al., 2019, Ono et al., 2019, Segarra et al., 2015, Regateiro et al., 2017). The trigger of the ALF is often a feverish illness but is not necessarily a prerequisite (Chavany et al., 2020, Ono et al., 2019, Haack et al., 2015). Hepatic insult can resolve spontaneously although affected individuals can suffer multiple crises (up to 12 has been described) with or without going into ALF (Staufner et al., 2016).

The biochemical derangement from ALF in NBAS deficiency is notably hyperacute with rapid, significant elevations in aspartate aminotransferase (AST) and ALT - typically, in the tens of thousands alluding to the degree of hepatocellular necrosis (Chavany et al., 2020, Calvo et al., 2017). This is accompanied by a sharp rise in INR ranging between 4 to 20 (Chavany et al., 2020). Elevations in lactic acid and ammonia are seen at the time of liver crisis as a general marker of critical illness but no specific, diagnostic biomarkers are currently available.

Histological understanding of the liver is derived from samples obtained from autopsy, explants following LT and elective biopsies between liver crises. Typical features include microvesicular steatosis, cytoplasmic vacuolations with minimal, background fibrosis (Li et al., 2017, Ono et al., 2019, Staufner et al., 2016) or no abnormalities (Segarra et al., 2015). Periportal cytokeratin 7 staining can be positive and is indicative of the ductular proliferation and metaplasia secondary to extra-acinar cholestasis (Haack et al., 2015). Ultrastructurally, dilation of the ER and peripherally orientated Golgi can be observed (Li et al., 2017). The mitochondria show a dense matrix and abnormal internal architecture with dilated, elongated cristae (Staufner et al., 2016).

Treatment for ALF secondary to NBAS deficiency is primarily supportive including glucose infusions and anti-pyretic therapy (Haack et al., 2015). The liver crises tend to resolve within 7-10 days if an affected individual can avoid LT – an accepted treatment for ALF as well as a preventative measure for future ALF (Chavany et al., 2020). However, the occurrence of crises seems to diminish or stop with age, therefore, the long-term need for LT should be considered very carefully (Chavany et al., 2020). Liver transplantation was carried out in 4/45 (11%) reported cases and a similar number have died without LT (Chavany et al., 2020).

1.3.2 NBAS deficiency as a multisystemic phenotype

There are two distinct groups of patients with NBAS deficiency: those that exhibit a pure hepatic phenotype and those with multisystemic involvement; a small minority exhibit features of both. The 3 patients diagnosed in our study had the hepatic phenotype.

SOPH syndrome is the archetypal description of multisystemic NBAS deficiency. These patients have short stature, optic nerve atrophy and Pelger-Huët neutrophil anomaly. Their skeletal features are most notable with short stature (-2 SD), clino-brachydactyly, osteopenia and facial dysmorphism including hypotelorism, thin upper-lip and pointed chin (Chavany et al., 2020). Neurologically, optic nerve atrophy is a key feature with visual and colour impairment being a relatively stationary symptom (Maksimova et al., 2010). Other features include inverted nipples at birth, lipodystrophy, joint laxity, dislocation of the lens, premature loss of milk teeth (connective tissue), relatively small foramen magnum, spinal cord compression with lower limb weakness (skeletal system), chronic lung disease with oxygen dependency and bilevel positive airway pressure (BiPAP) respiratory support, low immunoglobulin levels and recurrent bacterial pneumonia (respiratory system) (Staufner et al., 2020).

1.3.3 Genetics of NBAS deficiency

The *NBAS* gene is located on chromosome 2p and contains 52 exons spanning 15 megabases. Systematic analysis of NBAS variants and their associated clinical disease pattern was previously carried out in 2019 incorporating 33 publications reporting on 110 patients from 97 families (Staufner et al., 2020). Since then, two further reports have been published including the patients studied in this work making the total number of reported patients to be 115 (Chavany et al., 2020, Hegarty et al., 2021). Amongst them, there are a total of 91 variants including 43 missense variants, 14 frameshift variants, 12 nonsense variants, 5 exon deletions, 1 exon duplication, 2 in-frame deletions and 1 intronic variant (0). Seventeen of the 70 genotypes are homozygous. Apart from the homozygous missense variant c.5741G>A, p.Arg1914His reported in the Yakut population, no specific variant combination is present in more than two unrelated families which indicates allelic genetic heterogeneity amongst those with the ALF phenotype. There are no individuals with biallelic nonsense variants which may indicate that a complete absence of protein is incompatible with life.

1.3.4 The NBAS protein

The NBAS protein is 2,371 amino acids in length with a mass of 268,571 Da (Uniprot ID: A2RRP1). It is located in the ER in association with a complex of soluble NSF Attachment Protein (SNAP) receptors (SNAREs). The structure of the protein has been previously predicted using HHpred which is a web-based server that is able to predict protein structure based on homologous proteins (Zimmermann et al., 2018). According to this, NBAS has a partly disordered, partly helical N-terminus (residues 1–85), a region consisting of mostly β-strands in WD40 repeats (residues 86–446) with the remainder of the protein being predominantly helical (residues 447–2371) (Staufner et al., 2020). Amino acids 86-446 are thought to form a β propeller domain (InterPro ID: IPR011044) and amino acids 722-1369, a Sec39 domain (InterPro ID: IPR013244).

1.3.5 Genotype-phenotype correlation

The localisation of the reported, disease variants have provided insight into genotype-phenotype correlation according to the three domain-related subgroups: β-propeller, Sec39,

and C-terminal. Interestingly, variants in the coding region for the Sec39 domain are mainly associated with ALF, whilst variants in the coding region for the C-terminus including the c.5741G>A, p.Arg1914His variant seen in the Yakut population show a predominant multisystemic phenotype (Staufner et al., 2020, Carli et al., 2019). However, patients with variants in the region coding for the β-propeller domain present with a combined severe phenotype including both ALF and multisystemic features.

1.3.6 NBAS biology and pathobiology

1.3.7 Golgi-ER retrograde transport

The recycling of proteins from the Golgi to ER is carried out by a process known as retrograde transportation. In this process, vesicles containing proteins from the Golgi are coated by coat protein complex 1 (COP1) and transported along a microtubule to the ER. Here SNAP receptors – v-SNAREs for those arising from the vesicles; t-SNAREs for those that are anchored to the target-membrane – combine to tether the vesicle to the ER membrane so that the proteins can be released. Syntaxins are members of the t-SNARE family of proteins and specifically, syntaxin 18 is in the ER.

It has been shown that NBAS is a component of syntaxin 18 and implicated in the Golgi-to-ER retrograde transport (Figure 1-5) (Aoki et al., 2009). Disturbance in protein glycosylation as well as redistribution of Golgi recycling proteins were demonstrated when HeLa cells were transfected with NBAS siRNA (Aoki et al., 2009). Similarly, in affected patients' fibroblasts, immunofluorescence analyses of cells permeabilised with digitonin showed that Golgi recycling proteins were redistributed around the cell in comparison to controls (Staufner et al., 2016). These studies suggest that the tethering complex of the vesicles associated with Golgi-ER transportation is affected in NBAS deficiency.

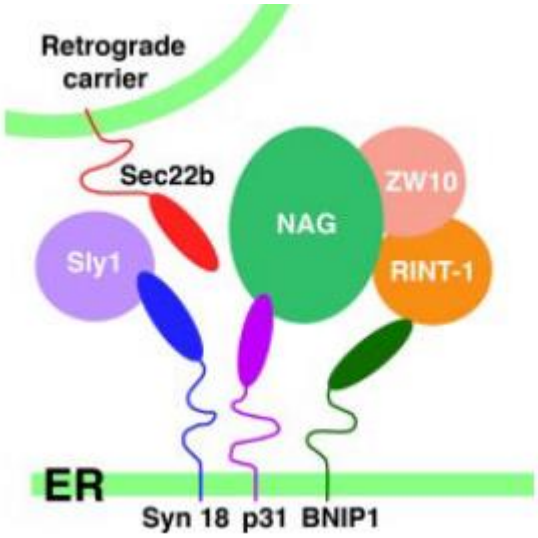

Figure 1-5 Schematic representation of the syntaxin 18 complex.
Neuroblastoma amplified gene interacts directly with other SNARES (p31, ZW10 and RINT-1) forming a large complex. The figure was adapted from (Aoki et al., 2009).

1.3.8 Nonsense mediated decay

Nonsense-mediated mRNA decay (NMD) is a highly conserved, post-transcriptional, regulatory mechanism of gene expression in eukaryotes. Originally, NMD was identified as an RNA surveillance machinery to downregulate prematurely terminated transcripts that are a consequence of naturally-occurring variants (Han et al., 2018). Recent progress in transcriptome wide high throughput sequencing estimates that NMD targets approximately 5–30% of physiological transcripts for the purpose of tuning gene expression in response to various environmental conditions (Kurosaki et al., 2019). The malfunction of NMD can result in serious, often multi-systemic consequences for the development of various organisms (Hwang and Maquat, 2011).

The mechanism of NMD is dependent on exon junction complexes (EJCs) that are deposited during splicing, approximately, 20-24 nucleotides upstream of exon/exon boundaries. These EJCs which importantly contain the key NMD factors are normally removed as the ribosome moves along the transcript during translation. Premature termination codons (PTCs) situated more than 50-55 nucleotides upstream of the last exon/exon junction leave the final EJC

allowing for the mRNA to be targeted for decay by NMD (Gatfield et al., 2003). On the contrary, PTCs positioned in the last exon will not be recognised for NMD producing a truncated protein which may have profound, deleterious effects (Figure 1-6).

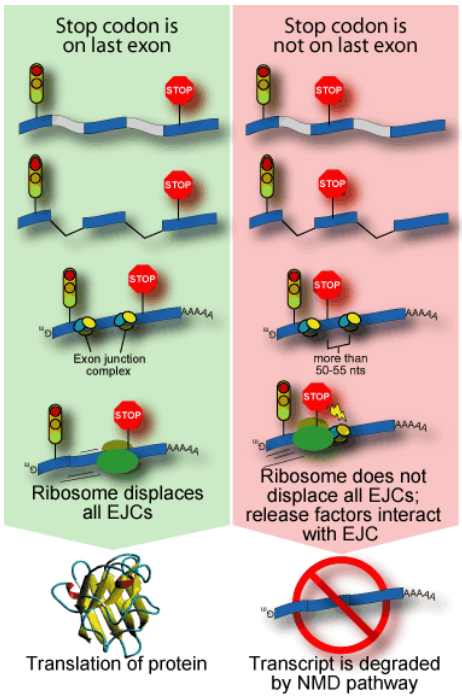

Figure 1-6 Nonsense mediated decay.
The location of the last EJC determines whether the transcript will be subject to NMD or not. On the left, the stop codon is located on the last exon and protein translation takes place as the ribosome traverses the mRNA and displaces EJC in its path. On the right, there is a premature stop codon that is more than 50-55 nucleotides upstream of the last EJC. As a result, there is an undisplaced EJC leading to the degradation of the transcript by NMD. The figure was adapted from (Lewis, 2003).

Evidence for the involvement of NBAS in NMD originates from studies using genetic screening. In the nematode, *Caenorhabditis elegans*, and fruit fly, *Drosophila*, the *smgl-1* (suppressor with morphogenetic effects on genitalia) gene was originally characterised as an NMD factor using RNA interference screens (Gatfield et al., 2003). These studies employed the use of green fluorescent protein probes and northern blot to ascertain relative expression levels of NMD targets when cells were transfected with short interfering RNA against NMD factors. The human ortholog of this highly conserved gene, *smgl-1*, is *NBAS* as identified by BLAST searches (Altschul et al., 1997). When *C. elegans* and zebrafish, *Daniorerio* were depleted of

smgl-1 many genes were shown to be upregulated, informing the landscape of transcripts that are targeted directly by NMD (Longman et al., 2013).

Conventional experimental set-ups looking at NMD as referenced above have been based on depleting an NMD factor and measuring relative changes in their targets in comparison to an untreated cell using northern blot, RT-qPCR and microarray techniques. More recent approaches are transcriptome-wide using RNA-Seq which highlights all mRNA that amount to a significant fold change (typically, greater than 1.5 or 2.0 times). Others have taken this further to calculate mRNA half-lives of NMD substrates, observing reduced decay in hundreds of transcripts after siRNA depletion of UPF-1, a key NMD factor (Tani et al., 2012). However, these experiments are complicated by issues such as: the fact that stabilised mRNAs may encode proteins that are involved in other aspects of RNA metabolism and, as a result, levels of mRNAs that are not direct NMD targets may change; the requirement for prolonged protein depletion when studying dynamic processes (Lykke-Andersen and Jensen, 2015).

A more practical approach of assessing whether NBAS has a role in NMD in humans will be to quantitatively evaluate endogenous NMD targets (personal communication, Maquat, Professor of Biochemistry & Biophysics and founding director of the Center for RNA Biology, University of Rochester). Growth arrest and DNA damage-inducible 45A and B (*GADD45A* and *GADD45B*) are two genes that are directly regulated by NMD in both fruit flies and mammals (Viegas et al., 2007, Hwang and Maquat, 2011). They have been shown to increase its expression upon knockdown of the NMD factor, UPF-1, confirming that it is sensitive to NMD (Nelson et al., 2016).

1.4 Research aims

As alluded to in previous sections, ALF in children is a heterogenous and complex condition in which there is a wide range of underlying aetiologies, both genetic and acquired. In recent years, “newer” monogenic causes of ALF have been described offering new aetiological insights. However, studies using NGS to investigate monogenic causes in a cohort of children with ALF are lacking. This is due to a few reasons. Firstly, ALF in children is rare which makes

larger meaningful studies difficult to carry out. Secondly, children with ALF are often critically ill, therefore, it is challenging to carry out research activities involving procedures that are in addition to those that are required for clinical care such as sampling of blood.

1.4.1 Genetics of acute liver failure in children

The Paediatric Liver, GI and Nutrition Centre at King's College Hospital (KCH), London, is an international referral centre for children with liver disease. It is uniquely placed to provide clinical care to children with liver disease from a large geographical area. Therefore, a study based at KCH has significant clinical relevance and potential to inform future clinical decision making.

The objectives were:

- To identify undiagnosed, monogenic diseases in children admitted to KCH who received a diagnosis of indeterminate ALF and to describe their characteristics.
- To provide the research foundation to construct a diagnostic, genetic panel using targeted NGS technology for future children with indeterminate ALF.

I hypothesised that in up to 20% of children previously admitted to KCH with indeterminate ALF there may be an underlying monogenic disorder given the reduced proportion of these cases from 49% (Squires et al., 2006) to 30% (Alonso et al., 2017) comparing the diagnostic rates prior to and after the advent of NGS.

1.4.2 Functional characterisation of NBAS deficiency

Our current understanding of NBAS deficiency is primarily based on clinical descriptions of patients with recurrent ALF whose diagnoses have come to light with genetic sequencing. The disease has been postulated to be secondary to defects in Golgi-ER retrograde transport and / or NMD. However, evidence is lacking to substantiate latter. A much better understanding of the disease mechanism is required to direct treatment in the future.

The objectives were:

- To investigate and describe the pathobiology of NBAS deficiency using skin fibroblasts obtained from affected patients.
- To determine if NMD is disrupted in patients with NBAS deficiency.

I hypothesised that the application of *stress* to skin fibroblasts from patients with NBAS deficiency will cause a negative effect on cell viability when compared to controls.

2 MATERIAL AND METHODS

2.1 Targeted NGS of children with indeterminate ALF

2.1.1 Patient identification

Children under 10 years of age admitted to KCH between 2000 and 2018 with indeterminate ALF were identified by carrying out a search of the electronic health records. The following search terms were used: acute liver failure, ALF and indeterminate. The clinical records were reviewed to ensure that the patients met the study criteria. Children were categorised as ALF of indeterminate aetiology when the diagnosis was not established despite thorough, age-appropriate investigations (APPENDIX A). Patients were selected for the study where valid consent and blood samples were available from the KCH Paediatric Liver Tissue Bank (research ethics committee reference number, 18/WA/00090). An age limit of 10 years was chosen as younger children are more likely to be affected by monogenic forms of ALF (Nicastro and D'Antiga, 2018). The year 2000 was the earliest year that a patient could be identified where the clinical records and blood samples were of sufficient quality for the study. A total of 41 children were selected for sequencing (Figure 2-1).

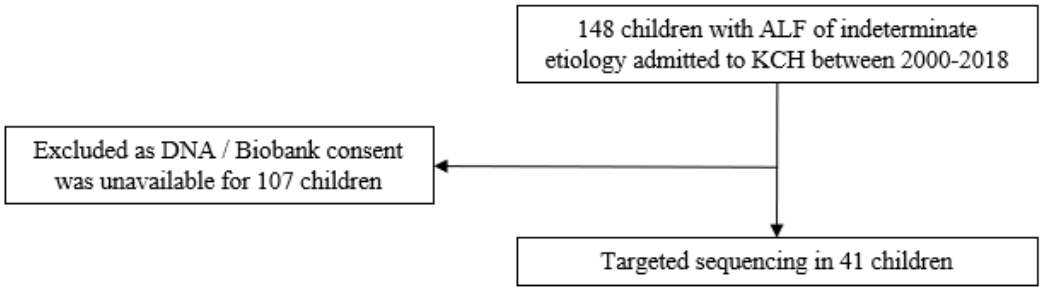

Figure 2-1 Identification of patients for targeted sequencing.
Samples from 41 children were available for sequencing amongst 148 who were admitted to KCH with indeterminate ALF between 2000 and 2018.

2.1.2 Next generation sequencing

Next generation sequencing is a form of short read, massively parallel sequencing technology that can determine the sequence of nucleic acids quickly and efficiently. Its advent since the mid-2000s has brought a revolutionary era in genomics and its utility has expanded exponentially. Prior to this, Sanger sequencing was considered the first generation of sequencing technology that used the chain termination methodology coupled with capillary electrophoresis. This method is slow and labour-intensive such that it took 13 years to complete the Human Genome Project at an approximate cost of $2.7 billion. Today NGS allows us to complete whole genome sequencing in under $1000 within the space of a few days.

Amongst the Illumina (Agilent Technology UK Ltd, Cheshire, UK) sequencing platforms there are several benchtop sequencers that can perform sequencing for clinical, diagnostic purposes. The choice depends on the purpose of the application. The NextSeq Series can produce the largest number of reads and can carry out exome, metagenomic and transcriptome sequencing. The middle-range MiSeq Series is more suited for targeted sequencing whilst the more affordable iSeq 100 range is ideal for small-scale sequencing of, for instance, bacteria and viruses.

2.1.2.1 DNA purification and quantification from whole blood

For the extraction of genomic DNA there are principally three methods that can be used including organic extraction (phenol–chloroform method), nonorganic method (salting out and proteinase K treatment) and adsorption method (silica–gel membrane) (Gupta, 2019). The QIAamp DNA Blood Mini kit (Qiagen Ltd, Manchester, UK)which uses a solid-phase extraction method of silica gel membrane columns was used for this work. Approximately, 200 µl of ethylenediaminetetraacetic acid (EDTA) buffer-preserved, patient's blood was used to yield 6 µg of DNA (Qiagen, 2018). One µl of purified DNA was subsequently quantified using Qubit 2.0 Fluorometer (ThermoFisher, Paisley, UK) to measure intact double stranded DNA (dsDNA) before NGS. The Qubit fluorometer uses fluorescent dyes specific to targets of interest such as DNA, RNA or protein and the intensity of the fluorescence indicates the quantity of DNA (ThermoFisher, 2018). This step was carried out with a staff member from the Liver Molecular Genetics laboratory to avoid sample mix-up and cross-contamination.

2.1.2.2 Probe design

A gene panel rather than whole exome / genome approach was used for the study using the resources available at the time in the Liver Molecular Genetics laboratory at KCH. Sixty-four monogenetic disorders that are known to cause metabolic liver disease in children, with or without acute liver failure, were selected (APPENDIX B). These genes were selected following a literature review of genetic conditions that are known to cause ALF or acute hepatitis and the final list decided upon consultation with Prof Richard Thompson, Primary Supervisor and Honorary Consultant Paediaric Hepatologist. To target these genes or regions of interest (ROI) for sequencing the Agilent SureSelectXT Target Enrichment kit for Illumina technology was used (Parshuram et al.). This method utilises biotinylated, single-stranded RNA to act as baits to capture the ROI. The probes were designed using Agilent eArray web portal (https://earray.chem.agilent.com/earray). Gene information was obtained from Ensembl (http://www.ensembl.org/index.html) and University of California Santa Cruz (UCSC; https://genome.ucsc.edu) genome browsers based on version GRCh37.p7/hg19 of the genome from February 2009.

2.1.2.3 Next generation sequencing: Illumina Paired-End Multiplexed Sequencing

Preparing the purified dsDNA for sequencing is known as the library preparation stage and requires the following three steps: sample preparation, hybridisation and post-capture sample processing. The Agilent SureSelect Target Enrichment System for Illumina Paired-End Multiplexed Sequencing was used for this (Agilent, 2017). In multiplex sequencing many libraries can be pooled and sequenced simultaneously owing to a unique sequence, or a 'barcode', being attached to each fragment of DNA. This greatly increases the number of samples that can be processed in a single NGS run.

2.1.2.4 Library preparation

The SureSelect Target Enrichment protocol was used for the library preparation where the DNA was enzymatically fragmented, end-repaired, dATP-tailed and ligated with a molecular-barcoded adaptor. This process was carried out in a single reaction by use of a mutant transposase enzyme that can fragment as well as attach synthetic oligonucleotides in an efficient manner (Kia et al., 2017). Next, the adaptor-tagged library was purified using Agencourt AMPure XP beads (Beckman Coulter, High Wycombe, UK) and PCR-amplified. The amplified library was again purified and measured for quantity and quality using 2200 TapeStation (Agilent, Santa Clara, USA). A peak DNA fragment size between 245bp and 325bp is necessary for optimum sequencing results.

2.1.2.5 Hybridisation

The sample library was hybridised to the previously designed, capture library targeted to the ROI. First, the sample library containing 500 to 850 ng of DNA was diluted to a final volume of 12 µl. This was then denatured using a thermal cycler and the capture library reagents were prepared in the mean time. Next, the sample and capture libraries were combined and hybridised. To pull the sample DNA hybridised to the biotinylated, capture library probes, Dynal MyOne Streptavidin T1 provided by Invitrogen (Life Technology) was used. This contains streptavidin-coupled magnetic beads that only allows the targeted genomic DNA

segments to be pulled down when applied to a magnetic field (Figure 2-2). Finally, the captured library was amplified by PCR and purified using Agencourt AMPure XP beads. The quality was assessed using Agilent TapeStation and High Sensitivity D1000 Screen Tape ensuring that the peak DNA fragment size was between 325 and 425 bp.

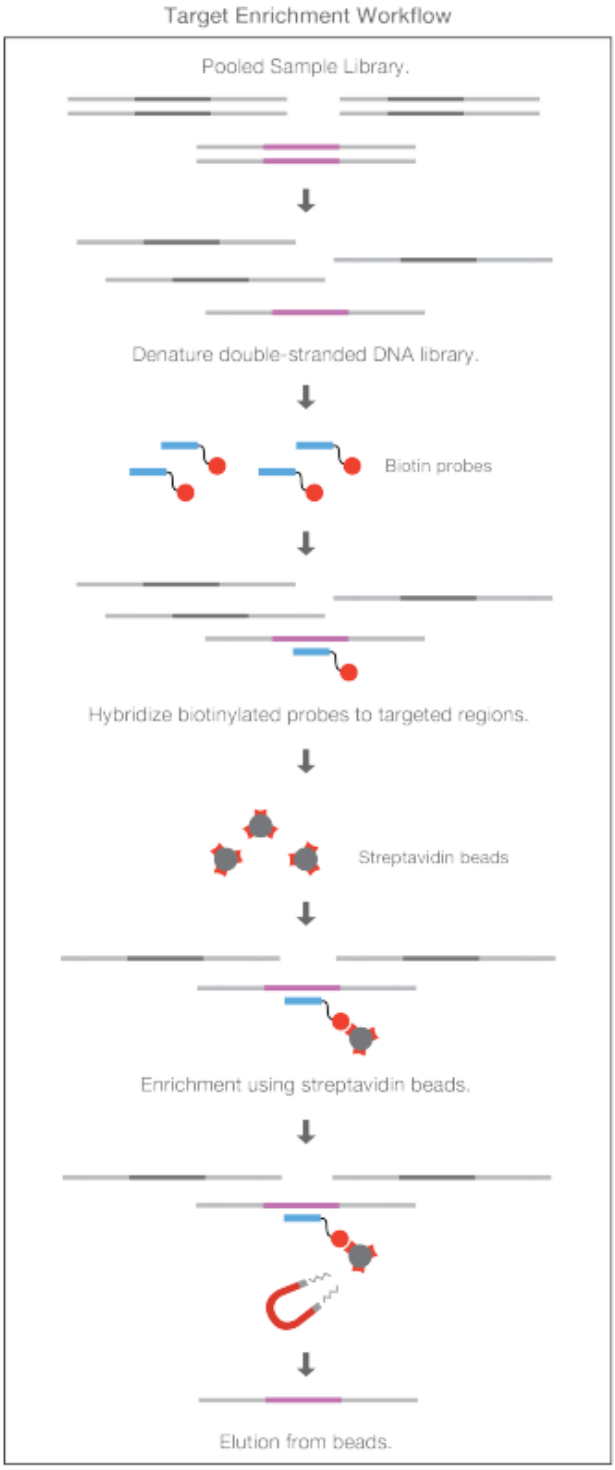

Figure 2-2 The SureSelect Target Enrichment protocol.

Biotinylated probes are employed to hybridize to specific regions of interest. This is then pulled down by streptavidin coated magnetic beads. The image was adapted from Illumina.

2.1.2.6 Cluster generation

The amplified, captured library was subsequently loaded onto an Illumina MiSeq sequencer at the Liver Molecular Genetics laboratory, KCH, to undergo sequencing using Illumina Sequencing Technology. Custom primers were added to the MiSeq cartridge and flow cell cleaned before they were loaded onto the MiSeq. The flow cell is a glass slide with a lane anchored with short oligonucleotides that are complementary to the adaptors ligated in the sample preparation stage. Sample DNA, once loaded on the flow cell, underwent 'bridge amplification' where DNA fragments are isothermally amplified using polymerase to form a double stranded 'bridge'. The 'bridge' is then denatured forming two complementary strands – repeating the process generates up to 1,000 copies of fragments to produce a unique cluster (Figure 2-3).

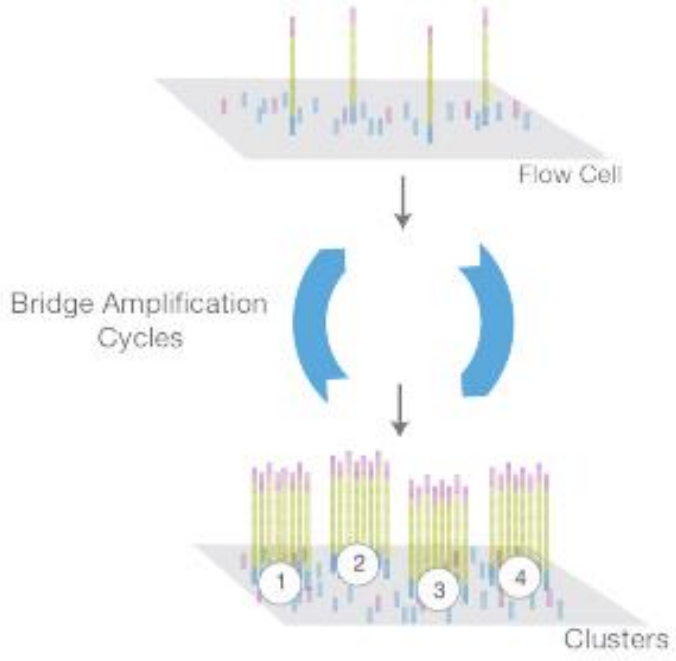

Figure 2-3 Bridge amplification.
During bridge amplification, the capture library bind to complimentary oligos on the surface of the flow cell. Once a double strand is formed by polymerase, priming occurs as the strand "bridges" to another complementary oligo forming clusters. The image was adapted from Illumina.

2.1.2.7 Sequencing by synthesis

Sequencing by synthesis technology uses DNA polymerase to sequentially extend multiple strands of DNA using nucleotides with an identifying tag which identifies the base type. Sequencing begins at the first sequencing primer and successively extending the DNA fragment using fluorescently labelled deoxyribonucleotide triphosphates (dNTPs) that compete to bind to the complementary strand. As polymerase extends the strand a light source is emitted, captured by a high sensitivity camera, leading to the base call. The completion of a DNA fragment, or a cluster of identical fragments, provides a 'read'. The same process is repeated on the opposite end of the DNA fragment creating forward and reverse reads (Illumina, 2017).

2.1.3 Sequence alignment, variant calling and annotation

Sequences from pooled sample libraries are separated based on the unique indices introduced during the sample preparation. For each sample reads with similar stretches of base calls are locally clustered. Forward and reverse reads are paired creating contiguous sequences. These contiguous sequences are then aligned to the reference genome.

2.1.3.1 Sequencing alignment and variant calling

The binary base call (BCL) file is the raw data files generated by Illumina sequencers. The FASTQ is a text file that contains the sequence data which can be incorporated to third-party tools for analysis. Demultiplexing and BCL file conversion to FASTQ was performed by Consensus Assessment of Sequence and Variation (CASAVA), installed in every Illumina machine, in a single step.

2.1.3.2 Variant annotation: *CLC bio*

The FASTQ files were then imported to CLC Genomics Workbench version *12.0*. *CLC bio* is a bioinformatics software that carries out variant alignment and annotation using a workflow constructed from a series of connected, data processing tools. Using the *map reads to*

reference tool the read depth and variant probability configurations were applied. The minimum read depth was set at 20, removing any variants with reads below this count. The minimum variant probability, which represents the probability of a specific variant being different to the reference, was set at 80. The coverage threshold of 20 can be compared to exome sequencing whereby the American College of Medical Genetics and Genomics (ACMG) recommends a minimum threshold of 10X (Sun et al., 2021). It highlights one of the advantages of gene-focussed, targeted sequencing which can achieve greater read depth increasing sequencing sensitivity and specificity. Information from reference databases such as database of single nucleotide polymorphisms (dbSNP) and 1000 Genomes Project were added using *annotate* from known variants tool. Similarly, the amino acid change tool was used to add amino acid information from Ensembl.

After the construction of the workflow, the FASTQ files were imported and the workflow applied generating a variant call format (VCF) file for each sample. The VCF file can be viewed, for instance, using Microsoft Excel where each row represents a variant with annotations on the columns.

2.1.4 Variant filtering and prioritisation

Sequence variants were filtered using Ingenuity Variant Analysis (IVA; Qiagen Bioinformatics) incorporating a filter excluding those with a minor allele frequency of >0.01 in the public databases as unlikely to be causative. The databases that were used were: Exome Aggregation Consortium (ExAC), Human Gene Mutation Database (HGMD), dbSNP, 1000 Genomes, Allele Frequency Community, Inova Genomes, Exome Variant Server (EVS) and Database of Genomic Variants (DGV). Non-synonymous (missense variants, stop gains or losses, frameshifts, small insertions and deletions) and intronic variants within 5 bp of exon-intron junctions were included. The prioritised genes with variants after filtering were investigated for pathogenicity using IVA whilst considering the effect of the candidate variants on the protein as predicted by Grantham score, Combined Annotation Dependent Depletion (CADD) score, Polymorphism Phenotyping-2 (PolyPhen-2), sorting intolerant from tolerant (SIFT) and MutationTaster:

- **Grantham score**. In this method, a score is provided to predict the distance between two amino acids in evolutionary terms (Grantham, 1974). The score ranges from 5 to 215 and the higher the score, the more distant the two amino acids are and, therefore, deleterious.
- **CADD score**. In this method, information from multiple, functional annotations are condensed to produce a single score (Kircher et al., 2014) (https://cadd-staging.kircherlab.bihealth.org/). A CADD score of 20 means that a variant is amongst the top 1% of deleterious variants in the human genome whilst a score of 30 means that the variant is in the top 0.1%.
- **PolyPhen-2**. This is a web-based tool that predicts the possible impact of an amino acid substitution on the structure and function of a human protein http://genetics.bwh.harvard.edu/pph2/). It uses the UniProtKB/Swiss-Prot database (https://www.uniprot.org/) to gather sequence, phylogenetic and structural information characterising the substitution. It classifies the nonsynonymous SNPs as *benign*, *possibly damaging*, or *probably damaging*.
- **SIFT**. This is another web-based tool that predicts the possible impact of an amino acid substitution on the structure and function of a human protein (https://sift.bii.a-star.edu.sg/). It uses sequence homology and the physical properties of amino acids and categorises the score as *tolerant* (0.201–1.00) or *intolerant* (0.051–0.10) and *borderline* (0.101–0.20).
- **MutationTaster**. This is another web-based tool that classifies DNA sequence variants as *disease-causing* or *polymorphism* (http://mutationtaster.org/). Unlike PolyPhen-2 and SIFT, MutationTaster works on DNA level and allows insertions and deletions.

The relative performance of these computational methods in predicting the functional impact of variants can be variable as they all use slightly different methods (Wang et al., 2022). The prediction outcomes derived from SIFT is based on evolutionary conservation whilst PolyPhen-2 and MutationTaster are based on protein structure as well as evolutionary conservation. CADD uses annotations from derived alleles in humans and compares them to simulated variants. Therefore, the ACMG guidelines state that a range of methods in conjunction should be used when classifying variants (Richards et al., 2015).The variants

remaining after these filtering steps were evaluated by reviewing the latest literaturefor genotype phenotype correlation. For the biallelic variants felt to be contributing to the patients' phenotype the ACMG classification was applied according to the 5-tier classification system (Richards et al., 2015). Under this system, there are two sets of criteria including one for classification of pathogenic or likely pathogenic variants and another for benign or likely benign variants where each pathogenic criterion is weighted as very strong (PVS1), strong (PS1–4); moderate (PM1–6), or supporting (PP1–5) and each benign criterion is weighted as stand-alone (BA1), strong (BS1–4) or supporting (BP1–6).

2.1.5 Quantitative real-time PCR using Universal ProbeLibrary System Technology

Quantitative PCR (q-PCR) is an established method in quantifying nucleic acid sequences. It was chosen as the method to confirm the x2 copy number variant (CNV) found in *NBAS* exon 17 - 19 in patient #9.

2.1.5.1 Primer design

Universal ProbeLibrary (UPL) System Technology (Roche) was used where available. This technology uses hydrolysis probes that are labelled at the 5' end with fluorescein (FAM) and at the 3' end with a dark quencher dye. These probes, 8-9 nucleotides in length, contain locked nucleic acids (LNA) which are nucleotide analogues with a higher binding strength in comparison to standard DNA nucleotides. Locked nucleic acids are, therefore, able to withstand the required, higher melting temperature. The FAM-labelled probes emit a fluorescent signal that corresponds to the doubling of the product. In total, there are 165 hydrolysis probes which can bind to 7000 human transcripts.

To select the appropriate probes to capture exon 17 and 19 of *NBAS* gene, the UPL Assay Design Center was used (https://www.lifescience.roche.com).

Each primer was screened with Basic Local Alignment Search Primers Tool (BLAST) (http://www.ncbi.nlm.nih.gov/tools/primer-blast/). Primers flanking the exon were then

purchased from Sigma Life Science (Mercke). For the control, a gene unrelated to ALF with a low germline mutation rate, bile salt export pump (BSEP; *ABCB11*), was selected. The primers and probes that were used in this study is listed in APPENDIX C.

2.1.5.2 qPCR protocol

The volume of reagents required (Table 2-1) was calculated for an 18x reaction mix and aliquoted in a 96 well PCR plate in technical duplicates. DNA samples were diluted to a concentration of 4 ng/µl and 2 µl of each sample were added to the wells.

	Volume (µl)	Concentration
Forward primer (10 µM)	0.8	0.4 µM
Reverse primer (10 µM)	0.8	0.4 µM
UPL probe (10 µM)	0.4	0.2 µM
ABI Taqman Universal Mastermix	10	
Sterile water	6	

Table 2-1 Volume and concentration of reagents used for the UPL assay.

The plates were sealed with an adhesive optical film and PCR reaction performed using the protocol illustrated below (Table 2-2) using StepOne Real-Time PCR System (Life Technologies). The cycling conditions used included an initial step at 50°C for 2 minutes to activate the uracil N-glycosylase (UNG) enzyme included in the mastermix to remove uracil, normally found in RNA, from DNA that may result from carry-over contamination. This was followed by an initial denaturation step of 95°C for 10 minutes followed by 40 cycles of denaturation at 95°C for 15 seconds and annealing of primers and extension at 60°C for 1 minute.

Step	Temperature (°C)	Time	Cycles
Initial denaturation	95	10 minutes	1
Denaturation	95	15 seconds	40

Annealing and extension	60	60 seconds	

Table 2-2 qPCR thermal cycling protocol used in the StepOne version 2.3 system.

2.1.5.3 qPCR data analysis

StepOne version 2.3 (Life Technologies) was used for the analysis of qPCR data incorporating an automatic function to set baseline and cycle threshold (C_T) values. The quantification of the target gene against a control gene was then calculated using the absolute quantification method. The quantities of DNA were calculated for the target gene (*NBAS*) and control (*ABCB11*) using their respective standard curves of a 5-fold dilution series. The data were exported to Excel 2017 (Microsoft) and the amount of target gene was divided by control to determine their ratio.

2.2 Functional characterisation of NBAS deficiency

2.2.1 Cell culture methods

The following section describes the material and methods set out to:

- Investigate the cell viability of fibroblasts from patients affected by NBAS deficiency when stressed by culturing in low glucose medium or incubating at 40 °C.
- Carry out NBAS western blot on protein extracts from fibroblasts from patients affected by NBAS deficiency.
- Measure *GADD45A* and *GADD45B* expression by RT-qPCR using fibroblasts from patients affected by NBAS deficiency.

2.2.1.1 Cell sources

The experiments described in this work were performed on dermal fibroblasts obtained from patients and human foreskin fibroblast 1 (HFF1; control) cells after confirming that *NBAS*, *GADD45A* and *GADD45B* are expressed in skin (https://www.proteinatlas.org/ENSG00000151779-NBAS). Human foreskin fibroblasts are commercially available cells that are obtained following circumcision that would have been discarded otherwise. They are widely used in research and considered a standard model of human cells (Hovatta et al., 2003) and have been previously used to study the mechanism of NMD (Brown et al., 2011). Fibroblasts from patients NBAS 1 to 4 were obtained using a 5mm punch biopsy, minced and placed in culture. The maintenance and storage of cells were carried out by Viapath Services at the Biochemical Genetics Laboratory, Guy's Hospital, London, UK.

The patient cells and the variants identified were as follows (Table 2-3).

Patient	NBAS variants (NM_015909.4, NP_056993.2)
NBAS1	c.exons 17-19 dup, p.? / c.exons 17-19 dup, p.?
NBAS2	c.4731_4733dup, p.Tyr1578dup / c.4731_4733dup, p.Tyr1578dup
NBAS3	c.1702G>A, p.Val568Ile /c.191G>A, p.Val568Ile
NBAS4	c.2191A>C, p.Thr731Pro / c.2191A>C, p.Thr731Pro

Table 2-3 Genotypes of patient fibroblasts used.
Four patients (NBAS1, 2, 3, 4) with a diagnosis of NBAS deficiency selected for the functional studies and their respective genotypes.

2.2.1.2 Reagent preparation and storage

Dulbecco's Modified Eagle Medium (DMEM; ThermoFisher, Paisley, UK) containing 4.5 g/L of glucose, 10% foetal bovine serum (FBS; GE Healthcare Bio-Sciences, Pasching, Austria), 1% L-glutamine and 1% pen-strep were used for routine cell culture. To prepare the culture medium, 50 ml of stock FBS was thawed overnight at 4 °C and added to 500 ml of DMEM along with 50,000 units of penicillin and 50 mg streptomycin (pen-strep; Sigma-aldrich, Suffolk, UK).

Temperature sensitive solutions were stored at 4 °C when not in use. Working aliquots of 50 ml were prepared as a precautionary measure to minimise the risk of contamination of the stock solutions as much as possible. All media solutions were equilibrated to 37 °C prior to use.

2.2.1.3 Maintenance

Cells were grown and maintained in a sterile, humidified incubator at 37 °C with 5% CO_2. T75 or T175 flasks were used to depending on the number of cells being cultured.

2.2.1.4 Passage

Cells were passaged using TrypLE Express Enzyme (ThermoFisher) which is a recombinant enzyme used widely to dissociate adherent cells. First, the medium was aspirated and discarded. Next, the cell monolayer was rinsed twice with phosphate-buffered saline, pH 7.4 (PBS; ThermoFisher) followed by 2 min incubation with 2 ml TrypLE at 37 °C. The flasks were gently tapped and checked for dissociation of cells under a light microscope and incubated for a further 1 min in TrypLE if they were found not to be fully dissociated. Once dissociated, the cells were collected in a 50ml Falcon tube using 20 ml of DMEM (4.5 g/L glucose) and centrifuged at 1400 revolutions/minute (RPM) for 5 min at 4 °C. The resulting pellet, after discarding the supernatant, was flicked gently and resuspended in 10 ml of medium before transferring into a T175 flask. A further 10ml of medium was used to rinse the original Falcon tube and added to the flask. Cell health was monitored daily and routinely passaged at 1:2 to 1:3 ratios every 4-5 days when, typically, 80-100% confluence was achieved.

2.2.1.5 Freezing and thawing

For freezing, cryopreservation medium with 50% DMEM, 40% FBS and 10% dimethylsulphoxide (DMSO; Sigma-aldrich) was prepared by adding 2 ml of FBS and 0.5 ml of DMSO to 2.5 ml of DMEM. Cells were dissociated from the flasks as described above. After centrifugation and complete removal of the supernatant, the cell pellet was resuspended in cryopreservation medium x 10 the volume of the cell pellet. The final cell suspension was transferred to a labelled cryovial, placed in a freezing container, Mr Frosty (ThermoFisher),

and frozen at -80 °C for 24 hours for controlled freezing at 1 °C/minute. For long-term storage, the cells were kept at -140 °C.

Cells were thawed in a water bath at 37 °C before being resuspended in 2 ml of medium and spun at 1400 RPM for 5 min at 4 °C. The supernatant was aspirated and plated in a flask corresponding to the number of cells being recovered.

2.2.1.6 Cell microscopy, counting and viability

Assessment of cell viability and death was carried out using Trypan Blue Staining Solution (Abcam, Cambridge, UK). In this method, dead cells are coloured as the stain penetrates through the cell membrane, a process that does not occur in viable cells. For every 25 µl of cell suspension solution, 25 µl of Tryphan Blue was added. Cell number was determined by manual counting of adherent cells using an Olympus microscope and haemocytometer. Images were captured with a 10X objective lens adapted with an Olympus camera.

2.2.1.7 Cell viability and effect of heat and glucose deprivation on NBAS deficient cells

Immunofluorescence of fibroblasts were carried out using 96 well glass-bottomed black plates. First, the total number of available cells in suspension was estimated by manual counting. Cells were then seeded to the wells at 500, 1000 and 2000 cells per well. The final volume of medium per well was adjusted to give a total volume of 200 µl. The assays were performed the next day, after the cells had sufficient time to adhere, using PrestoBlue Cell Viability Reagent (ThermoFisher) and a FLUOstar Omega plate reader (BMG Labtech, Aylesbury, UK). In this method, fluorescence is measured in relative fluorescence units (RFU) following the application of a redox-sensitive dye, resazurin. It is based on the principle of the reducing environment of viable cells that convert resazurin to a red-fluorescent colour. Twenty µl PrestoBlue was added to each well for 60 minutes and absorbance measured at 560 nm correcting for background. Each experiment was performed three times.

The cells were placed under *stress* by incubating them at 40 °C as well as removing glucose from the culture medium and their viability was measured. The results were expressed as relative fluorescence units (RFU) which correlates to the cell density within a culture plate well. Patient and control fibroblasts were incubated at 37 °C with glucose-containing medium for 24 hours and their cell viabilities measured as baseline. Then the incubation temperature was increased to 40 °C in half of the cell culture plates and the other half was maintained at 37 °C. The cell viabilities were remeasured after a further 24 hours (48 hours since plating). For the glucose deprivation experiments, the medium was exchanged with one that does not contain glucose whilst maintaining the incubation temperature at 37 °C.

2.2.1.8 Statistical analysis

Statistical analysis was performed using GraphPad Prism 8.4.3. P values were considered significant when <0.05.

Kruskal-Wallis test was used for the comparison of cell viability of each cell line against the others which involved the use of three or more data sets, not normally distributed.

2.2.1.9 Protein isolation from fibroblasts

Cells cultured for the purpose of protein isolation were cultured in 10cm petri dishes. Once the cultures were established, the cells were removed non-enzymatically, working quickly on ice to minimise the risk of disruption of the target molecule. First, the cells were scraped off the petri dishes in the culture medium and transferred to a 50 ml falcon tube followed by a wash using 5 ml of ice-cold PBS. The cells were then centrifuged at 1400 RPM for 5 min at 4 °C and the supernatant was removed. The resulting pellet was flicked gently and resuspended in 500 µl of PBS, twice, and transferred to cryovials. These were spun down at 12,000g for 5 min at 4 °C and the supernatant was removed. The cell pellets were then diluted with 2 to 3X volume of lysis buffer and pipetted vigorously and left for 10 mins. The resultant lysate was frozen at -80 °C.

2.2.1.10 Protein quantification

Protein concentrations were measured using BCA protein assay (Bio-Rad Laboratories, Hemel Hempstead, UK) and bovine serum albumin (BSA) protein standards, serially, diluted in water (0.25 mg/ml, 0.5 mg/ ml, 1 mg/ml, 2 mg/ml, 4 mg/ml, 6 mg/ml, 8 mg/ml and 10 mg/ml). In a 96-well plate, 1 µl of each BSA standard was loaded in duplicates and 1 µl patient sample in triplicates. Then 200 µl of alkaline copper regent was added in each well and mixed using a microplate shaker before incubating for 30 minutes at 37 °C. The absorbance of the standards and samples were measured at 562 nm using a FLUOstar Omega plate reader. The standard curve generated from the BSA was used to interpolate sample concentrations whilst correcting for the background, lysis buffer readings.

2.2.2 Western blot

2.2.2.1 Sample preparation

The concentrations of the quantified proteins were adjusted to 1 mg/ml. The loading buffer was prepared using 0.4 M sodium dodecyl sulphate (SDS), 1 M Tris(hydoxymethyl)aminomethane-hydrochloric acid (Tris-HCl), pH 6.8, 25% glycerol, 0.15 M bromophenol blue and 20% β-mercaptoethanol, the latter of which was added fresh prior to use. Ten to 15 µg of each sample was mixed with 5X loading buffer and boiled at 100 °C for 5 minutes. The samples, once cooled on ice, were ready for loading on to the electrophoretic gel.

2.2.2.2 Electrophoresis

The proteins were resolved by SDS-polyacrylamide gel electrophoresis (PAGE), using Any kD Mini-Protean TGX precast 4-12 % gels (Bio-Rad). The gels were fitted onto the inner chamber of a running tank (Bio-Rad). The inner and outer chambers were filled with running buffer made of 5X 20 % Tris-Glycine. Then the combs were removed and the exposed wells were washed with running buffer. Ten µl of Precision Plus Protein Dual Color Standards (Bio-Rad) was loaded along with the samples. The samples were electrophoresed at 100 Volts (V) usually for 2 hours when the protein markers reached the bottom of the gel.

2.2.2.3 Protein transfer

Once the proteins were separated by gel electrophoresis, the gels were removed from the inner chamber. The Trans-Blot Turbo Nitrocellulose Transfer Pack and Transfer System (both Bio-Rad) were then used for the transfer of proteins. The transfer pack is composed of blotting papers, a nitrocellulose membrane and a sponge soaked in a buffer. This system supplies an electric current allowing transfer of proteins from negative to positive electrode in a matter of minutes.

2.2.2.4 Immunoblotting

Blocking of the background proteins to prevent non-specific binding of the antibody was carried out by mixing the blotting membrane in a solution containing 3 % fat free milk, in 4% tris-buffered saline (TBS) and 0.1% Tween-20 (TBST; Sigma-aldrich) for 30 minutes. For the primary immunoblotting 3 anti-NBAS antibodies were used (Table 2-4). The primary anti-NBAS antibody in 3% milk in TBST was added to a 50 ml falcon tube containing the blotting membrane. This was incubated overnight at 4 °C under constant rocking. After 18-24 hours, the blotting membrane was equilibrated to room temperature before washing it in TBST three times to remove any excess antibodies. The secondary antibody and anti-rabbit IgG horseradish peroxidase (HRP) were then added and incubated for 1.5 hours at room temperature. The membrane was then washed 3 times for 10 minutes with TBST then 2 times with TBS. Visualisation of the membrane was performed using the Clarity Max Western ECL Substrate and a ChemiDoc XRS+ System (both Bio-Rad) located in the Institute of Hepatology, London. The membrane was incubated with the enhanced chemiluminescence detection reagents or 5 minutes before being exposed to X-rays. The exposure time was 10 to 70 seconds whilst digital images were acquired.

Antibody name	**Product number**	**Epitope**	**Primary antibody dilution**	**Secondary antibody dilution**

Anti-NBAS Rabbit Polyclonal	HPA036817-100 UL (Atlas Antibodies)	Residue 961-1047	1 : 2,000	1 : 40,000
Anti-NBAS Rabbit Polyclonal	DF9686-BP (Affiniti)	Unspecified	1 : 2,000	1 : 40,000
Anti-NBAS Rabbit Polyclonal	A305-636A-M (Bethyl Laboratories)	Residue 350-400	1 : 1,000	1 : 40,000

Table 2-4 Antibodies and dilutions used in western blot.

2.2.3 Polymerase chain reaction

Polymerase chain reaction was used to amplify DNA for Sanger sequencing. The volumes and concentrations of reagents used are specified below (Table 2-5).

	Volume (µl)	Concentration
5X Fast start buffer	2	1 X
Fast start GC buffer	4	1 X
Fast start Taq (5 U/µl)	0.25	1.25 U
Forward and reverse primers (10 µM)	1	1 µM
Sterile water	9.35	
DNA (50 ng/µl)	2	2.5 ng/µl

Table 2-5 Volume and concentration of reagents used for the PCR reaction.

The reagents were mixed and 18 µl aliquoted in in a 96-well PCR plate. Two µl of DNA (concentration 50 ng/µl) was added to make a final reaction volume of 20 µl. The thermal cycling conditions below were used (Table 2-6). Once finished the PCR plate was stored in the fridge.

Step	Temperature	Time
1	96°C	8 minutes
2	96°C	1 minutes
3	50-60°C	20 seconds
4	72°C	30 seconds
5	Repeat from Step 2 to Step 4 for 35 times	
6	72°C	7 minutes
Hold	4°C	∞

Table 2-6 Thermal cycling conditions for the PCR reaction.

2.2.3.1 Agarose gel electrophoresis

Agarose gel electrophoresis was used to check the abundance and specificity of the PCR products after amplification. One and a half grams of agarose (Helena Bioscience) was melted in 100ml of 1X tris-acetate-EDTA (TAE) buffer and the molten agarose was left to cool. One µl of Nancy-520 (Merck) was added to fluorescently stain dsDNA visible under UV light. The gel was left to cool in a mould with combs. DNA samples were mixed with 6X loading dye (Life technologies) and ran for approximately 20 minutes at 260 V. The agarose gel was then imaged with 2UV Benchtop trans illuminator.

2.2.4 Sanger sequencing

Sanger sequencing is a DNA sequencing technology developed in the 1970s by Fred Sanger and colleagues and considered the first efficient, genetic sequencing methodology. It relies on the selective incorporation of chain-terminating dideoxynucleotides (ddNTPs; ddA, ddC, ddG and ddT) producing partially replicated DNA strands. The terminators are now fluorescently labelled. The amplicons of different sizes with ddNTPs at the 3' end is then passed through a polyacrylamide gel capillary to separate the DNA strands by electrophoresis.

Each ddNTP fluorescent dye is then laser detected using a camera. A chromatograph is reconstructed and analysed using a specific software.

Sanger sequencing was employed to sequence *GADD45A* and *GADD45B* PCR products before qPCR due to previously unsuccessful qPCR attempts and to check the primers were sequencing the correct amplicon (APPENDIX C). Successful Sanger sequencing requires the removal of excess buffers, nucleotides, salts, primers and enzymes which can interfere with the sequencing reaction. This was done using 27µl of AMPure XP beads which was added to the plate with the PCR products and pipetted up and down 10 times. The plate was incubated for 5 minutes before placing the plate in a DynaMag-96 Side Magnet for 10 minutes until the solutions became clear. Whilst keeping the plate in the magnet holder the supernatant from each well was discarded and the undisturbed beads washed with 100 µl 70% ethanol to remove any impurities. The beads were air dried in the plate for 10 minutes before being eluted with 30 µl of High Performance Liquid Chromatography (HPLC) water.

For the sanger sequencing set up, Big Dye Terminator v3.1 (Life Technologies) and Big Dye Terminator v3.1 sequencing buffer (Life Technologies) were used
Table 2-7). Using a 96 well sequencing plate 8 µl of sequencing reaction was mixed with 2 µl of PCR product. This was then amplified by PCR (Table 2-8).

	Volume (µl)	Final concentration
BigDye Terminator v3.1 2.5X	1	0.25X
BigDye Terminator v3.1 sequencing buffer 5X	1.5	1.5X
Forward or reverse primer (10 µM)	1	1 µM
Sterile water	4.5	

Table 2-7 Volume and concentration of reagents used for Sanger sequencing.

Step	Temperature	Time
1	96°C	5 minutes
2	96°C	1 minutes

3	54°C	20 seconds
4	60°C	30 seconds
5	Repeat from Step 2 to Step 4 for 40 times	
6	60°C	5 minutes
Hold	4°C	∞

Table 2-8 Thermal cycling conditions for the PCR reaction.

The sequencing products must be purified prior to running on the sequencer. This was carried out using the BigDye XTerminator Purification Kit which incorporates XTerminator Solution for scavenging unincorporated dye terminators and SAM Solution which stabilises the post-purification reactions. For each reaction, 11 µl of BigDye XTerminator and 49.5 µl XTerminator Solution were used. The plate was then placed on a plate shaker for 30 minutes at a speed of 1800 rpm and centrifuged at 1000 rpm for 2 minutes.

The plate was loaded on to an ABI Prism 3730xl Genetic Analyzer (Life Technologies) located in the Liver Virology Department, KCH. The ABI Prism Sequencing Analyzer software was used to analyse the sequences on chromatograms depicted by 4 colour peaks representing each base (adenine = green, cytosine = blue, guanine = black, thymine = red). Mutation Surveyor (SoftGenetics, Pennsylvania, USA) was used to compare the sample sequence trace to reference.

2.2.5 RNA isolation from cultured cells

The role of *NBAS* in NMD was evaluated by relative quantification of *GADD45A* and *GADD45B*, two of several genes that are directly regulated by NMD. Firstly, cells were cultured as described in section 2.2.1. Total RNA using TRIzol Reagents (Thermofisher) was isolated from cultured fibroblasts from patients NBAS1 and NBAS2 (Table 2-3) and from control fibroblasts. First, the cells were removed from the culture plate and spun down to form a pellet as described in section 2.2.1.4. One ml of TRIzol was used to lyse and homogenise approximately, 10,000,000 cells. The sample was incubated for 5 minutes to allow complete dissociation of

the nucleoproteins complex. Then 0.2 mL of chloroform per 1 mL of TRIzol was added and thoroughly mixed and incubated for 2-3 minutes. The sample was centrifuged for 15 minutes at 12,000g at 4 °C. The mixture separates into a lower red phenol-chloroform, an interphase, and a colourless upper aqueous phase. The upper aqueous phase containing the RNA was pipetted out. For the precipitation of RNA, for every 1 mL of TRIzol, 0.5 mL of isopropanol was added and incubated for 10 minutes at 4 °C. Following centrifugation for 10 minutes at 12,000g at 4 °C the RNA precipitate forms a white gel-like pellet at the bottom of the tube. The RNA pellet was then washed in 1 mL of 75% ethanol per 1 mL of TRIzol and resuspended in 20-50 µl of RNase-free water (Thermofisher) before incubating on a heat block set at 55 °C for 10 minutes. The RNA solution was temporarily stored on ice for quantity and quality controls using the Qubit 2.0 Fluorometer and Agilent 2200 TapeStation system (described previously in sections 2.1.2.1 and 2.1.2.4, respectively). The RNA integrity is represented below (Figure 2-4).

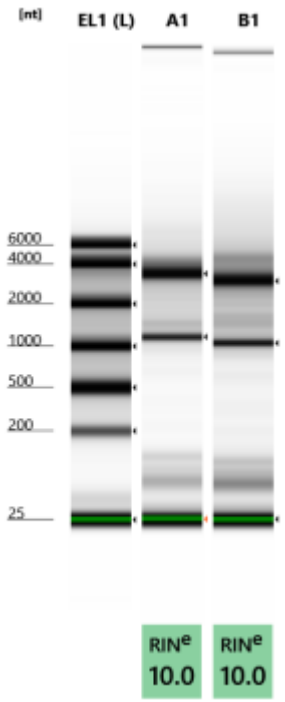

Figure 2-4 RNA integrity number (RIN) of RNA extracted from HFF1 (A1) and NBAS1 (B1) alongside an electronic ladder (EL1).
The image shows electrophoretic separation of RNA across a gel. The higher and lower bands represent the ribosomal subunits 28S and 18S, respectively. The quality of RNA is represented by the RIN number on a scale of 1 to 10 where a high RIN indicates highly intact RNA. The RIN number is calculated based on the ratio of the 28S and 18S peaks and any presence of degraded material.

2.2.5.1 DNase treatment

DNase I is an endonuclease that digests DNA. Treatment with recombinant DNase (ThermoFisher) was incorporated to deplete genomic DNA that could later interfere with the qPCR step. Five µg of RNA was dissolved in 25 µl of RNase free water and the tube flicked gently. Twenty-five µl of 10X reaction buffer and 5 µl of DNase enzyme was added. The final volume was made up to 50 µl with nuclease free water (ThermoFisher) and incubated at 37 °C for 30 minutes at the thermoshaker with flicking of the tubes at 5-minute intervals. After incubation, the DNase was inactivated by adding 2.5 of DNase Inactivation Agent and the tubes flicked gently. This was incubated at room temperature for 2 minutes. The tubes were centrifuged at 10,000g for 1.5 minutes and the supernatant transferred.

2.2.6 Reverse transcription

The ThermoFisher High-Capacity RNA-to-cDNA Kit was used to synthesise first strand cDNA from the RNA isolated from NBAS1, 2 and control cells. Ten µl of the RT Buffer Mix containing dNTPs and RT random primers, 1 µl of RT Enzyme Mix containing MultiScribe Reverse Transcriptase and up to 9 µl of DNase-treated RNA were added to a PCR plate (ThermoFisher). The final reaction volume was made up to 20 µl by adding nuclease free water (Table 2-9). The reaction was incubated at 37 °C for 60 minutes and stopped by heating to 95 °C for 5 minutes using thermal cycler.

Component	**Volume per reaction**	
	+RT reaction	**-RT control**
2X RT buffer	10 µl	10 µl
20X RT enzyme mix	1 µl	-
RNA sample	Up to 9 µl	Up to µl
Nuclease-free water	Q.S. to 20 µl	Q.S. to 20 µl
Total per reaction	20 µl	20 µl

Table 2-9 Reverse transcription protocol.

2.2.7 Quantitative PCR of *GADD45A* and *GADD45B*

Primer sequences for the qPCR of *GADD45A* and *GADD45B* designed to amplify mRNA and pre-mRNA were obtained from a previous publication below (APPENDIX C) (Kurosaki et al., 2014). BLAST was used to check the primer sequences using the reference sequence ENST00000370986.9 for *GADD45A* and ENST00000215631.9 for *GADD45B* (www.ensembl.org). For the amplification of mRNA, primer sequences were checked to ensure they spanned across exon-exon junctions and, therefore, will only amplify mRNA and not pre-mRNA. For the amplification of pre-mRNA, the primers were checked to ensure that at least one was within an intron. Consideration was also given to the annealing temperature (range of 60-65°C), GC content (40-60%) and the formation of self-complementary dimers or primer-dimer. The primers were purchased from Sigma-aldrich. To verify that these primers amplified cDNA by PCR, the synthesised PCR products were run on a 1.5% agarose gel as described previously.

Quantitative PCR on cDNA from NBAS1, 2 and control cells were carried out using Power SYBR Green PCR Master Mix (ThermoFisher). The cDNA samples were mixed with primers at a concentration of 0.2 μM and 2X SYBR Green diluted to a volume of 25 μl with RNAse free water (Table 2-10). They were then aliquoted to black, 96 well plates (ThermoFisher) in technical triplicates.

Component	**Volume per well**
2X Power SYBR Green PCR Master Mix	12.5 μl
Nuclease-free water	7.2 μl
Forward Primer	0.15 μl
Reverse Primer	0.15 μl
Sample (cDNA)	5 μl
Total per reaction	25 μl

Table 2-10 Two-step quantitative reverse-transcription protocol.

The plate was loaded on to a Step-One Plus Real-Time PCR System (Thermofisher) with the run protocol illustrated below (Table 2-11). For every plate run, a negative control was added where cDNA was replaced with water. Glyceraldehyde 3-phosphate dehydrogenase (GAPDH) expression was also determined for additional information. To check for the specificity of the PCR amplicon, a melt curve was produced for every plate run plotting fluorescence against a function of temperature. The experiment was performed triplicates and their averages calculated.

Step	Temperature	Time	Cycles
First denaturation	95 °C	10 minutes	1
Denaturation Annealing	95 °C 60 °C	15 seconds 60 seconds	40
Hold	4 °C	Until needed	1

Table 2-11 qPCR run module on the Step-One plus.

The expression of *GADD45A* and *GADD45B* mRNA relative to pre-mRNA was determined using the comparative Cr (ΔΔCt) method as previously described in section 2.1.5.

3 RESULTS

3.1 Targeted NGS of children with indeterminate ALF

A targeted NGS method, as described in section 2.1.2 was used for the detection of causative variants. Multiplex sequencing can be performed simultaneously for up to 16 samples per lane of flow cell. Therefore, three separate runs were carried out to sequence 41 samples: 16 in the first run, 15 in the second and 10 in the final.

3.1.1 Quality of NGS

The quality of sequencing is determined by accuracy of each step of the sequencing process including library preparation, base calling, read alignment, and variant calling. The coverage describes the number of reads that align to or "cover" a particular base position. More confidence to the base call is given at higher levels of coverage. For the three runs performed the fraction of targets with coverage of at least 30 was >99.0%.

3.1.2 Description of the 41 children with ALF

The full cohort for the study consisted of 41 children (23 boys) from 41 families. They were primarily of European ancestry: United Kingdom (20 children), Middle East (6 children), Africa (5 children), Asian (4 children) and other (6 children). Consanguinity, defined by a relation of second cousins or closer, was observed in 4 families but none had a family history of ALF. The median age of the children at diagnosis was 2.5 years (minimum, 7 days and maximum, 8.6 years).

3.1.3 Results of variant prioritisation

Data was annotated using the CLC Genomics Workbench version *12.0*. *CLC bio* as described previously in section 2.1.3.2. Subsequently, variants of interest were filtered and prioritised according to the strategy described in section 2.1.4.

A total of 17,452 variants were detected in this cohort. After the above filtering strategy was applied, a total of 69 prioritised variants (29 children) were identified in 40 genes (Table 3-1) (Figure 3-1).

Filtering rationale	Number of variants
Total unfiltered variants	17,452
< 1% MAF (or novel) and nonsynonymous	69
Biallelic	9

Table 3-1 Number of variants filtered after each step of prioritisation process.
A total of 17,452 variants were identified amongst the 41 study patients. Sixty-one variants were identified after filtering using a MAF cut-off of 1 % and removing nonsynonymous variants. Amongst these variants 9 were biallelic.

Amongst these prioritised variants 9 biallelic variants, including a child with a CNV, were identified in 8 children: *NBAS* (3 children); *TWNK* (1 child); *CPT1A* (1 child); *SUCLG1* and *POLG* (1 child); *MPV17* (1 child); *DLD* (1 child) (Table 3-2). Further details regarding their genetic and clinical information are described in section 3.1.4.

In addition, 60 monoallelic variants were identified in 27 children: 48 missense (24 children), 2 deletion, 1 duplication, 1 nonsense and 8 splice site. In addition, CNVs (all monoallelic) were identified in 2 children (Table 3-3). With this information, further interrogation seeking a second pathogenic variant was carried out but was unrevealing.

ID	Sex	Age at presentation	Clinical	Gene	Genotype	Protein	MAF	CADD / Pathogenicity	Classification	LT	Outcome	Age at last visit
1	F	1 m	x1 ALF	*DLD*	c.826A>T	p.Thr276Ser	5.42E-04	25	Uncertain	Yes	Alive	15 y
					c.911T>C	p.Ile304Thr	1.57E-04	26	Uncertain			
3	M	6 m	Recurrent ALF	*NBAS*	c.4731_4733dup	p.Tyr1578dup	Not reported	*Pathogenicity likely*	Likely pathogenic	Yes	Lost to follow up	
8	M	2 m	x1 ALF	*TWINK*	c.1471C>G	p.Ser491Thr	3.99E-06	24	Uncertain	Yes	Alive; NDD	7 y
					c.1697A>G	p.Lys566Arg	4.00E-03	22	Uncertain			
9	M	6 m	Recurrent ALF	*NBAS*	c.exons 17-19 dup	p.?	Not reported	*Pathogenicity likely*	Likely pathogenic	No	Alive	7 y
12	M	3 y	x1 ALF	*NBAS*	c.1702G>A	p.Val568Ile	0.0012	15	Uncertain	No	Alive	16 y
					c.191G>A	p.Arg64His	6.30E-05	19	Uncertain			
17	M	18 m	x1 ALF	*MPV17*	c.338C>T	p.Pro98Leu	5.31E-05	25	Pathogenic	Yes	Alive; NDD	20 y
18	M	17 m	x1 ALF	*SUCLG1*	c.601A>G	p.Arg201Gly	1.99E-05	30	Likely pathogenic	Yes	Alive; cardiomyopathy	17 y
					c.236G>A	p.Gly79Asp	0.0013	27	Uncertain			
				POLG	c.153_158delGCAGCA	p.Gln54_Gln55del	0.0036	*	Uncertain			
					c.803G>C	p.Gly268Ala	0.0039	27	Uncertain			
19	M	2 y	x1 ALF	*CPT1A*	c.2198A>G	p.Asn733Ser	0.0018	16	Uncertain	No	Alive	10 y

MAF, minor allele frequency; LT, liver transplantation; NA, not applicable; NDD, neurodevelopmental delay; Pat, patient; * Polyglutamine tract expansion

Table 3-2 Summary of patients found to have biallelic, rare, non-synonymous variants.
Nine biallelic variants including a child with a CNV were identified in 8 children in 7 genes.

ID	Sex	Age at presentation	Clinical	Gene	Zygosity	Genotype	Protein	MAF	CADD / Pathogenicity	LT	Outcome	Age at last visit
Pat 1	F	1 m	x1 ALF	*ALG8*	Het	c.1090C>T	p.Arg364*	6.36-E4	*Pathogenicity likely*	Yes	Alive	15 y
Pat 2	M	1 y	x1 ALF	*NPC2*	Het	c.441+1G>A	p.?	0.0038	*Pathogenicity likely*	Yes	Alive	16 y
Pat 4	M	1 y	x1 ALF	*CPT2*	Het	c.877A>G	p.Ser293Gly	1.23E-04	22	Yes	Alive	11 y
				ACADM		c.362C>T	p.Thr125Ile	1.19E-05	30			
Pat 5	M	3 y	x1 ALF	*DBT*	Het	c.1051G>C	p.Glu351Gln	7.45E-04	21	Yes	Alive	4 y
Pat 6	M	8 y	x1 ALF	*TSFM*	Het	c.797T>A	p.Leu287His	2.36E-04	26	No	Alive	23 y
				MPI		c.1049C>T	p.Thr350Met	0.0018	17			
				SCO1		c.167G>A	p.Gly56Gln	0.0015	13			
				GALE		c.140A>C	p.Gln47Ala	4.98-E4	28			
				ETFB		c.278_279insC	p.Pro94Thrfs*8	0.0033	*Likely benign*			
Pat 7	M	1 y	x1 ALF	*CPT1A*	Het	c.173G>A	p.Ser58Ala	7.98E-06	22	No	Alive	14y
Pat 8	M	2 m	x1 ALF	*HADHA*	Het	c.1072C>A	p.Gln358Lys	8.10E-03	19	Yes	Alive	7 y
				TALDO1		c.962A>G	p.Lys321Arg	0.0067	27			
				TSFM		c.5C>T	p.Ser2Leu	0.0015	26			
				ACAD		c.*5G>A	p.?	0.0077	*Likely benign*			
Pat 9	M	6 m	Recurrent ALF	*LIPA*	Het	c.539-5C>A	p.?	0.0034	*Likely benign*	Yes	Alive	7 y
Pat 10	M	1 y	x1 ALF	*SMPD1*	Het	c.1460C>T	p.Ala487Val	6.44E-04	21	Yes	Alive	9 y
Pat 13	M	6 y	x1 ALF	*GALE*	Het	c.997C>A	p.Leu333Ile	1.87E-04	19	Yes	Alive	16 y
				TWNK		c.737A>G	p.Asp246Asn	*Not reported*	26			
				FAH		c.466C>T	p.Pro156Ser	3.98E-05	26			

				POLG		c.2492A>G	p.Tyr831Cys	6.75E-04	23			
Pat 14	F	5 y	x1 ALF	*HADHA*	Het	c.1491G>A	p.Met497Ile	1.41E-04	29	Yes	Alive	16 y
				LIPA		c.539-5C>A	p?	3.89E-04	*Likely benign*			
Pat 15	F	4 y	x1 ALF	*ACADVL*	Het	c.1534C>T	p.Arg535Trp	4.79E-04	26	Yes	Alive	15 y
				TRMU		c.442G>A	p.Glu148Lys	9.62-E4	17			
				POLG		c.1515C>A	p.Gly517Val	4.71-E5	14			
				FAH		c.1180+4A>G	p.?	0.0153	*Likely benign*			
Pat 16	M	2 m	x1 ALF	*CPT2*	Het	c.1598T>A	p.Val533Asp	0.0032	16	Yes	Alive	15 y
				DBT		c.506G>A	p.Arg169Gly	0.0012	18			
				EIF2AK3		c.1264G>A	p.Arg422Ser	3.40E-04	20			
				SLC22A5		c.59T>A	p.Leu20His	0.0125	24			
				ACADVL		c.264C>T	p.Pro88Leu	0.0109	16			
Pat 17	M	1 y	x1 ALF	*ACAD9*	Het	c.1232C>T	p.Pro411Leu	3.53E-04	23	Yes	Alive	20 y
				NPC2		c.465delT	p.His156Thrfs *5	8.57-E05	*Pathogenicity likely*			
				BCKDHA		c.376-4C>T	p.?	0.0033	*Likely benign*			
				MPV17		c.293C>T	p.Pro98Leu	5.31E-04	26			
Pat 18	M	1 y	x1 ALF	*NBAS*	Het	c.1093G>C	p.Asp365His	0.0078	27	Yes	Alive	17 y
				SUCLG1		c.601A>G	p.Arg201Gly	1.99E-04	29			
				POLG		c.803G>C	p.Gly268Ala	0.0034	26			
Pat 19	M	2 y	x1 ALF	*SCO1*	Het	c.16C>G	p.Leu6Val	0.0036	16	Yes	Alive	10 y
Pat 20	M	2 y	x1 ALF	*EIF2AK3*	Het	c.1264G>T	p.Ala422Ser	3.98E-05	17	No	Dead	NA
				SLC22A5		c.1645C>T	p.Pro549Ser	0.0074	18			
				ASL		c.34T>C	p.Tyr12His	1.20E-04	31			
				LIPA		c.1046A>G	p.Asp349Gly	0.068	24			
				POLG		c.128A>G	p.Gly43Arg	0.00629	16			

Pat 21	M	2 y	x1 ALF	*FARS2*	Het	c.737C>T	p.Thr246Met	0.0041	23	Yes	Alive	11 y
Pat 26	M	2 y	x1 ALF	*HMGCL*	Het	c.208G>C	p.Val70Leu	7.07E-05	26	No	Alive	12 y
				ACADS		c.40C>G	p.Arg14Gln	1.23E-04	18			
Pat 30	M	2 y	x1 ALF	*HAHDA*	Het	c.1072C>A	p.Gln358Lys	0.0078	19	Yes	Alive	18 y
Pat 31	F	1 m	x1 ALF	*ACADS*	Het	c.509C>T	p.Ala170Val	8.00E-05	25	No	Alive	15 y
Pat 35	F	11 m	x1 ALF	*GFM1*	Het	c.1506G>A	p.Glu502Lys	4.10E-06	32	Yes	Dead	NA
				LARS1		c.3077A>G	p.Tyr1026Cys	0.0039	30			
				POLG		c.1550G>T	p.Gly517Val	0.0047	14			
Pat 36	M	8 y	x1 ALF	*HMGCS2*	Het	c.907C>T	p.Pro303Ser	3.18E-04	25	Yes	Alive	21 y
				CPT1A		967+3G>A	p.?	0.0031	*Likely benign*			
Pat 37	F	1 m	x1 ALF	*GFM1*	Het	c.568A>C	p.Met190Leu	0.0016	17	No	Alive	5 y
				ASS		c.766G>A	p.Gly256Lys	0.0029	23			
Pat 39	F	3 y	x1 ALF	*SMPD1*	Het	c.872G>A	p.Arg291His	0.0011	25	Yes	Alive	8 y
Pat 40	F	2 y	x1 ALF	*GALT*	Het	c.611G>A	p.Arg204Gln	6.36-E4	22	Yes	Alive	18 y

Hom, homozygous; het, heterozygous; LT, liver transplantation; MAF, minor allele frequency; NA, not applicable; NDD, neurodevelopmental delay; Pat, patient; * Polyglutamine tract expansion

Table 3-3 All prioritised, monoallelic missense, nonsense, insertion, deletion and splice site variants identified from the study cohort.
Patients were considered to be not affected by the conditions related to these genes given a second variant was not identified.

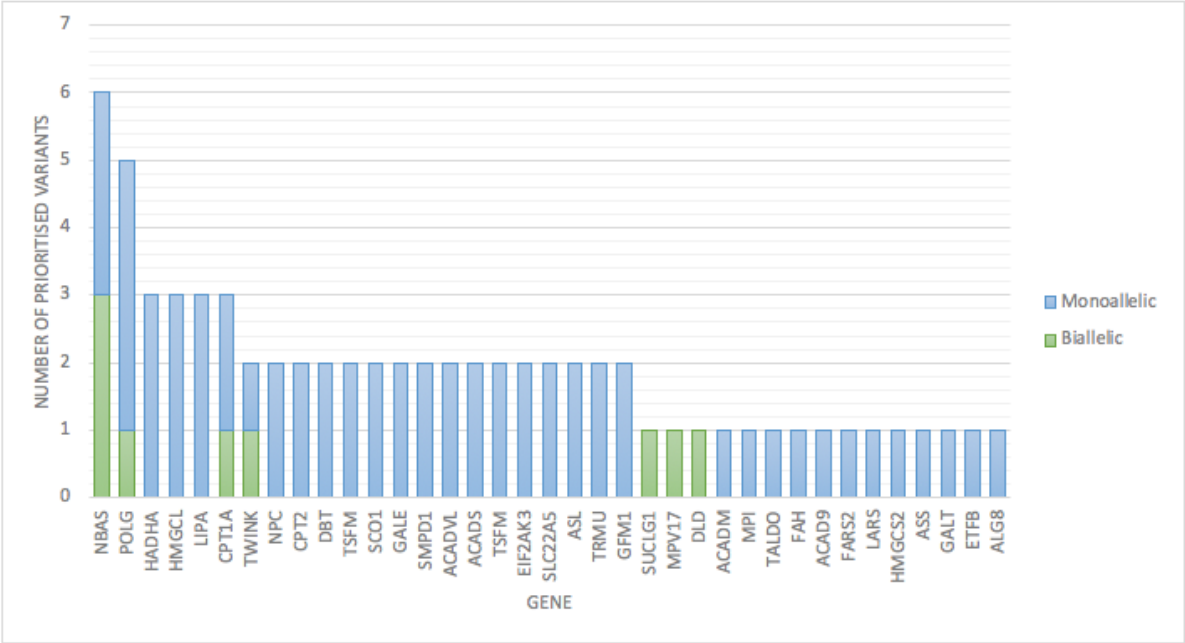

Figure 3-1 Bar chart representing all 69 prioritised variants in 29 children in 40 genes.
Variants in *NBAS* and nuclear genes encoding mitochondrial proteins were the most common findings.

3.1.4 Description of children with biallelic variants after prioritisation

3.1.4.1 Children with biallelic variants prioritised in *NBAS*

Three children were identified with biallelic variants prioritised in *NBAS* warranting further evaluation.

Patient #3

A 6-month-old boy was referred with history of recurrent ALF associated with intercurrent infections. He was born to consanguineous parents (1st cousins) of Middle Eastern origin and showed signs of motor developmental delay at presentation. He suffered from repeated episodes of ALF associated with hyperammonaemia, hypoglycaemia and lactic acidosis. Despite extensive investigations looking for metabolic causes a diagnosis was not made. Liver

transplantation was offered to avoid further episodes of ALF but the family returned to their country of origin when the child was 2 years and 2 months old.

A homozygous duplication was identified in *NBAS*: c.4731_4733dup, p.Tyr1578dup which results in an inframe insertion of a tyrosine (PVS1). The amino acid position is highly conserved and a duplication of tyrosine at 1578 has not been observed in population databases confirming that it is a rare variant (PM2). The classification of this variant is likely pathogenic supports a genetic diagnosis of the child's phenotype.

Patient #9

A 6-month-old boy, born to non-consanguineous parents from Southeast Asia presented with fever associated with adenovirus infection and was found to be in ALF. He was admitted to the paediatric intensive care unit for cardiorespiratory support, haemofiltration and was urgently listed for LT. He underwent transplantation with alginate microbead-encapsulated hepatocytes and delisted for LT 72 hours later. He suffered from recurrent ALF associated with intercurrent illnesses at 2 years and 5 months of age (parainfluenza) and 2 years and 7 months of age (influenza A) before undergoing LT. He does not have any signs of systemic disease nor graft dysfunction at the last follow up at 7 years.

A CNV ratio of 2 was identified for exons 17 – 19 in *NBAS,* which was confirmed by qPCR. Quantitative PCR spanning the same region on the healthy parents' DNA revealed a CNV ratio of 1.5 for each parent demonstrating their heterozygous status. Altogether, this provides evidence for the likelihood that the child has a duplication of exons 17 – 19 on each chromosome. If the duplication is in tandem, this is likely to alter the protein structure and function (PVS1), despite the total nucleotide length of exons 17 – 19 is 372 (divisible by 3, therefore, does not alter the reading frame). A CNV in *NBAS* has not been observed in population databases (PM2) nor reported previously in affected individuals. The classification of this variant is likely pathogenic and supports a genetic diagnosis of the child's phenotype.

Patient #12

A 3-year-old boy presented with vomiting, fever, hypoglycaemia and was found to be in ALF. The patient recovered but a diagnosis was not reached despite extensive metabolic work up. A liver biopsy was carried out at 12 years and 9 months of age showing diffuse macro- and micro-vesicular steatosis with mild lobular inflammation and periportal fibrosis. He does not have any signs of systemic disease, liver function tests are mildly elevated and the liver is fatty, at the last follow up at 16 years of age.

Compound heterozygous missense variants were identified in *NBAS*: c.191G>A, p.Arg64His; and c.1702G>A, p.Val568Ile. The arginine at position 64 and valine at position 568 are not conserved across species. They have been observed in populations databases at a frequency of 0.0012 (4 homozygotes; BS1) and $6.30e^{4}$ (0 homozygotes; PM2), respectively. *In silico* prediction using CADD were, 15 and 19, and PolyPhen-2, *benign* (BP4) for both variants. In the absence of further evidence, the classification of these variants are uncertain but may be part of the explanation of his milder phenotype.

3.1.4.2 Five children with biallelic variants after prioritisation in *TWNK*, *CPT1A, SUCLG1*, *POLG, MPV17* and *DLD*

Patient #8

A 10-week-old boy with a history of neonatal group B streptococcus infection presented with bleeding, icterus and hepatosplenomegaly. At presentation, he was coagulopathic but the international normalised ratio (INR) improved to 1.6 with treatment for sepsis. However, further deterioration lead to LT 6 weeks after initial the presentation and, intraoperatively, he underwent muscle and liver biopsies. The muscle respiratory chain enzymology demonstrated decreased respiratory chain complex IV activity of 0.006 relative to citrate synthase (reference range 0.014 – 0.034). Molecular genetic analysis of muscle and liver also showed evidence of DNA depletion: 19% and 33% of mean normal levels, respectively. However, subsequent molecular genetic testing for mitochondrial DNA maintenance disorders (*POLG*, *DGUOK*, *MPV17* and *TRMU*) did not identify any pathogenic variants. The child is now 7 years old and attends mainstream school although requires extra speech and language support and has been diagnosed with adrenal insufficiency and hyperinsulinism.

Compound heterozygous, missense variants were identified in *TWNK*: c.1471C>G, p.Ser491Thr; and c.1697A>G, p.Lys566Arg. These variants have been observed in populations databases at a frequency of $3.99e^{6}$ (PM2) and 0.004 (BS1), respectively, but have not been reported in a homozygous state. *In silico* prediction using CADD were, 24 and 22, respectively, and PolyPhen-2, *benign* (BP4) for both variants. They have not been previously reported to cause disease. In the absence of further evidence, the classification of these variants are uncertain but may be clinically significant given the child's phenotype.

Patient #19

A 2-year-old boy with a past medical history of achalasia was admitted with vomiting and fever and was found to be in ALF. Metabolic work up at the time was negative including repeated acylcarnitine profiles and respiratory chain enzymology from muscle which was within normal range. The patient is now 22 years old after being discharged at 10 years of age with no further episodes of ALF.

A homozygous missense variant was identified in *CPT1A*: c.2198A>G, p.Asn733Ser. This variant has been observed in populations databases at a frequency of 0.0018 (3 homozygotes; BS1). *In silico* prediction using CADD was 16, and PolyPhen-2, *benign* (BP4). They have not been previously reported to cause disease. In the absence of further evidence the classification of these variants are uncertain and may / may not be clinically significant

Patient #18

A 17-month-old, previously healthy boy presented with jaundice and lethargy. He was found to be in ALF and underwent auxiliary LT. His native liver fully recovered and immunosuppression was stopped when he was 5 years old. The child is now 17 years old and there have been no reported problems other than mild left ventricular hypertrophy.

Compound heterozygous missense variants were identified in two genes, *SUCLG1* and *POLG*. The variants in *SUCLG1* were c.601A>G, p.Arg201Gly; and c.236G>A, p.Gly79Asp. They have

been observed in population databases at a frequency of $1.99e^{5}$ (PM2) and 0.0014 (PM2), respectively, and neither in homozygous state. *In silico* prediction using CADD were, 30 and 27, respectively and PolyPhen-2, *probably damaging* (PP3), for both variants. The c.601A>G variant has been reported in the literature, with a second variant, in an infant diagnosed with MDS-9 (Chen et al., 2022) (PS4) and the c.236G>A variant in heterozygous state in a child with autism and MDS (Varga et al., 2018) (PM3). The classification of these variants are likely pathogenic and uncertain, respectively, providing a likely explanation of the child's phenotype.

The variants in *POLG* were c.153_158delGCAGCA, p.Gln54_Gln55del; and c.803G>C, p.Gly268Ala. The first variant is a highly polymorphic CAG-repeat encoding a polyglutamine tract (poly-Q) in the N-terminus. Most commonly the poly-Q tract comprises 10 repeats (10Q, frequency >80%) which has been reported to be associated with Parkinson's disease when <10Q (Anvret et al., 2010). The second variant has been observed in population databases at a frequency of 0.0039 (4 homozygotes; BS1). *In silico* prediction using CADD was 27 and PolyPhen-2, *deleterious* (PP3). It has been previously reported in several individuals with clinical suspicion of progressive external ophthalmoplegia (Tang et al., 2011, Di Fonzo et al., 2003, Del Bo et al., 2003) but also in heterozygous state without a second variant suggesting that it may be a modifier. Therefore, the evidence for this variant is conflicting. The classification of these are uncertain and do not provide an explanation but may have contributed to the child's phenotype.

Patient #17

An 18-month-old boy, born to consanguineous parents, presented with ALF and underwent LT. He has good graft function at 20 years of age but suffers from peripheral neuropathy and leads a semi-independent life with mild learning difficulties.

A homozygous missense variant was identified in *MPV17*: c.3338C>T, p.Pro98Leu. This variant has been observed in populations databases at a frequency of $5.31e^{5}$ and not in homozygous state (PM2). *In silico* prediction using CADD was 25 and PolyPhen-2, *deleterious* (PP3). This variant has been previously reported to cause disease (Kim et al., 2016) (PM3) and the

classification of this variant is pathogenic and supports a genetic diagnosis of *MPV17*-related MDS. The patient is now under the care of the regional mitochondrial disorders service.

Patient #1

A 1-month-old girl of presented with lethargy and vomiting and was found to be in ALF. No aetiology was found and she underwent LT at 2 months of age. She has fully recovered and at 15 years of age she has good academic performance and attends hospital infrequently.

Compound heterozygous missense variants were identified in *DLD* c.826A>T, p.Thr276Ser; and c.911T>C, p.Ile304Thr. They have been observed in populations databases at a frequency of $5.42e^{4}$ and $1.57e^{4}$ and neither in homozygous state. *In silico* prediction using CADD was, 25 and 26, and PolyPhen-2, *likely benign* (BP4) for both variants. Furthermore, the variant frequency specifically for the African population was 0.0056 (2 homozygotes; BS1) and 0.0016 (0 homozygotes; BS1), respectively. The classification of these variants are uncertain but may have contributed to the child's phenotype. The DLD gene encodes PDH, a subunit of the alpha-keto acid dehydrogenase complex. Subsequently, the activity of PDH was measured using the child's cultured skin fibroblasts. The result of 0.76 nmol/mg protein/min (normal range 0.60-0.90) was against a diagnosis of DLD deficiency. However, this has to be interpreted with caution as PDH activity in fibroblasts may not be representative of that in the liver.

3.2 Functional characterisation of NBAS deficiency

3.2.1 Cell culture studies

3.2.1.1 Effect of thermal stress on NBAS deficient cells

At 37 °C for 24 hours, cell viability increased in all cell lines in the 500, 1000 and 2000 cells/well experiments, as expected. A photomicrograph of the cells are shown in Figure 3-2. In the second 24 hours at 37 °C, cell viability increased in all cell lines except: Control in 500

cells/well; Control and NBAS1 in 1000 cells/well (Figure 3-3). Under 40 °C for the second 24 hours, cell viability did not increase in: Control, NBAS1 and 4 in 500 cells/well; Control and NBAS1 in 1000 cells/well; Control and NBAS3 in 2000 cells/well.

The ratio of the cell viabilities at 48 hours to 24 hours within the 37 °C and 40 °C plates were then calculated. The results were, in turn, expressed as a ratio of each other (Figure 3-4) allowing for the comparison of the cell viabilities of the 37 °C and 40 °C plates whilst correcting for any discrepancies that may have occurred within a plate. This showed that the control cells demonstrated a higher cell viability at 40 °C in the 500 cells/well experiment but this was not observed in the 1000 and 2000 cells/well experiments. Statistical analysis indicated no significance difference in cell viability between the control and patient cells.

A

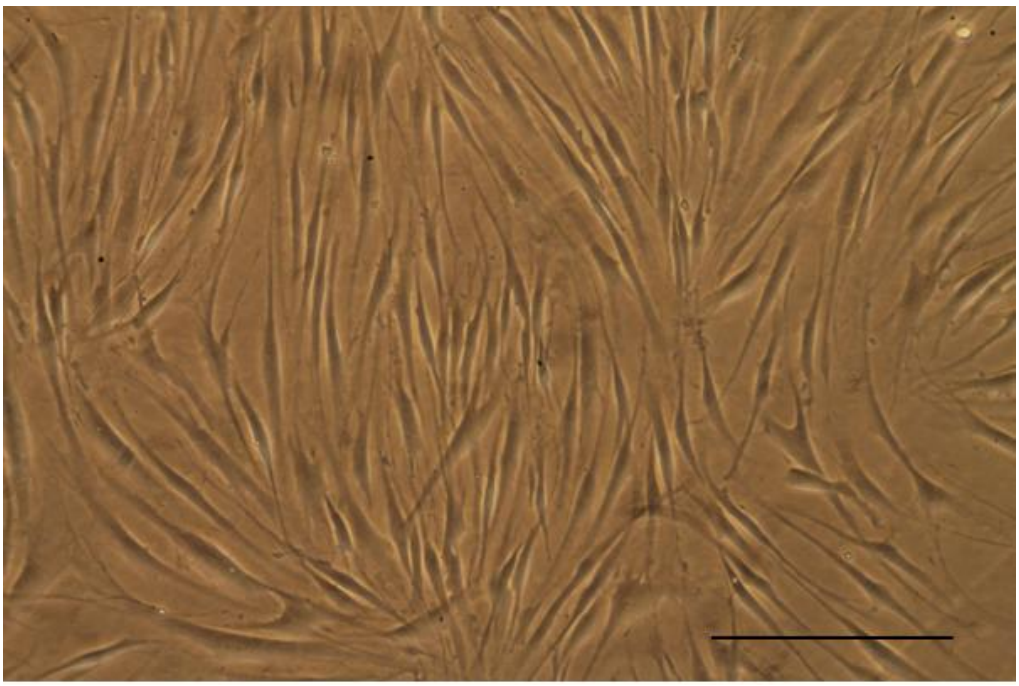

B

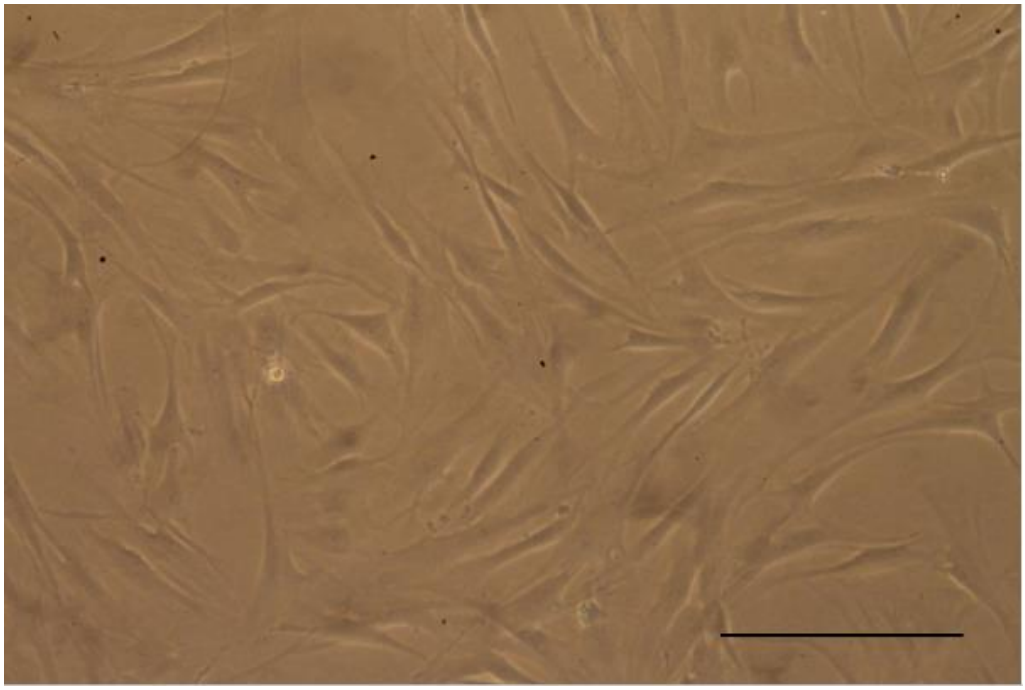

Figure 3-2 Photomicrograph of control and patient fibroblasts under normal culture conditions. Higher magnification (x 100) images of A, HFF1 cells, passage 8; B, NBAS1 patient cells, passage 11. Scale bars = 200 µm

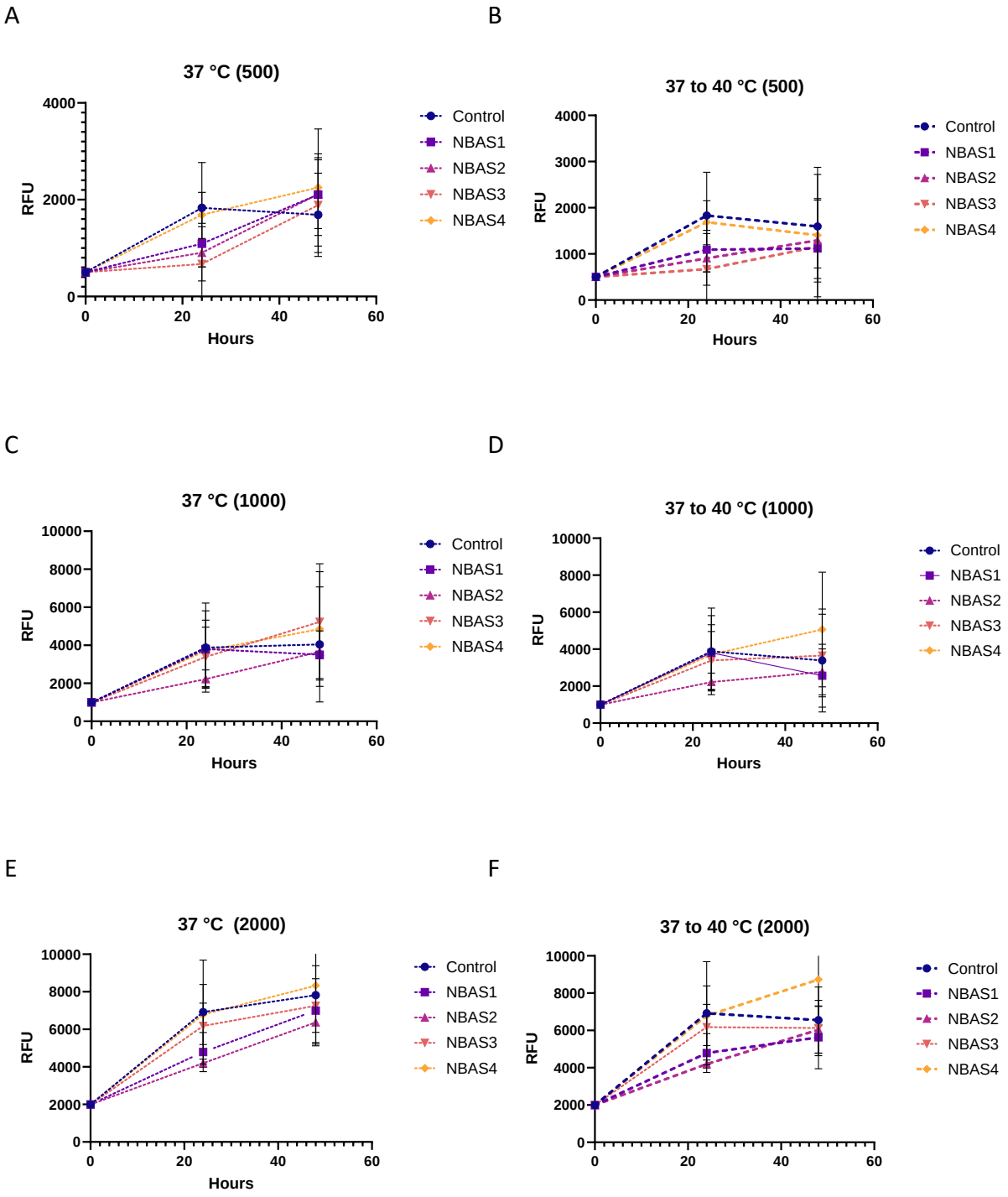

Figure 3-3 Cell viabilities of patient and control fibroblasts under *thermal stress*.
A, B and C represent cell viability of fibroblasts incubated at 37 °C for 48 hours; 500, 1000 and 2000 cells/well, respectively. D, E and F represent cell viability of fibroblasts incubated at 37 °C for 24 hours followed by 40 °C in the second 24 hours in; 500, 1000 and 2000 cells/well, respectively. Relative fluorescence units (RFU) shown as median ± range (n = 3).

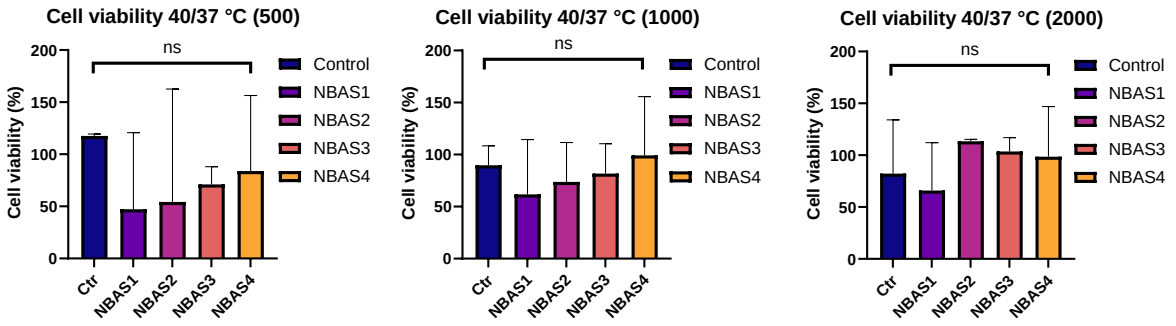

Figure 3-4 Cell viabilities of patient and control fibroblasts under *thermal stress* represented as a ratio of the second 24 hours to the first.
The results compare the cell viabilities of the 40 °C to the 37 °C plates after each were internally corrected for by obtaining a ratio of the cell viabilities at 48 hours to 24 hours within a plate. A, B, and C. = 500, 1000 and 2000 cells/well, respectively. Statistical analysis was carried out using Kruskal-Wallis test.

3.2.1.2 Effect of glucose deprivation on NBAS deficient cells

Patient and control fibroblasts were incubated for 24 hours in complete medium containing 4.5 g/L of glucose and their cell viabilities measured as baseline. Then the culture medium in the wells were replaced with medium containing 3 different concentrations of glucose: 0 g/L (*no glucose*), 1 g/L (*low glucose*) and 4.5 g

/L (*normal glucose*). The cell viabilities were measured after a further 24 and 48 hours of incubation (48 and 72 hours since plating, respectively; Figure 3-5).

Under a glucose concentration of 4.5 g/L, cell viability increased in all cell lines at 48 and 72 hours, as expected. However, cell viability also increased in all cell lines incubated with 1 g/L and 0 g/L of glucose. One exception to this was observed in NBAS3 in 0 g/L which did not demonstrate growth at 48 and 72 hours. However, statistical analysis indicated no significance difference in cell viability between the control and patient cells.

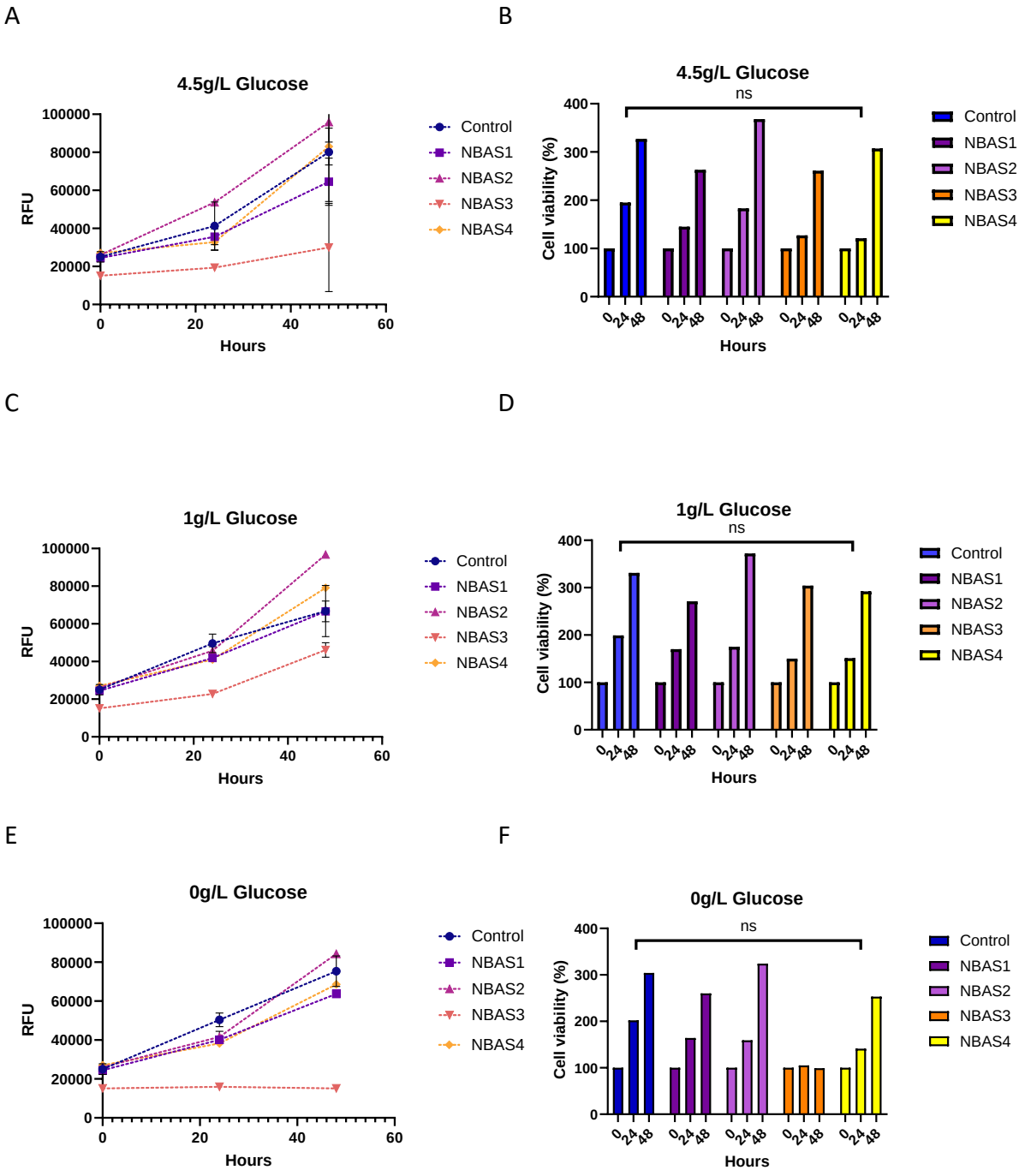

Figure 3-5 Cell viabilities of patient and control fibroblasts following *stress* by glucose deprivation. Fibroblasts were incubated in complete medium containing 4.5g/dL of glucose. After 24 hours of incubation, the culture medium was replaced with medium containing three different glucose concentrations and incubated for a further 24 and 48 hours. A and B = 4.5g/dL, C and D = 1g/dL and E and F = 0g/dL of glucose. The results are expressed as relative fluorescence units (RFU) shown as median ± range (n = 3) and percentage change in cell viability compared to baseline. Statistical analysis was carried out using Kruskal-Wallis test.

3.2.2 Protein expression analysis of NBAS

The expression of NBAS protein was investigated by western blot for the four patients and control cells. Three different antibodies which recognise different epitopes of the protein were tested. The first antibody from Atlas Antibodies (Stockholm, Sweden), which had not been validated in western blot but its use had been previously reported in the literature, was a polyclonal antibody raised in rabbit against amino acid residue 1011 to 1096. The second antibody from Affinity Biosciences (Cincinnati, US) was a polyclonal antibody raised in rabbit for which the epitope it was raised against was not made available.

These two antibodies were tested first in proteins extracted from NBAS1-4 cells and control cells that had not been placed under *stress*. Using the antibody from Atlas Antibody, two bands at approximately, 50 kD and 37 kD, were demonstrated from protein extracts from all the cell lines. Multiple bands were demonstrated from protein extracts from all the cell lines using the antibody from Affinity Biosciences. Neither antibody demonstrated a clear band at the expected molecular weight of 268 kD, therefore, the antibodies were considered not suitable for further protein expression analysis. A third antibody from Abcam (Cambridge, UK) which had been validated in western blot was then used - a polyclonal antibody raised in rabbit against amino acid residue 350 to 400. This showed a band, for the first time, at the expected molecular weight although multiple other, stronger bands were also shown at lower molecular weights. The antibody was, therefore, considered most appropriate for subsequent western blotting. Additionally, to improve the transferring of large molecular proteins such as NBAS, the transfer time was increased on the Trans-Blot Turbo System for subsequent experiments. β-actin with a molecular weight of approximately 42 kDa was used as the internal reference control.

Stripping of the NBAS antibody was carried out to blot a house keeping gene, β-actin, without interference from the non-specific bands from NBAS blotting. The BioRad protocol was used for this followed by re-blocking of the nitrocellulose membrane with 3% milk and following the protocol described previously for β-actin blotting and detection. For subsequent experiments, the membrane was cut to allow for differential blotting of NBAS and β-actin.

The western blot demonstrated multiple, non-specific bands suggesting interaction of the antibody with multiple proteins with similar epitopes (Figure 3-6). This may be due to the heterogenous antibody mixture raised typical of polyclonal antibodies which may have been avoided if monoclonal antibodies were available. Samples from NBAS1 and NBAS2 did not demonstrate bands at the expected molecular weight of 268 kDa whilst those from control, NBAS3 and NBAS4 did.

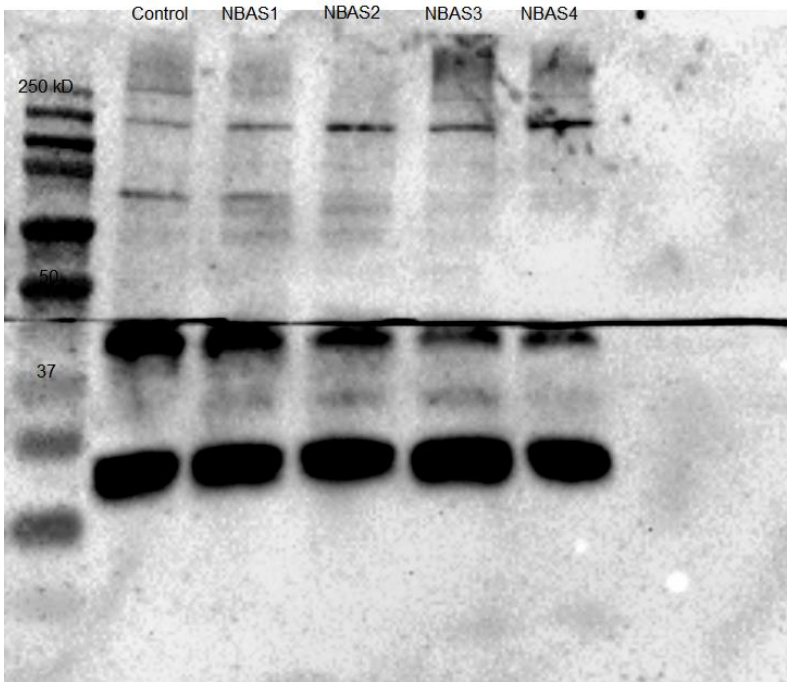

Figure 3-6 Western blot of NBAS using a polyclonal antibody raised in rabbit.
A band is not demonstrated at the expected molecular weight of 268kD for NBAS1 and NBAS2 whilst a band is demonstrated in all other cell lines (top half). β-actin with a molecular weight of 42kD was used as internal control (bottom half).

3.2.3 *GADD45A* and *GADD45B* expression analysis

The expression of *GADD45A* and *GADD45B* was investigated by qPCR for two patients (NBAS1 and NBAS2) and control cells (HFF1 and HFF2). These two patient samples were selected for the experiments because their variants were considered to be most significant (Table 2-3).

For *GADD45A*, satisfactory CT values were obtained using conventional qPCR conditions: an annealing temperature of 60 °C and primer concentration of 100 µM for both pre-mRNA and mRNA primers. For *GADD45B*, there was initial difficulty in generating PCR products. Using a primer concentration of 100 uM did not produce a CT value both for *GADD45A* and *GADD45B*. However, PCR products were generated when the primer concentrations were increased to 10 uM. Furthermore, qPCR using an annealing temperature of 60 °C produced CT values for mRNA primers > 35. Increasing the temperature sequentially to 62 °C and 64 °C lowered the CT values for mRNA primers but this, in turn, increased the CT values using the pre-mRNA primers. Therefore, it was necessary to carry out qPCR for *GADD45B* pre-mRNA and mRNA in separate experiments at 60 °C and 64 °C, respectively. To account for any differences in plating the ΔΔCT method was used.

The results for RT-qPCR on *GADD45A* and *GADD45B* demonstrated that their expression was lower in NBAS1 and NBAS2 in comparison to healthy controls (Figure 3-7). For GADD45A at 2X dilution this mounted to a 4.6-, 4.5-, 1.7- and 1.7-fold difference between mRNA and pre-mRNA for Control 1, Control 2, NBAS1 and NBAS2 cell lines, respectively. For GADD45A at 10X dilution this mounted to a 2.9-, 3.3-, 1.2- and 1.1-fold difference between mRNA and pre-mRNA for Control 1, Control 2, NBAS1 and NBAS2 cell lines, respectively. For GADD45B at 2X dilution this mounted to a 7.4-, 5.7-, 2.6- and 4.0-fold difference between mRNA and pre-mRNA for Control 1, Control 2, NBAS1 and NBAS2 cell lines, respectively. For GADD45B at 10X dilution this mounted to a 7.3-, 6.1-, 3.4- and 4.9-fold difference between mRNA and pre-mRNA for Control 1, Control 2, NBAS1 and NBAS2 cell lines, respectively.

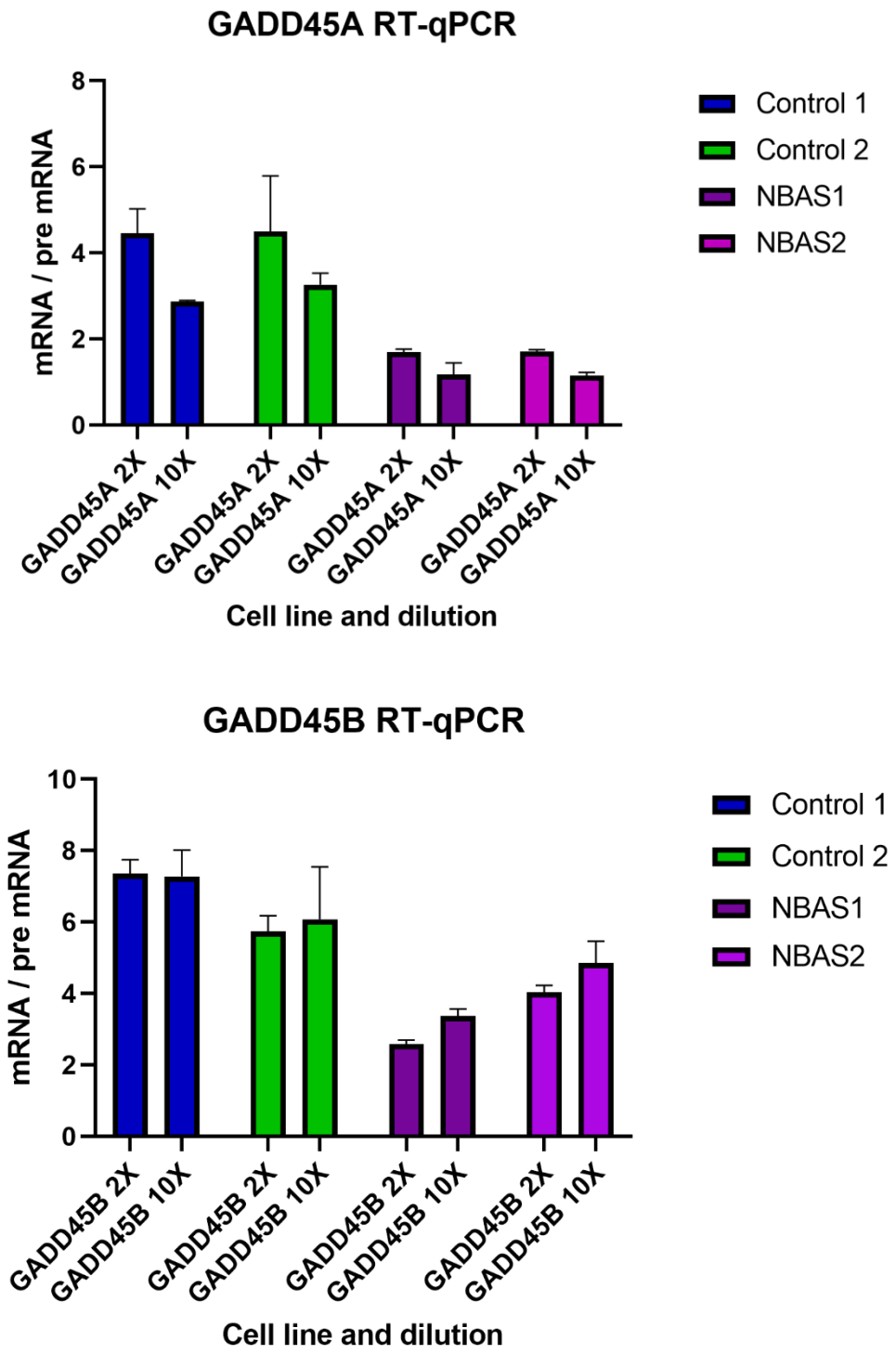

Figure 3-7 RT-qPCR for *GADD45A* and *GADD45B* mRNA and pre-mRNA expressed as a ratio.
Expression of *GADD45A* and *GADD45B* when expressed as a ratio of mRNA to pre-mRNA was lower in NBAS1 and NBAS2 when compared to healthy controls. *GAPDH* was used as an internal reference gene.

4 DISCUSSION AND FUTURE WORKS

4.1 Genetics of acute liver failure in children

The clinical phenotype of ALF is a reflection of the nature and extent of liver damage, its rate of evolution and ability of hepatic regeneration (Bernal and McPhail, 2021). In children, ALF is defined as a *rare multisystem disorder in which there is severe impairment of liver function, with or without encephalopathy, that occurs in association with hepatocellular necrosis in a patient with no recognised underlying chronic liver disease* (Bhaduri and Mieli-Vergani, 1996). This in an inclusive description which inevitably covers numerous underlying aetiologies. Reaching a diagnosis can be difficult (Narkewicz et al., 2009) and it remains a challenge to reduce the rate of indeterminate cases (Alonso et al., 2017). Monogenic disorders causing metabolic disease are thought to contribute to 10-28% of these cases (Hegarty et al., 2015, Squires et al., 2006) and are thought to be more likely in younger children or infants (Nicastro and D'Antiga, 2018).

4.1.1 Improving diagnostic yield in paediatric ALF

Biallelic variants of varying evidence for pathogenicity were identified in 8 / 41 (20%) children in whom targeted sequencing was carried out. Their median age at presentation was 2.5 years of age. Six children presented with one episode of ALF whilst 2 children suffered from recurrent ALF. Liver transplantation was performed in 5 children. All children who were followed up are alive. The genes involved were those that maintain mitochondrial DNA (*TWNK, MPV17, SUCLG1* and *POLG*), carry out mitochondrial energy production (*DLD*) and intracellular protein transport (*NBAS*). Most of the variants were missense variants although insertions were found in two patients (patients #3 and #9).

After sequencing, the genetic information was compared against the disease phenotype and thought to provide the diagnosis with confidence in 5 (patients #3, #8, #9, #17 and #18). However, in others the significance of the genetic findings was less clear. In patient #1, PDH

enzymology using skin fibroblasts demonstrated normal enzyme activity going against a diagnosis of DLD deficiency. Furthermore, in patient #19, repeat profiles of plasma acylcarnitines suggested that the carnitine transporter was not impaired. A possible interpretation of these results is that susceptibility to ALF was increased genetically but the variants were not the cause of a monogenic disease.

In 33 children, biallelic variants were not identified. However, 60 monoallelic variants were identified in 27 children. The phenotypes of those children found to have a variant that could lead to nonfunctional allele were, subsequently, interrogated further. These variants were observed in: patient #2, c.441+1G>A, p.? in *NPC2*; patient #6, c.278_279insC, p.Pro94Thrfs*8 in *ETFB*; patient #17, c.465delT, p.His156Thrfs*5 in *NPC2.* However, without functional studies to look specifically at the impact of these variants, it was not possible to state beyond the fact that the variant may have contributed in risk to ALF.

These findings demonstrate that genetic sequencing was successful in identifying causative variants in genes known to cause ALF in children from a historical group admitted to KCH. Traditionally, as much as half of cases of children with ALF were undiagnosed (Squires et al., 2006) whilst more recent figures are nearer to 30% (Alonso et al., 2017). However, these figures are quoted from clinical experiences based on the era prior to widespread use of NGS not accounting for more recently identified aetiologies such as those caused by variants in *NBAS*, *LARS* and *RINT1* (Cousin et al., 2019, Haack et al., 2015, Casey et al., 2012). Therefore, in the future diagnostic rates will be expected to improve further. The challenges will be around determining the pathogenicity and relevance of the genetic findings with enough confidence to influence therapeutic decision making.

4.1.2 Mitochondrial DNA depletion syndromes and ALF

Mitochondrial DNA depletion syndromes are caused by nuclear gene defects affecting genes responsible for the maintenance and replication of the mtDNA (Davison and Rahman, 2017). Liver transplantation for MDS is controversial because of the possibility of offering an organ transplant to a child with a multi-systemic, life-limiting disorder. In this work, 3 children were

found to have compound heterozygous or homozygous variants in mtDNA maintenance genes all of whom received LT and are alive at follow up. In a series of 29 patients with MPV17-associated hepatocerebral MDS, LT was performed in about 40% in whom half died afterwards (El-Hattab et al., 2010). It has been suggested that the degree of mtDNA depletion in the most commonly identified p.Arg50Gln, missense variant may result in a milder severity of the disease whilst nonsense, splice site and frameshift variants and deletions lead to death in infancy or early childhood (El-Hattab et al., 2010). In *POLG*-associated MDS, progressive neurological deterioration ensues even if they were to survive with LT (Tzoulis et al., 2006, Wong et al., 2008, Rahman and Copeland, 2019). There are no published reports of LT in TWNK or SUCLG1 deficiency.

The increasing use of NGS will be accompanied by an increase in the number of reported variants of potential pathogenicity. Genotyping is far from providing the phenotypic clarity that is required for therapeutic decision making in MDS – one of the risks is the possibility of over-interpretating genotypic information. This will be particularly relevant to MDS where LT may be contraindicated. Therefore, conventional biochemical and enzymatic tests should, for the time-being, continue to be carried out in parallel to help complement the genetic findings. In the future, it may be possible to consider gene therapy as a treatment option (Rahman and Copeland, 2019).

4.1.3 Rapid sequencing for ALF

Targeted, as well as exome sequencing have been successful in identifying molecular diagnoses in children with rare diseases (Sawyer et al., 2016, Wright et al., 2015). However, genome sequencing using trio testing is being used with superior diagnostic rates and cost-effectiveness (French et al., 2019, Mestek-Boukhibar et al., 2018). Children with ALF pose specific challenges due to the short time frame between presentation to therapeutic decision making as they can lose hepatic function within days (Squires et al., 2006, Hegarty et al., 2015). Therefore, a short time frame to results is critical to its practical application.

Efforts to develop rapid NGS pipelines for neonatal and paediatric intensive care patients has shown some early promise. A genome sequencing study carried out in the UK demonstrated a mean turnaround time of around 11 days from library preparation to analysis of candidate genes using specific, fast data processing software for variant mapping and calling and a tiered approach in the analysis of genes (French et al., 2019, Mestek-Boukhibar et al., 2018). It has even been possible to arrive at molecular diagnosis in as short as 50 hours. This was achieved by: 1) manufacturer reconfiguration of the sequencer; 2) 24-hour availability of laboratory staff for sequencing and; 3) use of a specific, clinicopathological correlation tool to narrow down the candidate genes (Saunders et al., 2012, van Diemen et al., 2017). This shows promise for the application of NGS to reach a diagnosis in paediatric ALF in time to help make therapeutic decisions. Future efforts should concentrate around building the appropriate technology, infrastructure and resources to reduce the turnaround time even further in order maximise its clinical utility.

4.1.4 Limitations

This work has some limitations. Targeted sequencing did not identify a molecular diagnosis in 80% of the cohort. The reasons for this can be divided into *biological factors* where the patient's DNA was, in fact, free of disease-causing variants and a molecular diagnosis was not to be made or *technical factors* where a molecular diagnosis was to be made but was somehow missed.

Biological factors

- A significant proportion of those who remained *indeterminate* after sequencing may not have a monogenic aetiology as ALF is a condition with a wide range of underlying causes. Currently, there are no reliable, clinical indicators to help identify those who may have a monogenic disorder versus those who do not although in the publication related to this research, younger age and worse clinical outcome characterised the *biallelic* group (Hegarty et al., 2021).
- It is also possible that the current, targeted sequencing method was not able to capture the causative gene because the disease-causing gene was not included in the

design in the first place. As stated in section 1.4.1, the aim of this research was to identify known, monogenic causes of ALF in a historical cohort of children in whom the diagnosis may have been missed. Given that over 180 novel genes are added to the list of disease-causing genes each year (Directors, 2015), it is likely that there are still undiscovered, monogenic causes of ALF that are yet to be described.

Technical factors

- Targeted NGS analyses specific genomic ROI which are isolated by magnetic pulldown during the library preparation stage. It has a robust workflow that can reliably sequence many genes (50 – 100) with ample read depth to make interpretation and generation of a final report manageable within a reasonable timeframe. However, on the other hand, coverage outside the coding regions is lacking in targeted NGS. Therefore, the main pitfall is the exclusion of introns including promotor and enhancer variants escaping interpretation. In this work, it is possible that even amongst the genes in which monoallelic variants were detected, a second intronic variant *in trans* may have been present.
- Although the capture efficiency and depth of coverage was good overall (section 3.1.1), varying GC content, small and variable DNA fragment sizes and the presence of repetitive sequences can all contribute to inconsistent coverage and variants being missed. The effects of this are over- or underrepresentation of certain sequences and may require additional sanger sequencing to fill the regions missed. Further biases could be introduced due to preferential enrichment of the reference allele which is used to design the capture probe (De Cario et al., 2020). Additionally, CNVs and large genomic rearrangements may be missed in short-read sequencing.
- The genetic interpretation carried out in this work assumed an autosomal recessive Mendelian inheritance pattern, the usual mode of inheritance of the conditions that were tested for. However, alleles for a given trait can be complicated by interactions between different genes or inconsistent inheritance patterns. For instance, penetrance as defined by the proportion of individuals in a population who carry a specific gene and express the related trait of a disease may not be 100%. Furthermore, individuals with the same genotype can also show different degrees of the same phenotype due to variable expressivity. Therefore, genotype-phenotype associations

can be difficult to predict without understanding genetic regulation and its molecular mechanisms.

4.2 Functional characterisation of NBAS deficiency

4.2.1 Stress treatment

Acute liver failure secondary to NBAS deficiency can be considered as the archetypal form of ALF where there is rapid and significant derangement in AST and ALT, typically, in the tens of thousands (Chavany et al., 2020, Calvo et al., 2017). This is accompanied by a sharp rise in INR ranging between 4 to 20 (Chavany et al., 2020). Fever is the typical trigger and glucose infusion for the patient is advocated as a supportive treatment measure (Chavany et al., 2020, Ono et al., 2019, Haack et al., 2015). In this work, attempts to mimic the biology of NBAS deficiency were made by placing fibroblasts obtained from affected patients and placing them under *stress*. This included incubating the cells at 40 °C as well as removing glucose from the culture medium and measuring their effects on cell viability. Under *thermal stress*, control cells demonstrated a higher cell viability at 40 °C in the 500 cells/well experiment but this did not amount to statistical significance and was not observed in the 1000 and 2000 cells/well experiments. Under glucose deprivation, cell viability increased in all cell lines except for NBAS3.

Western blot was performed on protein extracts from NBAS 1-4. This demonstrated multiple, non-specific bands suggesting interaction of the antibody with multiple proteins with similar epitopes. Samples from NBAS1 and NBAS2 did not show a band at the expected molecular weight of 268 kDa whilst those from HFF1, NBAS1, NBAS3 and NBAS4 did.

These results provided an insight into the pathobiology of NBAS deficiency - that the application of *stress* by heat and deprivation of glucose impaired cell viability in patient cells compared to controls although it was not a consistent finding across all experimental conditions. Therefore, it was not possible to conclusively demonstrate *in vitro* replication of the liver phenotype of NBAS deficiency. Further studies using alternate methods to assay cell

proliferation will be required such as those that measure metabolic activity or ATP assays (Espinosa et al., 2021, Adan et al., 2016). Furthermore, it may be possible to ascertain whether the trigger of ALF is fever or an infection by carrying out these assays following inoculation of the affected cells with a virus at 37 °C. With such insights it may be possible to direct treatment in the future for those affected.

4.2.2 Nonsense mediated decay

The *NBAS* gene is the human ortholog of a highly conserved gene *smgl-1* identified by BLAST searches (Altschul et al., 1997). Published literature on human disease caused by NBAS deficiency allude to the possibility of a disruption in NMD leading to disease (Staufner et al., 2016, Haack et al., 2015). However, evidence is lacking to substantiate this. Furthermore, human disease caused by NBAS deficiency is usually seen as a disease that primarily affects the liver without neurological involvement. This is contrary to diseases that are caused by disrupted NMD which are usually multisystemic and involves the neurological system because of the broad way in which NMD controls gene expression (Pawlicka et al., 2020).

GADD45A and *GADD45B* are genes implicated in stress signalling. They interact with other cellular proteins implicated in cell cycle regulation and response to stress resulting in cell cycle arrest, DNA repair, cell survival and senescence, or apoptosis (Liebermann and Hoffman, 2008). More specific and recent data suggest the role of *GADD45A* in epigenetics by binding to R-loops which are DNA-RNA hybrids that can regulate chromatin states (Arab et al., 2019). In doing so it mediates DNA demethylation. It has a unique property of being expressed in low quantities at steady state regulated by NMD in both fruit flies and mammals (Viegas et al., 2007, Hwang and Maquat, 2011). It has been shown to increase its expression upon knockdown of the NMD factor, UPF-1, confirming that it is sensitive to NMD (Nelson et al., 2016). Therefore, it can act as a model to study NMD (Morris et al., 2007, Kurosaki et al., 2014, Nelson et al., 2016).

In this work, fibroblasts obtained from the skin from two patients known to be affected by NBAS deficiency were used to delineate their involvement in NMD. They were from patients

NBAS1 and NBAS2 in whom the homozygous variants c.exons 17-19 dup, p.? and c.4731_4733dup, p.Tyr1578dup were detected, respectively (Table 2-3). In both cases, the variants are significant: NBAS1 may produce protein but likely to be non-functional (as a duplication of 372 nucleotides will not alter the reading frame) and NBAS2 is likely to result in no protein formation in the presence of NMD (or disrupted protein in the absence of NMD). The RT-qPCR experiments demonstrated that the expression of both *GADD45A* and *GADD45B* was not elevated in comparison to controls. This goes against the previous suggestions that disease causing mutations in NBAS may disrupt NMD (Staufner et al., 2020, Staufner et al., 2016, Rius et al., 2019, Ono et al., 2019, Li et al., 2017, Haack et al., 2015, Chavany et al., 2020, Carli et al., 2019, Capo-Chichi et al., 2015, Calvo et al., 2017).

However, it must be borne in mind that there are limitations in the use of commercially obtained human foreskin fibroblasts. The conditions in which these cells were cultured and stored as well as their senescence may not be consistent with the patient cells. It is possible that such differences had an influence on the results on *GADD45A* and *GADD45B* expression levels. Another limitation is that foreskin fibroblasts may not be representative of NMD activity in the liver. Fibroblasts are commonly used in experiments to study physiological conditions at cellular level (Nadalutti and Wilson, 2020). It has been used, for instance, to study the expression of NMD factors in cytoplasmic stress granules where mRNA regulation occurs under genotoxic stress (Brown et al., 2011). However, it remains a possibility that fibroblasts from skin and their response to stress are not fully representative of hepatocytes. Variation in NMD efficiency has been demonstrated in murine models where up to a two-fold difference in NMD activity occurred depending on the organ evaluated (Zetoune et al., 2008).

Additionally, more recent evidence suggests that there may be an ER-specific NMD pathway regulated by *NBAS* that encode for the secretome or membrane-associated genes that lead to neurodegeneration when disrupted (Longman et al., 2020). However, there are a few considerations that need to be taken into account before accepting this hypothesis by Longman *et al* in entirety.

1. NBAS deficiency can manifest as a single organ, hepatic disease (0). Human disease that affect NMD are usually multisystemic so it seems unlikely that there is a disease

process in NBAS deficiency that fully disrupts NMD. Certainly, a localised ER-specific NMD pathway that affects the secretome but not the wider transcriptome is plausible.

2. With relevance to the *GADD45A* and *GADD45B* experiments carried out in this work, it seems unlikely that *GADD45A* and *GADD45B* are part of this ER-specific NMD pathway given that its expression is in the nucleus and function related to chromatin states and demethylation (https://reactome.org/). Therefore, whilst this work suggested that NMD is not disrupted it is still plausible that there is a more localised NMD pathway separate to *GADD45A* and *GADD45B* expression.

3. Finally, there are limitations to experiments carried out by Longman *et al* using: 1) HeLa cells such as cross-contamination, false cell lines and genetic drift (Masters, 2002) and 2) *C elegans* in which NMD is not essential (Longman et al., 2013). An *in vitro* model using induced pluripotent stem cells derived hepatocytes from patients may offer the possibility to model the human disease further (Lenz et al., 2019, Ng et al., 2018).

The following approaches may be considered in the future to add further evidence to the experiments carried out in this work.

1. *GADD45A* and *GADD45B* are the most frequently cited endogenous NMD targets (Kurosaki et al., 2014, Kurosaki et al., 2019). However, it is possible that *GADD45A* and *GADD45B* do not use *NBAS* in their decay pathway. Alternative genes that demonstrate similar properties may be used to provide further evidence such as *TBL2* and *NAT9* (Viegas et al., 2007).

2. The fibroblasts used in this work were obtained from patients NBAS1 and NBAS2 both of whom were considered as having single organ disease. Therefore, it is possible that NMD was not disrupted in fibroblasts in these particular patients. Given that NBAS deficiency can also manifest as a multisystemic phenotype named SOPH syndrome (MIM 614800), repeating the experiments from fibroblasts obtained from patients with SOPH syndrome may provide alternative results.

3. Alternative approaches of detecting targets of NMD may be used such as investigating the transcriptome by RNA sequencing (Nguyen et al., 2012). In another approach, decay rates of transcripts or mRNA half-lives were determined by 5'-bromo-uridine immunoprecipitation chase - deep sequencing analysis (BRIC-seq) (Tani et al., 2012).

4. Finally, another experimental approach is the use of human induced pluripotent stem cell (iPSC) derived hepatocytes as a disease model. This has the advantage of overcoming any biological differences in *NBAS* that may exist between hepatocytes and fibroblasts. Furthermore, the iPSC line can be generated from affected patients or from CRISPR/Cas9 edited human iPSC by gene knockout or knock-in, gene interference or activation (Ran et al., 2013). These cells can exhibit phenotypes close to human pathology and represent a disease model this clinically relevant (De Masi et al., 2020).

5 FINAL CONCLUSION

This work demonstrated the benefits of using NGS in reaching a diagnosis in children with ALF. Functional studies employed to elucidate the pathobiology of NBAS deficiency showed that NMD was intact, but unfortunately, failed to replicate the effects of *stress*, *in vitro*. Despite these results, the pursuit to understand the pathobiology of NBAS deficiency should continue: not only because of the possibility to provide insights to treatment in NBAS deficiency but to understand ALF in a broader sense given the archetypal ALF phenotype that NBAS deficiency represents. The knowledge gained in studying NBAS deficiency is likely to be applicable to other causes of ALF.

From a diagnostic perspective, the discovery of NBAS deficiency in 2015 paved the way to the discovery of several other novel monogenic causes of ALF. This was achieved by use of exome sequencing technology and multicentre collaboration studies. Nonetheless, as our understanding of variations within the coding DNA improves the rate of gene discovery in rare diseases may be reaching a plateau. The focus is now shifting towards the completeness of the genetic diagnostic evaluation including variations that occur in non-coding regions and the role of gene expression regulators. Whole genome sequencing can close some of this gap but in the future, it is likely to be a combination of tests that be required.

Progress is still required for the clinical application of NGS in children with ALF, a rapidly progressive condition with devastating complications. Firstly, the timeframe required to reach a molecular diagnosis is still too long to influence clinical decisions regarding redirection of care, LT and specialised treatments. Furthermore, the molecular diagnosis must be supported with sufficient phenotypic evidence so that clinical decisions can be made with confidence. Future efforts should focus on overcoming these challenges by close inter-disciplinary working between hepatologists and geneticists so that accessibility and incorporation of genomic data into clinical care be maximised. Until then conventional diagnostic tests should continue be carried out in conjunction with genetic sequencing. This work provides a basis towards a future with more informed and individualised therapeutic decision making for children affected by ALF where NGS-based, diagnostic evaluation will become the standard of care.

6 REFERENCES

ADAN, A., KIRAZ, Y. & BARAN, Y. 2016. Cell Proliferation and Cytotoxicity Assays. *Curr Pharm Biotechnol,* 17**,** 1213-1221.

ADEVA-ANDANY, M. M., CARNEIRO-FREIRE, N., SECO-FILGUEIRA, M., FERNANDEZ-FERNANDEZ, C. & MOURINO-BAYOLO, D. 2019. Mitochondrial beta-oxidation of saturated fatty acids in humans. *Mitochondrion,* 46**,** 73-90.

AGILENT. 2017. *SureSelectXT Low Input Target Enrichment System for Illumina Paired-End Multiplexed Sequencing Library* [Online]. Available: https://www.agilent.com/cs/library/usermanuals/public/G9702-90000.pdf [Accessed 01/02/2018 2017].

AKIYAMA, N., SHIMURA, M., YAMAZAKI, T., HARASHIMA, H., FUSHIMI, T., TSURUOKA, T., EBIHARA, T., ICHIMOTO, K., MATSUNAGA, A., SAITO-TSURUOKA, M., YATSUKA, Y., KISHITA, Y., KOHDA, M., NAMBA, A., KAMEI, Y., OKAZAKI, Y., KOSUGI, S., OHTAKE, A. & MURAYAMA, K. 2021. Prenatal diagnosis of severe mitochondrial diseases caused by nuclear gene defects: a study in Japan. *Sci Rep,* 11**,** 3531.

ALONSO, E. M. 2005. Acute liver failure in children: the role of defects in fatty acid oxidation. *Hepatology,* 41**,** 696-9.

ALONSO, E. M., HORSLEN, S. P., BEHRENS, E. M. & DOO, E. 2017. Pediatric acute liver failure of undetermined cause: A research workshop. *Hepatology,* 65**,** 1026-1037.

ALTSCHUL, S. F., MADDEN, T. L., SCHAFFER, A. A., ZHANG, J., ZHANG, Z., MILLER, W. & LIPMAN, D. J. 1997. Gapped BLAST and PSI-BLAST: a new generation of protein database search programs. *Nucleic Acids Res,* 25**,** 3389-402.

ANVRET, A., WESTERLUND, M., SYDOW, O., WILLOWS, T., LIND, C., GALTER, D. & BELIN, A. C. 2010. Variations of the CAG trinucleotide repeat in DNA polymerase gamma (POLG1) is associated with Parkinson's disease in Sweden. *Neurosci Lett,* 485**,** 117-20.

AOKI, T., ICHIMURA, S., ITOH, A., KURAMOTO, M., SHINKAWA, T., ISOBE, T. & TAGAYA, M. 2009. Identification of the neuroblastoma-amplified gene product as a component of the syntaxin 18 complex implicated in Golgi-to-endoplasmic reticulum retrograde transport. *Mol Biol Cell,* 20**,** 2639-49.

APTE, U., GKRETSI, V., BOWEN, W. C., MARS, W. M., LUO, J. H., DONTHAMSETTY, S., ORR, A., MONGA, S. P., WU, C. & MICHALOPOULOS, G. K. 2009. Enhanced liver regeneration following changes induced by hepatocyte-specific genetic ablation of integrin-linked kinase. *Hepatology,* 50**,** 844-51.

APTOWITZER, I., SAADA, A., FABER, J., KLEID, D. & ELPELEG, O. N. 1997. Liver disease in the Ashkenazi-Jewish lipoamide dehydrogenase deficiency. *J Pediatr Gastroenterol Nutr,* 24**,** 599-601.

ARAB, K., KARAULANOV, E., MUSHEEV, M., TRNKA, P., SCHAFER, A., GRUMMT, I. & NIEHRS, C. 2019. GADD45A binds R-loops and recruits TET1 to CpG island promoters. *Nat Genet,* 51**,** 217-223.

BALASUBRAMANIAM, S., CHOY, Y. S., TALIB, A., NORSIAH, M. D., VAN DEN HEUVEL, L. P. & RODENBURG, R. J. 2012. Infantile Progressive Hepatoencephalomyopathy with Combined OXPHOS Deficiency due to Mutations in the Mitochondrial Translation Elongation Factor Gene GFM1. *JIMD Rep,* 5**,** 113-22.

BALASUBRAMANIAM, S., WAMELINK, M. M., NGU, L. H., TALIB, A., SALOMONS, G. S., JAKOBS, C. & KENG, W. T. 2011. Novel heterozygous mutations in TALDO1 gene causing transaldolase deficiency and early infantile liver failure. *J Pediatr Gastroenterol Nutr,* 52**,** 113-6.

BALASUBRAMANIAN, M., HURST, J., BROWN, S., BISHOP, N. J., ARUNDEL, P., DEVILE, C., POLLITT, R. C., CROOKS, L., LONGMAN, D., CACERES, J. F., SHACKLEY, F., CONNOLLY, S., PAYNE, J. H., OFFIAH, A. C., HUGHES, D., STUDY, D. D. D., PARKER, M. J., HIDE, W. & SKERRY, T. M. 2017. Compound heterozygous variants in NBAS as a cause of atypical osteogenesis imperfecta. *Bone,* 94**,** 65-74.

BANTEL, H. & SCHULZE-OSTHOFF, K. 2012. Mechanisms of cell death in acute liver failure. *Front Physiol,* 3**,** 79.

BARAK, N., HUMINER, D., SEGAL, T., BEN ARI, Z., HALEVY, J. & TUR-KASPA, R. 1998. Lipoamide dehydrogenase deficiency: a newly discovered cause of acute hepatitis in adults. *J Hepatol,* 29**,** 482-4.

BARUTEAU, J., SACHS, P., BROUE, P., BRIVET, M., ABDOUL, H., VIANEY-SABAN, C. & OGIER DE BAULNY, H. 2014. Clinical and biological features at diagnosis in mitochondrial fatty acid beta-oxidation defects: a French pediatric study from 187 patients. Complementary data. *J Inherit Metab Dis,* 37**,** 137-9.

BERNAL, W., AUZINGER, G., DHAWAN, A. & WENDON, J. 2010. Acute liver failure. *Lancet,* 376**,** 190-201.

BERNAL, W., LEE, W. M., WENDON, J., LARSEN, F. S. & WILLIAMS, R. 2015. Acute liver failure: A curable disease by 2024? *J Hepatol,* 62**,** S112-20.

BERNAL, W. & MCPHAIL, M. J. 2021. Acute liver failure. *J Hepatol,* 74**,** 1489-1490.

BHADURI, B. R. & MIELI-VERGANI, G. 1996. Fulminant hepatic failure: pediatric aspects. *Semin Liver Dis,* 16**,** 349-55.

BHAVE, V. S., MARS, W., DONTHAMSETTY, S., ZHANG, X., TAN, L., LUO, J., BOWEN, W. C. & MICHALOPOULOS, G. K. 2013. Regulation of liver growth by glypican 3, CD81, hedgehog, and Hhex. *Am J Pathol,* 183**,** 153-9.

BLACKMORE, L. & BERNAL, W. 2015. Acute liver failure. *Clin Med (Lond),* 15**,** 468-72.

BOWER, W. A., JOHNS, M., MARGOLIS, H. S., WILLIAMS, I. T. & BELL, B. P. 2007. Population-based surveillance for acute liver failure. *Am J Gastroenterol,* 102**,** 2459-63.

BRASSIER, A., OTTOLENGHI, C., BOUTRON, A., BERTRAND, A. M., VALMARY-DEGANO, S., CERVONI, J. P., CHRETIEN, D., ARNOUX, J. B., HUBERT, L., RABIER, D., LACAILLE, F., DE KEYZER, Y., DI MARTINO, V. & DE LONLAY, P. 2013. Dihydrolipoamide dehydrogenase deficiency: a still overlooked cause of recurrent acute liver failure and Reye-like syndrome. *Mol Genet Metab,* 109**,** 28-32.

BRETHERICK, A. D., CRAIG, D. G., MASTERTON, G., BATES, C., DAVIDSON, J., MARTIN, K., IREDALE, J. P. & SIMPSON, K. J. 2011. Acute liver failure in Scotland between 1992 and 2009; incidence, aetiology and outcome. *QJM,* 104**,** 945-56.

BROWN, J. A., ROBERTS, T. L., RICHARDS, R., WOODS, R., BIRRELL, G., LIM, Y. C., OHNO, S., YAMASHITA, A., ABRAHAM, R. T., GUEVEN, N. & LAVIN, M. F. 2011. A novel role for hSMG-1 in stress granule formation. *Mol Cell Biol,* 31**,** 4417-29.

CALVO, P. L., TANDOI, F., HAAK, T. B., BRUNATI, A., PINON, M., OLIO, D. D., ROMAGNOLI, R. & SPADA, M. 2017. NBAS mutations cause acute liver failure: when acetaminophen is not a culprit. *Ital J Pediatr,* 43**,** 88.

CAPO-CHICHI, J. M., MEHAWEJ, C., DELAGUE, V., CAILLAUD, C., KHNEISSER, I., HAMDAN, F. F., MICHAUD, J. L., KIBAR, Z. & MEGARBANE, A. 2015. Neuroblastoma Amplified

Sequence (NBAS) mutation in recurrent acute liver failure: Confirmatory report in a sibship with very early onset, osteoporosis and developmental delay. *Eur J Med Genet,* 58**,** 637-41.

CARLI, D., GIORGIO, E., PANTALEONI, F., BRUSELLES, A., BARRESI, S., RIBERI, E., LICCIARDI, F., GAZZIN, A., BALDASSARRE, G., PIZZI, S., NICETA, M., RADIO, F. C., MOLINATTO, C., MONTIN, D., CALVO, P. L., CIOLFI, A., FLEISCHER, N., FERRERO, G. B., BRUSCO, A. & TARTAGLIA, M. 2019. NBAS pathogenic variants: Defining the associated clinical and facial phenotype and genotype-phenotype correlations. *Hum Mutat,* 40**,** 721-728.

CASEY, J. P., MCGETTIGAN, P., LYNAM-LENNON, N., MCDERMOTT, M., REGAN, R., CONROY, J., BOURKE, B., O'SULLIVAN, J., CRUSHELL, E., LYNCH, S. & ENNIS, S. 2012. Identification of a mutation in LARS as a novel cause of infantile hepatopathy. *Mol Genet Metab,* 106**,** 351-8.

CHAPIN, C. A., BURN, T., MEIJOME, T., LOOMES, K. M., MELIN-ALDANA, H., KREIGER, P. A., WHITINGTON, P. F., BEHRENS, E. M. & ALONSO, E. M. 2018. Indeterminate pediatric acute liver failure is uniquely characterized by a CD103(+) CD8(+) T-cell infiltrate. *Hepatology,* 68**,** 1087-1100.

CHAPIN, C. A., BURN, T. M., DIAMOND, T., LOOMES, K. M., ALONSO, E. M. & BEHRENS, E. M. 2023. Effector memory CD8 T-cells as a novel peripheral blood biomarker for activated T-cell pediatric acute liver failure. *PLoS One,* 18**,** e0286394.

CHAVANY, J., CANO, A., ROQUELAURE, B., BOURGEOIS, P., BOUBNOVA, J., GAIGNARD, P., HOEBEKE, C., REYNAUD, R., RHOMER, B., SLAMA, A., BADENS, C., CHABROL, B. & FABRE, A. 2020. Mutations in NBAS and SCYL1, genetic causes of recurrent liver failure in children: Three case reports and a literature review. *Arch Pediatr,* 27**,** 155-159.

CHEN, Y. M., CHEN, W., XU, Y., LU, C. S., ZHU, M. M., SUN, R. Y., WANG, Y., CHEN, Y., SHI, J. & WANG, D. 2022. Novel compound heterozygous SUCLG1 variants may contribute to mitochondria DNA depletion syndrome-9. *Mol Genet Genomic Med,* 10**,** e2010.

COUSIN, M. A., CONBOY, E., WANG, J. S., LENZ, D., SCHWAB, T. L., WILLIAMS, M., ABRAHAM, R. S., BARNETT, S., EL-YOUSSEF, M., GRAHAM, R. P., GUTIERREZ SANCHEZ, L. H., HASADSRI, L., HOFFMANN, G. F., HULL, N. C., KOPAJTICH, R., KOVACS-NAGY, R., LI, J. Q., MARX-BERGER, D., MCLIN, V., MCNIVEN, M. A., MOUNAJJED, T., PROKISCH, H., RYMEN, D., SCHULZE, R. J., STAUFNER, C., YANG, Y., CLARK, K. J., LANPHER, B. C. & KLEE, E. W. 2019. RINT1 Bi-allelic Variations Cause Infantile-Onset Recurrent Acute Liver Failure and Skeletal Abnormalities. *Am J Hum Genet,* 105**,** 108-121.

DAVISON, J. E. & RAHMAN, S. 2017. Recognition, investigation and management of mitochondrial disease. *Arch Dis Child,* 102**,** 1082-1090.

DE CARIO, R., KURA, A., SURACI, S., MAGI, A., VOLTA, A., MARCUCCI, R., GORI, A. M., PEPE, G., GIUSTI, B. & STICCHI, E. 2020. Sanger Validation of High-Throughput Sequencing in Genetic Diagnosis: Still the Best Practice? *Front Genet,* 11**,** 592588.

DE MASI, C., SPITALIERI, P., MURDOCCA, M., NOVELLI, G. & SANGIUOLO, F. 2020. Application of CRISPR/Cas9 to human-induced pluripotent stem cells: from gene editing to drug discovery. *Hum Genomics,* 14**,** 25.

DEL BO, R., BORDONI, A., SCIACCO, M., DI FONZO, A., GALBIATI, S., CRIMI, M., BRESOLIN, N. & COMI, G. P. 2003. Remarkable infidelity of polymerase gammaA associated with mutations in POLG1 exonuclease domain. *Neurology,* 61**,** 903-8.

DI FONZO, A., BORDONI, A., CRIMI, M., SARA, G., DEL BO, R., BRESOLIN, N. & COMI, G. P. 2003. POLG mutations in sporadic mitochondrial disorders with multiple mtDNA deletions. *Hum Mutat,* 22**,** 498-9.

DIRECTORS, A. B. O. 2015. Clinical utility of genetic and genomic services: a position statement of the American College of Medical Genetics and Genomics. *Genet Med,* 17**,** 505-7.

EGUCHI, A., WREE, A. & FELDSTEIN, A. E. 2014. Biomarkers of liver cell death. *J Hepatol,* 60**,** 1063-74.

EL-HATTAB, A. W., LI, F. Y., SCHMITT, E., ZHANG, S., CRAIGEN, W. J. & WONG, L. J. 2010. MPV17-associated hepatocerebral mitochondrial DNA depletion syndrome: new patients and novel mutations. *Mol Genet Metab,* 99**,** 300-8.

ESCORSELL, A., MAS, A., DE LA MATA, M. & SPANISH GROUP FOR THE STUDY OF ACUTE LIVER, F. 2007. Acute liver failure in Spain: analysis of 267 cases. *Liver Transpl,* 13**,** 1389-95.

ESPINOSA, J. A., POHAN, G., ARKIN, M. R. & MARKOSSIAN, S. 2021. Real-Time Assessment of Mitochondrial Toxicity in HepG2 Cells Using the Seahorse Extracellular Flux Analyzer. *Curr Protoc,* 1**,** e75.

ESPINOZA-LEWIS, R. A. & WANG, D. Z. 2012. MicroRNAs in heart development. *Curr Top Dev Biol,* 100**,** 279-317.

FAUSTO, N., CAMPBELL, J. S. & RIEHLE, K. J. 2006. Liver regeneration. *Hepatology,* 43**,** S45-53.

FERREIRA, C. R., RAHMAN, S., KELLER, M., ZSCHOCKE, J. & GROUP, I. A. 2021. An international classification of inherited metabolic disorders (ICIMD). *J Inherit Metab Dis,* 44**,** 164-177.

FRENCH, C. E., DELON, I., DOLLING, H., SANCHIS-JUAN, A., SHAMARDINA, O., MEGY, K., ABBS, S., AUSTIN, T., BOWDIN, S., BRANCO, R. G., FIRTH, H., DISEASE, N. B.-R., NEXT GENERATION CHILDREN, P., ROWITCH, D. H. & RAYMOND, F. L. 2019. Whole genome sequencing reveals that genetic conditions are frequent in intensively ill children. *Intensive Care Med,* 45**,** 627-636.

GATFIELD, D., UNTERHOLZNER, L., CICCARELLI, F. D., BORK, P. & IZAURRALDE, E. 2003. Nonsense-mediated mRNA decay in Drosophila: at the intersection of the yeast and mammalian pathways. *EMBO J,* 22**,** 3960-70.

GIL-BORLADO, M. C., GONZALEZ-HOYUELA, M., BLAZQUEZ, A., GARCIA-SILVA, M. T., GABALDON, T., MANZANARES, J., VARA, J., MARTIN, M. A., SENECA, S., ARENAS, J. & UGALDE, C. 2009. Pathogenic mutations in the 5' untranslated region of BCS1L mRNA in mitochondrial complex III deficiency. *Mitochondrion,* 9**,** 299-305.

GILGENKRANTZ, H. & COLLIN DE L'HORTET, A. 2018. Understanding Liver Regeneration: From Mechanisms to Regenerative Medicine. *Am J Pathol,* 188**,** 1316-1327.

GRANTHAM, R. 1974. Amino acid difference formula to help explain protein evolution. *Science,* 185**,** 862-4.

GUPTA, N. 2019. DNA Extraction and Polymerase Chain Reaction. *J Cytol,* 36**,** 116-117.

HAACK, T. B., STAUFNER, C., KOPKE, M. G., STRAUB, B. K., KOLKER, S., THIEL, C., FREISINGER, P., BARIC, I., MCKIERNAN, P. J., DIKOW, N., HARTING, I., BEISSE, F., BURGARD, P., KOTZAERIDOU, U., KUHR, J., HIMBERT, U., TAYLOR, R. W., DISTELMAIER, F., VOCKLEY, J., GHALOUL-GONZALEZ, L., ZSCHOCKE, J., KREMER, L. S., GRAF, E., SCHWARZMAYR, T., BADER, D. M., GAGNEUR, J., WIELAND, T., TERRILE, C., STROM, T. M., MEITINGER, T., HOFFMANN, G. F. & PROKISCH, H. 2015. Biallelic Mutations in NBAS Cause Recurrent Acute Liver Failure with Onset in Infancy. *Am J Hum Genet,* 97**,** 163-9.

HAN, X., WEI, Y., WANG, H., WANG, F., JU, Z. & LI, T. 2018. Nonsense-mediated mRNA decay: a 'nonsense' pathway makes sense in stem cell biology. *Nucleic Acids Res,* 46**,** 1038-1051.

HEGARTY, R., GIBSON, P., SAMBROTTA, M., STRAUTNIEKS, S., FOSKETT, P., ELLARD, S., BAPTISTA, J., LILLIS, S., BANSAL, S., VARA, R., DHAWAN, A., GRAMMATIKOPOULOS, T.

& THOMPSON, R. J. 2021. Study of Acute Liver Failure in Children Using Next Generation Sequencing Technology. *J Pediatr*.

HEGARTY, R., HADZIC, N., GISSEN, P. & DHAWAN, A. 2015. Inherited metabolic disorders presenting as acute liver failure in newborns and young children: King's College Hospital experience. *Eur J Pediatr,* 174**,** 1387-92.

HOVATTA, O., MIKKOLA, M., GERTOW, K., STROMBERG, A. M., INZUNZA, J., HREINSSON, J., ROZELL, B., BLENNOW, E., ANDANG, M. & AHRLUND-RICHTER, L. 2003. A culture system using human foreskin fibroblasts as feeder cells allows production of human embryonic stem cells. *Hum Reprod,* 18**,** 1404-9.

HWANG, J. & MAQUAT, L. E. 2011. Nonsense-mediated mRNA decay (NMD) in animal embryogenesis: to die or not to die, that is the question. *Curr Opin Genet Dev,* 21**,** 422-30.

ILLUMINA, I. 2017. *An introduction to Next-Generation Sequencing Technology* [Online]. USA. Available: https://emea.illumina.com/content/dam/illumina-marketing/documents/products/illumina_sequencing_introduction.pdf [Accessed 25/05/2019].

IVERSON, S. V., COMSTOCK, K. M., KUNDERT, J. A. & SCHMIDT, E. E. 2011. Contributions of new hepatocyte lineages to liver growth, maintenance, and regeneration in mice. *Hepatology,* 54**,** 655-63.

JANSEN, J. C., CIRAK, S., VAN SCHERPENZEEL, M., TIMAL, S., REUNERT, J., RUST, S., PEREZ, B., VICOGNE, D., KRAWITZ, P., WADA, Y., ASHIKOV, A., PEREZ-CERDA, C., MEDRANO, C., ARNOLDY, A., HOISCHEN, A., HUIJBEN, K., STEENBERGEN, G., QUELHAS, D., DIOGO, L., RYMEN, D., JAEKEN, J., GUFFON, N., CHEILLAN, D., VAN DEN HEUVEL, L. P., MAEDA, Y., KAISER, O., SCHARA, U., GERNER, P., VAN DEN BOOGERT, M. A., HOLLEBOOM, A. G., NASSOGNE, M. C., SOKAL, E., SALOMON, J., VAN DEN BOGAART, G., DRENTH, J. P., HUYNEN, M. A., VELTMAN, J. A., WEVERS, R. A., MORAVA, E., MATTHIJS, G., FOULQUIER, F., MARQUARDT, T. & LEFEBER, D. J. 2016. CCDC115 Deficiency Causes a Disorder of Golgi Homeostasis with Abnormal Protein Glycosylation. *Am J Hum Genet,* 98**,** 310-21.

KARKHANIS, J., VERNA, E. C., CHANG, M. S., STRAVITZ, R. T., SCHILSKY, M., LEE, W. M., BROWN, R. S., JR. & ACUTE LIVER FAILURE STUDY, G. 2014. Steroid use in acute liver failure. *Hepatology,* 59**,** 612-21.

KIA, A., GLOECKNER, C., OSOTHPRAROP, T., GORMLEY, N., BOMATI, E., STEPHENSON, M., GORYSHIN, I. & HE, M. M. 2017. Improved genome sequencing using an engineered transposase. *BMC Biotechnol,* 17**,** 6.

KIM, J., KANG, E., KIM, Y., KIM, J. M., LEE, B. H., MURAYAMA, K., KIM, G. H., CHOI, I. H., KIM, K. M. & YOO, H. W. 2016. MPV17 mutations in patients with hepatocerebral mitochondrial DNA depletion syndrome. *Mol Genet Metab Rep,* 8**,** 74-6.

KIRCHER, M., WITTEN, D. M., JAIN, P., O'ROAK, B. J., COOPER, G. M. & SHENDURE, J. 2014. A general framework for estimating the relative pathogenicity of human genetic variants. *Nat Genet,* 46**,** 310-5.

KOPAJTICH, R., MURAYAMA, K., JANECKE, A. R., HAACK, T. B., BREUER, M., KNISELY, A. S., HARTING, I., OHASHI, T., OKAZAKI, Y., WATANABE, D., TOKUZAWA, Y., KOTZAERIDOU, U., KOLKER, S., SAUER, S., CARL, M., STRAUB, S., ENTENMANN, A., GIZEWSKI, E., FEICHTINGER, R. G., MAYR, J. A., LACKNER, K., STROM, T. M., MEITINGER, T., MULLER, T., OHTAKE, A., HOFFMANN, G. F., PROKISCH, H. & STAUFNER, C. 2016. Biallelic IARS

Mutations Cause Growth Retardation with Prenatal Onset, Intellectual Disability, Muscular Hypotonia, and Infantile Hepatopathy. *Am J Hum Genet,* 99**,** 414-22.

KUROSAKI, T., LI, W., HOQUE, M., POPP, M. W., ERMOLENKO, D. N., TIAN, B. & MAQUAT, L. E. 2014. A post-translational regulatory switch on UPF1 controls targeted mRNA degradation. *Genes Dev,* 28**,** 1900-16.

KUROSAKI, T., MYERS, J. R. & MAQUAT, L. E. 2019. Defining nonsense-mediated mRNA decay intermediates in human cells. *Methods,* 155**,** 68-76.

LEFKOWITCH, J. H. 2016. The Pathology of Acute Liver Failure. *Adv Anat Pathol,* 23**,** 144-58.

LENZ, D., MCCLEAN, P., KANSU, A., BONNEN, P. E., RANUCCI, G., THIEL, C., STRAUB, B. K., HARTING, I., ALHADDAD, B., DIMITROV, B., KOTZAERIDOU, U., WENNING, D., IORIO, R., HIMES, R. W., KULOGLU, Z., BLAKELY, E. L., TAYLOR, R. W., MEITINGER, T., KOLKER, S., PROKISCH, H., HOFFMANN, G. F., HAACK, T. B. & STAUFNER, C. 2018. SCYL1 variants cause a syndrome with low gamma-glutamyl-transferase cholestasis, acute liver failure, and neurodegeneration (CALFAN). *Genet Med,* 20**,** 1255-1265.

LENZ, D., STAUFNER, C., WACHTER, S., HAGEDORN, M., EBERSOLD, J., GOHRING, G., KOLKER, S., HOFFMANN, G. F. & JUNG-KLAWITTER, S. 2019. Generation of an iPSC line from a patient with infantile liver failure syndrome 2 due to mutations in NBAS: DHMCi004-A. *Stem Cell Res,* 35**,** 101398.

LEWIS, B. P. 2003. *Regulated Unproductive Splicing and Translation (RUST)* [Online]. Available: https://compbio.berkeley.edu/people/ed/rust/ [Accessed January 18 2021].

LI, J. Q., GONG, J. Y., KNISELY, A. S., ZHANG, M. H. & WANG, J. S. 2019. Recurrent acute liver failure associated with novel SCYL1 mutation: A case report. *World J Clin Cases,* 7**,** 494-499.

LI, J. Q., QIU, Y. L., GONG, J. Y., DOU, L. M., LU, Y., KNISELY, A. S., ZHANG, M. H., LUAN, W. S. & WANG, J. S. 2017. Novel NBAS mutations and fever-related recurrent acute liver failure in Chinese children: a retrospective study. *BMC Gastroenterol,* 17**,** 77.

LIEBERMANN, D. A. & HOFFMAN, B. 2008. Gadd45 in stress signaling. *J Mol Signal,* 3**,** 15.

LINDROOS, P. M., ZARNEGAR, R. & MICHALOPOULOS, G. K. 1991. Hepatocyte growth factor (hepatopoietin A) rapidly increases in plasma before DNA synthesis and liver regeneration stimulated by partial hepatectomy and carbon tetrachloride administration. *Hepatology,* 13**,** 743-50.

LONGMAN, D., HUG, N., KEITH, M., ANASTASAKI, C., PATTON, E. E., GRIMES, G. & CACERES, J. F. 2013. DHX34 and NBAS form part of an autoregulatory NMD circuit that regulates endogenous RNA targets in human cells, zebrafish and Caenorhabditis elegans. *Nucleic Acids Res,* 41**,** 8319-31.

LONGMAN, D., JACKSON-JONES, K. A., MASLON, M. M., MURPHY, L. C., YOUNG, R. S., STODDART, J. J., HUG, N., TAYLOR, M. S., PAPADOPOULOS, D. K. & CACERES, J. F. 2020. Identification of a localized nonsense-mediated decay pathway at the endoplasmic reticulum. *Genes Dev,* 34**,** 1075-1088.

LYKKE-ANDERSEN, S. & JENSEN, T. H. 2015. Nonsense-mediated mRNA decay: an intricate machinery that shapes transcriptomes. *Nat Rev Mol Cell Biol,* 16**,** 665-77.

MAKSIMOVA, N., HARA, K., NIKOLAEVA, I., CHUN-FENG, T., USUI, T., TAKAGI, M., NISHIHIRA, Y., MIYASHITA, A., FUJIWARA, H., OYAMA, T., NOGOVICINA, A., SUKHOMYASOVA, A., POTAPOVA, S., KUWANO, R., TAKAHASHI, H., NISHIZAWA, M. & ONODERA, O. 2010. Neuroblastoma amplified sequence gene is associated with a novel short stature syndrome characterised by optic nerve atrophy and Pelger-Huet anomaly. *J Med Genet,* 47**,** 538-48.

MARQUES-DA-SILVA, D., DOS REIS FERREIRA, V., MONTICELLI, M., JANEIRO, P., VIDEIRA, P. A., WITTERS, P., JAEKEN, J. & CASSIMAN, D. 2017. Liver involvement in congenital disorders of glycosylation (CDG). A systematic review of the literature. *J Inherit Metab Dis,* 40**,** 195-207.

MASTERS, J. R. 2002. HeLa cells 50 years on: the good, the bad and the ugly. *Nat Rev Cancer,* 2**,** 315-9.

MESTEK-BOUKHIBAR, L., CLEMENT, E., JONES, W. D., DRURY, S., OCAKA, L., GAGUNASHVILI, A., LE QUESNE STABEJ, P., BACCHELLI, C., JANI, N., RAHMAN, S., JENKINS, L., HURST, J. A., BITNER-GLINDZICZ, M., PETERS, M., BEALES, P. L. & WILLIAMS, H. J. 2018. Rapid Paediatric Sequencing (RaPS): comprehensive real-life workflow for rapid diagnosis of critically ill children. *J Med Genet,* 55**,** 721-728.

MICHALOPOULOS, G. K. 2007. Liver regeneration. *J Cell Physiol,* 213**,** 286-300.

MOLINA-BERENGUER, M., VILA-JULIA, F., PEREZ-RAMOS, S., SALCEDO-ALLENDE, M. T., CAMARA, Y., TORRES-TORRONTERAS, J. & MARTI, R. 2022. Dysfunctional mitochondrial translation and combined oxidative phosphorylation deficiency in a mouse model of hepatoencephalopathy due to Gfm1 mutations. *FASEB J,* 36**,** e22091.

MORITA, A., IMAGAWA, K., ASAYAMA, K., TERAKADO, T., TAKAHASHI, S., YAITA, K., TAGAWA, M., MATSUBARA, D. & TAKADA, H. 2022. Immunological characteristics of severe acute hepatitis of unknown origin in a child post SARS-CoV-2 infection. *Clin Immunol,* 245**,** 109138.

MORRIS, C., WITTMANN, J., JACK, H. M. & JALINOT, P. 2007. Human INT6/eIF3e is required for nonsense-mediated mRNA decay. *EMBO Rep,* 8**,** 596-602.

MULLANY, L. K., WHITE, P., HANSE, E. A., NELSEN, C. J., GOGGIN, M. M., MULLANY, J. E., ANTTILA, C. K., GREENBAUM, L. E., KAESTNER, K. H. & ALBRECHT, J. H. 2008. Distinct proliferative and transcriptional effects of the D-type cyclins in vivo. *Cell Cycle,* 7**,** 2215-24.

NADALUTTI, C. A. & WILSON, S. H. 2020. Using Human Primary Foreskin Fibroblasts to Study Cellular Damage and Mitochondrial Dysfunction. *Curr Protoc Toxicol,* 86**,** e99.

NARKEWICZ, M. R., DELL OLIO, D., KARPEN, S. J., MURRAY, K. F., SCHWARZ, K., YAZIGI, N., ZHANG, S., BELLE, S. H., SQUIRES, R. H. & PEDIATRIC ACUTE LIVER FAILURE STUDY, G. 2009. Pattern of diagnostic evaluation for the causes of pediatric acute liver failure: an opportunity for quality improvement. *J Pediatr,* 155**,** 801-806 e1.

NARKEWICZ, M. R., HORSLEN, S., HARDISON, R. M., SHNEIDER, B. L., RODRIGUEZ-BAEZ, N., ALONSO, E. M., NG, V. L., LEONIS, M. A., LOOMES, K. M., RUDNICK, D. A., ROSENTHAL, P., ROMERO, R., SUBBARAO, G. C., LI, R., BELLE, S. H., SQUIRES, R. H. & PEDIATRIC ACUTE LIVER FAILURE STUDY, G. 2018. A Learning Collaborative Approach Increases Specificity of Diagnosis of Acute Liver Failure in Pediatric Patients. *Clin Gastroenterol Hepatol,* 16**,** 1801-1810 e3.

NELSON, J. O., MOORE, K. A., CHAPIN, A., HOLLIEN, J. & METZSTEIN, M. M. 2016. Degradation of Gadd45 mRNA by nonsense-mediated decay is essential for viability. *Elife,* 5.

NG, S. S., SAEB-PARSY, K., BLACKFORD, S. J. I., SEGAL, J. M., SERRA, M. P., HORCAS-LOPEZ, M., NO, D. Y., MASTORIDIS, S., JASSEM, W., FRANK, C. W., CHO, N. J., NAKAUCHI, H., GLENN, J. S. & RASHID, S. T. 2018. Human iPS derived progenitors bioengineered into liver organoids using an inverted colloidal crystal poly (ethylene glycol) scaffold. *Biomaterials,* 182**,** 299-311.

NGUYEN, L. S., JOLLY, L., SHOUBRIDGE, C., CHAN, W. K., HUANG, L., LAUMONNIER, F., RAYNAUD, M., HACKETT, A., FIELD, M., RODRIGUEZ, J., SRIVASTAVA, A. K., LEE, Y.,

LONG, R., ADDINGTON, A. M., RAPOPORT, J. L., SUREN, S., HAHN, C. N., GAMBLE, J., WILKINSON, M. F., CORBETT, M. A. & GECZ, J. 2012. Transcriptome profiling of UPF3B/NMD-deficient lymphoblastoid cells from patients with various forms of intellectual disability. *Mol Psychiatry,* 17**,** 1103-15.

NICASTRO, E. & D'ANTIGA, L. 2018. Next generation sequencing in pediatric hepatology and liver transplantation. *Liver Transpl,* 24**,** 282-293.

O'GRADY, J. G., SCHALM, S. W. & WILLIAMS, R. 1993. Acute liver failure: redefining the syndromes. *Lancet,* 342**,** 273-5.

OCHOA, B., SYN, W. K., DELGADO, I., KARACA, G. F., JUNG, Y., WANG, J., ZUBIAGA, A. M., FRESNEDO, O., OMENETTI, A., ZDANOWICZ, M., CHOI, S. S. & DIEHL, A. M. 2010. Hedgehog signaling is critical for normal liver regeneration after partial hepatectomy in mice. *Hepatology,* 51**,** 1712-23.

ODAIB, A. A., SHNEIDER, B. L., BENNETT, M. J., POBER, B. R., REYES-MUGICA, M., FRIEDMAN, A. L., SUCHY, F. J. & RINALDO, P. 1998. A defect in the transport of long-chain fatty acids associated with acute liver failure. *N Engl J Med,* 339**,** 1752-7.

OLAHOVA, M., CECCATELLI BERTI, C., COLLIER, J. J., ALSTON, C. L., JAMESON, E., JONES, S. A., EDWARDS, N., HE, L., CHINNERY, P. F., HORVATH, R., GOFFRINI, P., TAYLOR, R. W. & SAYER, J. A. 2019. Molecular genetic investigations identify new clinical phenotypes associated with BCS1L-related mitochondrial disease. *Hum Mol Genet,* 28**,** 3766-3776.

OLPIN, S. E. 2013. Pathophysiology of fatty acid oxidation disorders and resultant phenotypic variability. *J Inherit Metab Dis,* 36**,** 645-58.

ONO, S., MATSUDA, J., WATANABE, E., AKAIKE, H., TERANISHI, H., MIYATA, I., OTOMO, T., SADAHIRA, Y., MIZUOCHI, T., KUSANO, H., KAGE, M., UENO, H., YOSHIDA, K., SHIRAISHI, Y., CHIBA, K., TANAKA, H., MIYANO, S., OGAWA, S., HAYASHI, Y., KANEGANE, H. & OUCHI, K. 2019. Novel neuroblastoma amplified sequence (NBAS) mutations in a Japanese boy with fever-triggered recurrent acute liver failure. *Hum Genome Var,* 6**,** 2.

PARANJPE, S., BOWEN, W. C., MARS, W. M., ORR, A., HAYNES, M. M., DEFRANCES, M. C., LIU, S., TSENG, G. C., TSAGIANNI, A. & MICHALOPOULOS, G. K. 2016. Combined systemic elimination of MET and epidermal growth factor receptor signaling completely abolishes liver regeneration and leads to liver decompensation. *Hepatology,* 64**,** 1711-1724.

PARK, J. W. & LEE, S. J. 2017. Foveal hypoplasia in short stature with optic atrophy and Pelger-Huet anomaly syndrome with neuroblastoma-amplified sequence (NBAS) gene mutation. *J AAPOS*.

PARSHURAM, C. S., DUNCAN, H. P., JOFFE, A. R., FARRELL, C. A., LACROIX, J. R., MIDDAUGH, K. L., HUTCHISON, J. S., WENSLEY, D., BLANCHARD, N., BEYENE, J. & PARKIN, P. C. 2011. Multicentre validation of the bedside paediatric early warning system score: a severity of illness score to detect evolving critical illness in hospitalised children. *Crit Care,* 15**,** R184.

PAWLICKA, K., KALATHIYA, U. & ALFARO, J. 2020. Nonsense-Mediated mRNA Decay: Pathologies and the Potential for Novel Therapeutics. *Cancers (Basel),* 12.

PEROUTKA, C., SALAS, J., BRITTON, J., BISHOP, J., KRATZ, L., GILMORE, M. M., FAHRNER, J. A., GOLDEN, W. C. & WANG, T. 2019. Severe Neonatal Manifestations of Infantile Liver Failure Syndrome Type 1 Caused by Cytosolic Leucine-tRNA Synthetase Deficiency. *JIMD Rep,* 45**,** 71-76.

QIAGEN. 2018. *Quick-Start Protocol: QIAamp DNA Mini Kit* [Online]. Qiagen. Available: https://www.qiagen.com/gb/resources/resourcedetail?id=566f1cb1-4ffe-4225-a6de-6bd3261dc920&lang=en [Accessed 06/01/2018 2018].

QUAGLIA, A., PORTMANN, B. C., KNISELY, A. S., SRINIVASAN, P., MUIESAN, P., WENDON, J., HENEGHAN, M. A., O'GRADY, J. G., SAMYN, M., HADZIC, D., DHAWAN, A., MIELI-VERGANI, G., HEATON, N. & RELA, M. 2008. Auxiliary transplantation for acute liver failure: Histopathological study of native liver regeneration. *Liver Transpl,* 14**,** 1437-48.

RAHMAN, S. & COPELAND, W. C. 2019. POLG-related disorders and their neurological manifestations. *Nat Rev Neurol,* 15**,** 40-52.

RAN, F. A., HSU, P. D., WRIGHT, J., AGARWALA, V., SCOTT, D. A. & ZHANG, F. 2013. Genome engineering using the CRISPR-Cas9 system. *Nat Protoc,* 8**,** 2281-2308.

REGATEIRO, F. S., BELKAYA, S., NEVES, N., FERREIRA, S., SILVESTRE, P., LEMOS, S., VENANCIO, M., CASANOVA, J. L., GONCALVES, I., JOUANGUY, E. & DIOGO, L. 2017. Recurrent elevated liver transaminases and acute liver failure in two siblings with novel bi-allelic mutations of NBAS. *Eur J Med Genet,* 60**,** 426-432.

RICCI, S., LODI, L., SERRANTI, D., MORONI, M., BELLI, G., MANCANO, G., LA BARBERA, A., FORZANO, G., MANGONE, G., INDOLFI, G. & AZZARI, C. 2019. Immunological Features of Neuroblastoma Amplified Sequence Deficiency: Report of the First Case Identified Through Newborn Screening for Primary Immunodeficiency and Review of the Literature. *Front Immunol,* 10**,** 1955.

RICHARDS, S., AZIZ, N., BALE, S., BICK, D., DAS, S., GASTIER-FOSTER, J., GRODY, W. W., HEGDE, M., LYON, E., SPECTOR, E., VOELKERDING, K., REHM, H. L. & COMMITTEE, A. L. Q. A. 2015. Standards and guidelines for the interpretation of sequence variants: a joint consensus recommendation of the American College of Medical Genetics and Genomics and the Association for Molecular Pathology. *Genet Med,* 17**,** 405-24.

RIEDL, S. J. & SHI, Y. 2004. Molecular mechanisms of caspase regulation during apoptosis. *Nat Rev Mol Cell Biol,* 5**,** 897-907.

RIUS, R., RILEY, L. G., GUO, Y., MENEZES, M., COMPTON, A. G., VAN BERGEN, N. J., GAYEVSKIY, V., COWLEY, M. J., CUMMINGS, B. B., ADAMS, L., ELLAWAY, C., THORBURN, D. R., HAKONARSON, H. & CHRISTODOULOU, J. 2019. Cryptic intronic NBAS variant reveals the genetic basis of recurrent liver failure in a child. *Mol Genet Metab,* 126**,** 77-82.

ROLLINS, M. F., VAN DER HEIDE, D. M., WEISEND, C. M., KUNDERT, J. A., COMSTOCK, K. M., SUVOROVA, E. S., CAPECCHI, M. R., MERRILL, G. F. & SCHMIDT, E. E. 2010. Hepatocytes lacking thioredoxin reductase 1 have normal replicative potential during development and regeneration. *J Cell Sci,* 123**,** 2402-12.

SAUDUBRAY, J. M., MOCHEL, F., LAMARI, F. & GARCIA-CAZORLA, A. 2019. Proposal for a simplified classification of IMD based on a pathophysiological approach: A practical guide for clinicians. *J Inherit Metab Dis,* 42**,** 706-727.

SAUNDERS, C. J., MILLER, N. A., SODEN, S. E., DINWIDDIE, D. L., NOLL, A., ALNADI, N. A., ANDRAWS, N., PATTERSON, M. L., KRIVOHLAVEK, L. A., FELLIS, J., HUMPHRAY, S., SAFFREY, P., KINGSBURY, Z., WEIR, J. C., BETLEY, J., GROCOCK, R. J., MARGULIES, E. H., FARROW, E. G., ARTMAN, M., SAFINA, N. P., PETRIKIN, J. E., HALL, K. P. & KINGSMORE, S. F. 2012. Rapid whole-genome sequencing for genetic disease diagnosis in neonatal intensive care units. *Sci Transl Med,* 4**,** 154ra135.

SAWYER, S. L., HARTLEY, T., DYMENT, D. A., BEAULIEU, C. L., SCHWARTZENTRUBER, J., SMITH, A., BEDFORD, H. M., BERNARD, G., BERNIER, F. P., BRAIS, B., BULMAN, D. E., WARMAN

CHARDON, J., CHITAYAT, D., DELADOEY, J., FERNANDEZ, B. A., FROSK, P., GERAGHTY, M. T., GERULL, B., GIBSON, W., GOW, R. M., GRAHAM, G. E., GREEN, J. S., HEON, E., HORVATH, G., INNES, A. M., JABADO, N., KIM, R. H., KOENEKOOP, R. K., KHAN, A., LEHMANN, O. J., MENDOZA-LONDONO, R., MICHAUD, J. L., NIKKEL, S. M., PENNEY, L. S., POLYCHRONAKOS, C., RICHER, J., ROULEAU, G. A., SAMUELS, M. E., SIU, V. M., SUCHOWERSKY, O., TARNOPOLSKY, M. A., YOON, G., ZAHIR, F. R., CONSORTIUM, F. C., CARE4RARE CANADA, C., MAJEWSKI, J. & BOYCOTT, K. M. 2016. Utility of whole-exome sequencing for those near the end of the diagnostic odyssey: time to address gaps in care. *Clin Genet,* 89**,** 275-84.

SEGARRA, N. G., BALLHAUSEN, D., CRAWFORD, H., PERREAU, M., CAMPOS-XAVIER, B., VAN SPAENDONCK-ZWARTS, K., VERMEER, C., RUSSO, M., ZAMBELLI, P. Y., STEVENSON, B., ROYER-BERTRAND, B., RIVOLTA, C., CANDOTTI, F., UNGER, S., MUNIER, F. L., SUPERTI-FURGA, A. & BONAFE, L. 2015. NBAS mutations cause a multisystem disorder involving bone, connective tissue, liver, immune system, and retina. *Am J Med Genet A,* 167A**,** 2902-12.

SEPTER, S., EDWARDS, G., GUNEWARDENA, S., WOLFE, A., LI, H., DANIEL, J. & APTE, U. 2012. Yes-associated protein is involved in proliferation and differentiation during postnatal liver development. *Am J Physiol Gastrointest Liver Physiol,* 302**,** G493-503.

SHOHET, A., COHEN, L., HAGUEL, D., MOZER, Y., SHOMRON, N., TZUR, S., BAZAK, L., BASEL SALMON, L. & KRAUSE, I. 2019. Variant in SCYL1 gene causes aberrant splicing in a family with cerebellar ataxia, recurrent episodes of liver failure, and growth retardation. *Eur J Hum Genet,* 27**,** 263-268.

SPARKS, S. E. & KRASNEWICH, D. M. 1993. PMM2-CDG (CDG-Ia). *In:* ADAM, M. P., ARDINGER, H. H., PAGON, R. A., WALLACE, S. E., BEAN, L. J. H., STEPHENS, K. & AMEMIYA, A. (eds.) *GeneReviews((R)).* Seattle (WA).

SQUIRES, R. H., JR., SHNEIDER, B. L., BUCUVALAS, J., ALONSO, E., SOKOL, R. J., NARKEWICZ, M. R., DHAWAN, A., ROSENTHAL, P., RODRIGUEZ-BAEZ, N., MURRAY, K. F., HORSLEN, S., MARTIN, M. G., LOPEZ, M. J., SORIANO, H., MCGUIRE, B. M., JONAS, M. M., YAZIGI, N., SHEPHERD, R. W., SCHWARZ, K., LOBRITTO, S., THOMAS, D. W., LAVINE, J. E., KARPEN, S., NG, V., KELLY, D., SIMONDS, N. & HYNAN, L. S. 2006. Acute liver failure in children: the first 348 patients in the pediatric acute liver failure study group. *J Pediatr,* 148**,** 652-658.

STARKEY LEWIS, P. J., DEAR, J., PLATT, V., SIMPSON, K. J., CRAIG, D. G., ANTOINE, D. J., FRENCH, N. S., DHAUN, N., WEBB, D. J., COSTELLO, E. M., NEOPTOLEMOS, J. P., MOGGS, J., GOLDRING, C. E. & PARK, B. K. 2011. Circulating microRNAs as potential markers of human drug-induced liver injury. *Hepatology,* 54**,** 1767-76.

STAUFNER, C., HAACK, T. B., KOPKE, M. G., STRAUB, B. K., KOLKER, S., THIEL, C., FREISINGER, P., BARIC, I., MCKIERNAN, P. J., DIKOW, N., HARTING, I., BEISSE, F., BURGARD, P., KOTZAERIDOU, U., LENZ, D., KUHR, J., HIMBERT, U., TAYLOR, R. W., DISTELMAIER, F., VOCKLEY, J., GHALOUL-GONZALEZ, L., OZOLEK, J. A., ZSCHOCKE, J., KUSTER, A., DICK, A., DAS, A. M., WIELAND, T., TERRILE, C., STROM, T. M., MEITINGER, T., PROKISCH, H. & HOFFMANN, G. F. 2016. Recurrent acute liver failure due to NBAS deficiency: phenotypic spectrum, disease mechanisms, and therapeutic concepts. *J Inherit Metab Dis,* 39**,** 3-16.

STAUFNER, C., PETERS, B., WAGNER, M., ALAMEER, S., BARIC, I., BROUE, P., BULUT, D., CHURCH, J. A., CRUSHELL, E., DALGIC, B., DAS, A. M., DICK, A., DIKOW, N., DIONISI-VICI, C., DISTELMAIER, F., BOZBULUT, N. E., FEILLET, F., GONZALES, E., HADZIC, N., HAUCK,

F., HEGARTY, R., HEMPEL, M., HERGET, T., KLEIN, C., KONSTANTOPOULOU, V., KOPAJTICH, R., KUSTER, A., LAASS, M. W., LAINKA, E., LARSON-NATH, C., LEIBNER, A., LURZ, E., MAYR, J. A., MCKIERNAN, P., MENTION, K., MOOG, U., MUNGAN, N. O., RIEDHAMMER, K. M., SANTER, R., PALAFOLL, I. V., VOCKLEY, J., WESTPHAL, D. S., WIEDEMANN, A., WORTMANN, S. B., DIWAN, G. D., RUSSELL, R. B., PROKISCH, H., GARBADE, S. F., KOLKER, S., HOFFMANN, G. F. & LENZ, D. 2020. Defining clinical subgroups and genotype-phenotype correlations in NBAS-associated disease across 110 patients. *Genet Med,* 22**,** 610-621.

STOLZ, D. B., MARS, W. M., PETERSEN, B. E., KIM, T. H. & MICHALOPOULOS, G. K. 1999. Growth factor signal transduction immediately after two-thirds partial hepatectomy in the rat. *Cancer Res,* 59**,** 3954-60.

SUN, Y., LIU, F., FAN, C., WANG, Y., SONG, L., FANG, Z., HAN, R., WANG, Z., WANG, X., YANG, Z., XU, Z., PENG, J., SHI, C., ZHANG, H., DONG, W., HUANG, H., LI, Y., LE, Y., SUN, J. & PENG, Z. 2021. Characterizing sensitivity and coverage of clinical WGS as a diagnostic test for genetic disorders. *BMC Med Genomics,* 14**,** 102.

SZE, Y. K., DHAWAN, A., TAYLOR, R. M., BANSAL, S., MIELI-VERGANI, G., RELA, M. & HEATON, N. 2009. Pediatric liver transplantation for metabolic liver disease: experience at King's College Hospital. *Transplantation,* 87**,** 87-93.

TANG, S., WANG, J., LEE, N. C., MILONE, M., HALBERG, M. C., SCHMITT, E. S., CRAIGEN, W. J., ZHANG, W. & WONG, L. J. 2011. Mitochondrial DNA polymerase gamma mutations: an ever expanding molecular and clinical spectrum. *J Med Genet,* 48**,** 669-81.

TANI, H., IMAMACHI, N., SALAM, K. A., MIZUTANI, R., IJIRI, K., IRIE, T., YADA, T., SUZUKI, Y. & AKIMITSU, N. 2012. Identification of hundreds of novel UPF1 target transcripts by direct determination of whole transcriptome stability. *RNA Biol,* 9**,** 1370-9.

TANIMIZU, N. & MITAKA, T. 2014. Re-evaluation of liver stem/progenitor cells. *Organogenesis,* 10**,** 208-15.

TAUB, R. 1996. Liver regeneration 4: transcriptional control of liver regeneration. *FASEB J,* 10**,** 413-27.

TAUB, R. 2004. Liver regeneration: from myth to mechanism. *Nat Rev Mol Cell Biol,* 5**,** 836-47.

THERMOFISHER. 2018. *The Next Generation in Nucleic Acid and Protein Quantitation* [Online]. Available: https://www.thermofisher.com/uk/en/home/references/newsletters-and-journals/bioprobes-journal-of-cell-biology-applications/bioprobes-issues-2011/bioprobes-64-april-2011/the-qubit-2-0-fluorometer-april-2011.html [Accessed 06/01/2018 2018].

TREY, C. & DAVIDSON, C. S. 1970. The management of fulminant hepatic failure. *Prog Liver Dis,* 3**,** 282-98.

TRUST, S. C. S. N. F. 2019. *Expanded Newborn Screening* [Online]. Sheffield, UK: Sheffield Children's NHS Foundation Trust. Available: http://www.expandedscreening.org/site/home/newbornscreening.asp [Accessed 20/05/2019 2019].

TZOULIS, C., ENGELSEN, B. A., TELSTAD, W., AASLY, J., ZEVIANI, M., WINTERTHUN, S., FERRARI, G., AARSETH, J. H. & BINDOFF, L. A. 2006. The spectrum of clinical disease caused by the A467T and W748S POLG mutations: a study of 26 cases. *Brain,* 129**,** 1685-92.

VAN DIEMEN, C. C., KERSTJENS-FREDERIKSE, W. S., BERGMAN, K. A., DE KONING, T. J., SIKKEMA-RADDATZ, B., VAN DER VELDE, J. K., ABBOTT, K. M., HERKERT, J. C., LOHNER, K., RUMP, P., MEEMS-VELDHUIS, M. T., NEERINCX, P. B. T., JONGBLOED, J. D. H., VAN RAVENSWAAIJ-ARTS, C. M., SWERTZ, M. A., SINKE, R. J., VAN LANGEN, I. M. &

WIJMENGA, C. 2017. Rapid Targeted Genomics in Critically Ill Newborns. *Pediatrics,* 140.

VARGA, N. A., PENTELENYI, K., BALICZA, P., GEZSI, A., REMENYI, V., HARSFALVI, V., BENCSIK, R., ILLES, A., PREKOP, C. & MOLNAR, M. J. 2018. Mitochondrial dysfunction and autism: comprehensive genetic analyses of children with autism and mtDNA deletion. *Behav Brain Funct,* 14**,** 4.

VEDRENNE, V., GALMICHE, L., CHRETIEN, D., DE LONLAY, P., MUNNICH, A. & ROTIG, A. 2012. Mutation in the mitochondrial translation elongation factor EFTs results in severe infantile liver failure. *J Hepatol,* 56**,** 294-7.

VERHOEVEN, N. M., WALLOT, M., HUCK, J. H., DIRSCH, O., BALLAUF, A., NEUDORF, U., SALOMONS, G. S., VAN DER KNAAP, M. S., VOIT, T. & JAKOBS, C. 2005. A newborn with severe liver failure, cardiomyopathy and transaldolase deficiency. *J Inherit Metab Dis,* 28**,** 169-79.

VIEGAS, M. H., GEHRING, N. H., BREIT, S., HENTZE, M. W. & KULOZIK, A. E. 2007. The abundance of RNPS1, a protein component of the exon junction complex, can determine the variability in efficiency of the Nonsense Mediated Decay pathway. *Nucleic Acids Res,* 35**,** 4542-51.

VOGEL, G. F., MOZER-GLASSBERG, Y., LANDAU, Y. E., SCHLIEBEN, L. D., PROKISCH, H., FEICHTINGER, R. G., MAYR, J. A., BRENNENSTUHL, H., SCHROTER, J., PECHLANER, A., ALKURAYA, F. S., BAKER, J. J., BARCIA, G., BARIC, I., BRAVERMAN, N., BURNYTE, B., CHRISTODOULOU, J., CIARA, E., COMAN, D., DAS, A. M., DARIN, N., DELLA MARINA, A., DISTELMAIER, F., EKLUND, E. A., ERSOY, M., FANG, W., GAIGNARD, P., GANETZKY, R. D., GONZALES, E., HOWARD, C., HUGHES, J., KONSTANTOPOULOU, V., KOSE, M., KERR, M., KHAN, A., LENZ, D., MCFARLAND, R., MARGOLIS, M. G., MORRISON, K., MULLER, T., MURAYAMA, K., NICASTRO, E., PENNISI, A., PETERS, H., PIEKUTOWSKA-ABRAMCZUK, D., ROTIG, A., SANTER, R., SCAGLIA, F., SCHIFF, M., SHAGRANI, M., SHARRARD, M., SOLER-ALFONSO, C., STAUFNER, C., STOREY, I., STORMON, M., TAYLOR, R. W., THORBURN, D. R., TELES, E. L., WANG, J. S., WEGHUBER, D. & WORTMANN, S. 2022. Genotypic and phenotypic spectrum of infantile liver failure due to pathogenic TRMU variants. *Genet Med*.

WANG, D., LI, J., WANG, Y. & WANG, E. 2022. A comparison on predicting functional impact of genomic variants. *NAR Genom Bioinform,* 4**,** lqab122.

WANG, K., ZHANG, S., MARZOLF, B., TROISCH, P., BRIGHTMAN, A., HU, Z., HOOD, L. E. & GALAS, D. J. 2009. Circulating microRNAs, potential biomarkers for drug-induced liver injury. *Proc Natl Acad Sci U S A,* 106**,** 4402-7.

WENG, H. L., CAI, X., YUAN, X., LIEBE, R., DOOLEY, S., LI, H. & WANG, T. L. 2015. Two sides of one coin: massive hepatic necrosis and progenitor cell-mediated regeneration in acute liver failure. *Front Physiol,* 6**,** 178.

WONG, L. J., NAVIAUX, R. K., BRUNETTI-PIERRI, N., ZHANG, Q., SCHMITT, E. S., TRUONG, C., MILONE, M., COHEN, B. H., WICAL, B., GANESH, J., BASINGER, A. A., BURTON, B. K., SWOBODA, K., GILBERT, D. L., VANDERVER, A., SANETO, R. P., MARANDA, B., ARNOLD, G., ABDENUR, J. E., WATERS, P. J. & COPELAND, W. C. 2008. Molecular and clinical genetics of mitochondrial diseases due to POLG mutations. *Hum Mutat,* 29**,** E150-72.

WRIGHT, C. F., FITZGERALD, T. W., JONES, W. D., CLAYTON, S., MCRAE, J. F., VAN KOGELENBERG, M., KING, D. A., AMBRIDGE, K., BARRETT, D. M., BAYZETINOVA, T., BEVAN, A. P., BRAGIN, E., CHATZIMICHALI, E. A., GRIBBLE, S., JONES, P., KRISHNAPPA, N., MASON, L. E., MILLER, R., MORLEY, K. I., PARTHIBAN, V., PRIGMORE, E., RAJAN, D.,

SIFRIM, A., SWAMINATHAN, G. J., TIVEY, A. R., MIDDLETON, A., PARKER, M., CARTER, N. P., BARRETT, J. C., HURLES, M. E., FITZPATRICK, D. R., FIRTH, H. V. & STUDY, D. D. D. 2015. Genetic diagnosis of developmental disorders in the DDD study: a scalable analysis of genome-wide research data. *Lancet,* 385**,** 1305-14.

YIMLAMAI, D., CHRISTODOULOU, C., GALLI, G. G., YANGER, K., PEPE-MOONEY, B., GURUNG, B., SHRESTHA, K., CAHAN, P., STANGER, B. Z. & CAMARGO, F. D. 2014. Hippo pathway activity influences liver cell fate. *Cell,* 157**,** 1324-1338.

ZETOUNE, A. B., FONTANIERE, S., MAGNIN, D., ANCZUKOW, O., BUISSON, M., ZHANG, C. X. & MAZOYER, S. 2008. Comparison of nonsense-mediated mRNA decay efficiency in various murine tissues. *BMC Genet,* 9**,** 83.

ZIMMERMANN, L., STEPHENS, A., NAM, S. Z., RAU, D., KUBLER, J., LOZAJIC, M., GABLER, F., SODING, J., LUPAS, A. N. & ALVA, V. 2018. A Completely Reimplemented MPI Bioinformatics Toolkit with a New HHpred Server at its Core. *J Mol Biol,* 430**,** 2237-2243.

ZORN, A. M. 2008. Liver development. *StemBook.* Cambridge (MA).

APPENDIX A Diagnostic work up for children presenting with ALF (subject to age of patient and suspected aetiology)

Condition	**Tests**
Autoimmune hepatitis	Autoantibody test (anti-nuclear antibody ≥1:40, anti-smooth muscle antibody ≥1:20, anti-liver-kidney microsomal antibody ≥1:20) Elevated immunoglobulin levels
Hepatitis A, B, C and E	Serology and / or polymerase chain reaction (PCR)
Viral infections	Positive IgM antibody and / or PCR
Wilson disease	Ceruloplasmin 24-hour urinary copper excretion
Alpha-1-antitrypsin deficiency	Alpha-1-antitrypsin isoelectrophoresis
Gestational alloimmune liver disease	Iron studies Lip biopsy for iron deposition
Hemophagocytic lymphocytic Histiocytosis	Perforin Soluble CD25 Bone marrow aspiration
Galactosemia	Galactose-1-phosphate uridylyltransferase enzymology
Urea cycle defects	Plasma amino acid Urine orotic acid
Organic acidemias	Urine organic acid
Fatty acid oxidation defects	Acylcarnitine profile Fatty acid flux studies using cultured skin fibroblasts
Mitochondrial enzyme defect	Respiratory chain enzymology from muscle and / or liver biopsy
Tyrosinemia	Urine organic acids Plasma amino acids
Niemann-Pick C disease	Chitotriosidase Filipin staining on cultured skin fibroblasts
Congenital disorder of glycosylation	Transferrin isoelectrophoresis
Peroxisomal disorders	Very long chain fatty acids
Dihydrolipoamide dehydrogenase deficiency	Pyruvate dehydrogenase enzymology using cultured skin fibroblasts
Drugs and toxins	Urine toxicology

APPENDIX B Paediatric ALF gene panel

Gene	Description
ACAD9	Acyl-CoA Dehydrogenase Family Member 9
ACADM	Acyl-CoA Dehydrogenase Medium Chain
ACADS	Acyl-CoA Dehydrogenase Short Chain
ACADVL	Acyl-CoA Dehydrogenase Very Long Chain
ALDOB	Aldolase, Fructose-Bisphosphate B
ALG6	ALG6 Alpha-1,3-Glucosyltransferase
ALG8	ALG8 Alpha-1,3-Glucosyltransferase
ARG1	Arginase 1
ASL	Argininosuccinate Lyase
ASS1	Argininosuccinate Synthase 1
BCKDHA	Branched Chain Keto Acid Dehydrogenase E1 Subunit Alpha
BCKDHB	Branched Chain Keto Acid Dehydrogenase E1 Subunit Beta
BCS1L	BCS1 Homolog, Ubiquinol-Cytochrome C Reductase Complex Chaperone
CPS1	Carbamoyl-Phosphate Synthase 1
CPT1A	Carnitine Palmitoyltransferase 1A
CPT2	Carnitine Palmitoyltransferase 2
DBT	Dihydrolipoamide Branched Chain Transacylase E2
DGUOK	Deoxyguanosine Kinase
DLD	Dihydrolipoamide Dehydrogenase
GFM1	G Elongation Factor Mitochondrial
TUFM	Tu Translation Elongation Factor, Mitochondrial
EIF2AK3	Eukaryotic Translation Initiation Factor 2 Alpha Kinase 3
ETFA	Electron Transfer Flavoprotein Subunit Alpha
ETFB	Electron Transfer Flavoprotein Subunit Beta
ETFDH	Electron Transfer Flavoprotein Dehydrogenase
FAH	Fumarylacetoacetate Hydrolase
FARS2	Phenylalanyl-TRNA Synthetase 2, Mitochondrial

GALE	UDP-Galactose-4-Epimerase
GALT	Galactose-1-Phosphate Uridylyltransferase
GBE1	1,4-Alpha-Glucan Branching Enzyme 1
GLDH	L-galactono-1,4-lactone dehydrogenase, mitochondrial
GLS	Glutaminase 1
GSK3B	Glycogen Synthase Kinase 3 Beta
HADHA	Hydroxyacyl-CoA Dehydrogenase Trifunctional Multienzyme Complex Subunit Alpha
HADHB	Hydroxyacyl-CoA Dehydrogenase Trifunctional Multienzyme Complex Subunit Beta
HMGCL	3-Hydroxy-3-Methylglutaryl-CoA Lyase
HMGCS2	3-Hydroxy-3-Methylglutaryl-CoA Synthase 2
LARS	Leucyl-TRNA Synthetase 1
LIPA	Lipase A, Lysosomal Acid Type
MGAT2	Alpha-1,6-Mannosyl-Glycoprotein 2-Beta-N-Acetylglucosaminyltransferase
MPI	Mannose Phosphate Isomerase
MPV17	Mitochondrial Inner Membrane Protein MPV17
MRPS16	Mitochondrial Ribosomal Protein S16
NBAS	Neuroblastoma-amplified sequence
NPC1	NPC Intracellular Cholesterol Transporter 1
NPC2	NPC Intracellular Cholesterol Transporter 2
OTC	Ornithine Carbamoyltransferase
PEX1	Peroxisomal Biogenesis Factor 1
PMM2	Phosphomannomutase 2
POLG	DNA Polymerase Gamma, Catalytic Subunit
SCO1	Synthesis Of Cytochrome C Oxidase 1
SCYL1	SCY1 Like Pseudokinase 1
SLC22A5	Solute Carrier Family 22 Member 5 – transports carnitine
SLC25A13	Solute Carrier Family 25 Member 13 – transports aspartate/glutamate at the mitochondrial inner membrane

SLC25A15	Solute Carrier Family 25 Member 15 – transports ornithine across the inner mitochondrial membrane
SLC25A20	Solute Carrier Family 25 Member 20 – carnitine-acylcarnitine translocase that transports long-chain acylcarnitines
SMPD1	Sphingomyelin Phosphodiesterase 1
SUCLG1	Succinate-CoA Ligase GDP/ADP-Forming Subunit Alpha
TALDO1	Transaldolase 1
TMEM70	Transmembrane Protein 70
TRMU	Ts Translation Elongation Factor, Mitochondrial
TSFM	Ts Translation Elongation Factor, Mitochondrial
TWNK	Twinkle MtDNA Helicase
TYMP	Thymidine Phosphorylase

Appendix B 1. Genes included in the paediatric, ALF, 64-gene panel (designed in 2018).

APPENDIX C Primer sequences

Gene	Forward primer	Reverse primer	UPL probe
NBAS Ex17 A	tgttgtaagatgtcatggattctg	ggatcgcttctttattttactctgc	6
NBAS Ex17 B	gacctggaggctcttttagca	ttctgtaaccaacctgccatc	68
NBAS Ex19 A	ggcctaacatagttattcaaaacagg	ccgtctacaacggcaaagtt	47
NBAS Ex19 B	ccaattatgttcatttgatctgtcat	cccagaaaaatagttctaaagaccaag	46
BSEP Ex15 A	gaaagggtggatgctctcag	agccctaactggaaagctcat	16
BSEP Ex15 B	gagggaaaacccaatgtcaa	tcctgcacagagaagcactg	83

Appendix C 1. Primer sequences and UPL probes used for Ex17 to Ex19 duplication analysis in patient #2.

Gene	Forward primer (5' to 3')	Reverse primer (5' to 3')	Temp.
GADD45A mRNA	ggaggaattctcggctggag	cgttatcggggtcgacgtt	60
GADD45A pre-mRNA	ttgcagggaacccaactacc	tccttccattgagatgaatgtgg	60
GADD45B mRNA	ttgtctcctggtcacgaacc	tgtggcagcaactcaacaga	60
GADD45B pre-mRNA	gatgaatgtgtgagtcagacc	gcagacgatacatcaggatac	64
GAPDH	gtcgccagccgagccacatc	ccaggcgcccaatacgacca	60

Appendix C 2. Primer sequences used for *GADD45A* and *GADD45B* mRNA and pre-mRNA and *GAPDH*.

APPENDIX D Publications related to this work

ARTICLE IN PRESS

THE JOURNAL OF PEDIATRICS • www.jpeds.com

ORIGINAL ARTICLES

Study of Acute Liver Failure in Children Using Next Generation Sequencing Technology

Robert Hegarty, MD[1,2,3], Philippa Gibson, PhD[2], Melissa Sambrotta, PhD[2], Sandra Strautnieks, PhD[1], Pierre Foskett, BSc[1], Sian Ellard, PhD[4], Julia Baptista, PhD[4], Suzanne Lillis, BSc[5], Sanjay Bansal, MD[3], Roshni Vara, MD[3], Anil Dhawan, MD[1,2,3], Tassos Grammatikopoulos, MD[1,2,3], and Richard J. Thompson, PhD[1,2,3]

Objective To use next generation sequencing (NGS) technology to identify undiagnosed, monogenic diseases in a cohort of children who suffered from acute liver failure (ALF) without an identifiable etiology.

Study design We identified 148 under 10 years of age admitted to King's College Hospital, London, with ALF of indeterminate etiology between 2000 and 2018. A custom NGS panel of 64 candidate genes known to cause ALF and/or metabolic liver disease was constructed. Targeted sequencing was carried out on 41 children in whom DNA samples were available. Trio exome sequencing was performed on 4 children admitted during 2019. A comparison of the clinical characteristics of those identified with biallelic variants against those without biallelic variants was then made.

Results Homozygous and compound heterozygous variants were identified in 8 out of 41 children (20%) and 4 out of 4 children (100%) in whom targeted and exome sequencing were carried out, respectively. The genes involved were *NBAS* (3 children); *DLD* (2 children); and *CPT1A, FAH, LARS1, MPV17, NPC1, POLG, SUCLG1,* and *TWINK* (1 each). The 12 children who were identified with biallelic variants were younger at presentation and more likely to die in comparison with those who did not: median age at presentation of 3 months and 30 months and survival rate 75% and 97%, respectively.

Conclusions NGS was successful in identifying several specific etiologies of ALF. Variants in *NBAS* and mitochondrial DNA maintenance genes were the most common findings. In the future, a rapid sequencing NGS workflow could help in reaching a timely diagnosis and facilitate clinical decision making in children with ALF. *(J Pediatr 2021;■:1-7).*

Historically, reports from Europe and North America of children with acute liver failure (ALF) identified infectious, metabolic, and drug-related etiologies but the cause remained unexplained in approximately one-half of all cases.[1-3] Despite the progress made over the last 40 years the rate of indeterminate cases remains ~30%.[4] Therefore, challenges remain when evaluating the indeterminate cohort who have a lower chance of spontaneous survival, and higher rates of liver transplantation and death when compared with other diagnostic categories.[4,5]

The rapid increase in the use of next generation sequencing (NGS) since its advent in 2004 has transformed the way children with rare diseases such as ALF are evaluated. This is particularly relevant when considering the more recently identified monogenic disorders such as those caused by variants in *NBAS*,[6] *SCYL1*,[7] and *RINT1*.[8] Therefore, the purpose of this study was to use NGS technology to identify undiagnosed, monogenic diseases in children who received a diagnosis of indeterminate ALF and to gain insight into how this information may assist us in making therapeutic decisions for affected children in the future.

Methods

This study was carried out at the Pediatric Liver, GI and Nutrition Centre at King's College Hospital, London. The department is an international referral center for children with liver disease. Children under 10 years of age were included in the study as they are considered more likely to suffer from ALF

ALF	Acute liver failure
CNV	Copy number variant
DLD	Dihydrolipoamide dehydrogenase
INR	International normalized ratio
MDS	mtDNA depletion syndromes
mtDNA	Mitochondrial DNA
NGS	Next generation sequencing

From the [1]Institute of Liver Studies, King's College Hospital; [2]Institute of Liver Studies, King's College London; [3]Pediatric Liver, GI and Nutrition Center and MowatLabs, King's College Hospital; [4]Exeter Genetics Laboratory at Royal Devon and Exeter Hospital, Exeter; and [5]Molecular Genetics Laboratory at Guy's Hospital, London, United Kingdom

The authors declare no conflicts of interest.

Portions of this study were presented at the American Association for the Study of Liver Diseases meeting, November 8, 2019 to November 12, 2019 in Boston.

https://doi.org/10.1016/j.jpeds.2021.05.041

because of a monogenic disease.[9] Targeted sequencing was carried out at King's College Hospital in a historical cohort of children admitted between 2000 and 2018 in whom stored blood was available. Trio exome sequencing was carried out in 3 patients admitted after 2019 at the Exeter Genetics Laboratory at Royal Devon and Exeter Hospital, Exeter, under the United Kingdom Genomics Medicine Rapid Exome Sequencing for acutely unwell children with a likely monogenic disorder service.[10] One patient had exome sequencing performed at the Molecular Genetics Laboratory at Guy's Hospital, London.

The Pediatric Acute Liver Failure study group definition for ALF was used: (1) children with no known evidence of chronic liver disease, (2) biochemical evidence of acute liver injury, and (3) hepatic-based coagulopathy defined as an international normalized ratio (INR) ≥1.5 not corrected by vitamin K in the presence of clinical hepatic encephalopathy or an INR ≥2.0 regardless of the presence or absence of clinical hepatic encephalopathy.[2]

Clinical data was collected retrospectively using the electronic health records on all children who underwent sequencing. Statistical analysis was carried out using GraphPad Prism v 9.1 for Windows (GraphPad Software). Mann-Whitney *U* test was used to compare medians of the clinical characteristics of those who were identified with biallelic variants vs not. The Fisher exact test was used to compare any categorical data.

Children were categorized as ALF of indeterminate etiology when the diagnosis was not established despite thorough, age-appropriate investigations as previously described (**Appendix 1**; available at www.jpeds.com).[2] Blood samples previously collected for research purposes were retrieved after institutional review board/ethics approval and parental consent (18/WA/0009). Genomic DNA was extracted from peripheral leukocytes using standard procedures.

Targeted NGS: Custom ALF Panel

For the target enrichment sequencing method, a custom ALF panel of 64 genes that are known to cause ALF or a liver based metabolic disorder was constructed (**Appendix 2**; available at www.jpeds.com) using the Agilent eArray web portal (https://earray.chem.agilent.com/earray/). The final design consisted of 14 720 probes covering 276.07 kbp. The enrichment of target regions and library preparation was performed using the SureSelectQXT Target Enrichment Kit (Agilent Technologies). Library quantity and quality were measured using 2200 TapeStation (Agilent Technologies). The pooled libraries were paired-end sequenced (2 × 300 bp) on a flow cell on a MiSeq instrument (Illumina). Demultiplexing and binary base call file conversion to FASTQ was performed by CASAVA (Consensus Assessment of Sequence and Variation). Sequencing quality control and primary analysis were performed using the Illumina Real Time Analysis Software. The FASTQ files were imported and annotated using the CLC Genomics Workbench (Qiagen) where the minimum coverage was set at 30.

Exome Sequencing

The affected child and unaffected parents were sequenced for the trio exome analysis, which were carried out at the aforementioned laboratories where slightly different methods were employed.[11] Exome library capture was performed using the SureSelectXT Human All Exon Kit V5 (Agilent Technologies). Paired-end sequencing was performed on an Illumina NextSeq 550 or HiSeq 2500. The resulting reads were aligned to the hg19/GRCh37 reference genome with BWA. Variants were called with GATK Unified Genotyper and annotated using ANNOVAR where the minimum coverage was set at 20.

NGS Data Analysis

Sequence variants were filtered to identify potentially disease-causing mutations using Ingenuity Variant Analysis (Qiagen) or Alamut (Interactive Biosoftware). Variants with a minor allele frequency of >0.01 in the public databases (ExAC, HGMD, dbSNP, 1000 Genomes, Allele Frequency Community, Inova Genomes, EVS and DGV) were excluded. Nonsynonymous (missense, stop gain or loss, frameshift, small insertion and deletion) and intronic variants within 5 bp of exon-intron junctions were included. The filtered variants were investigated for pathogenicity considering the effect on the protein as predicted by Grantham distance, combined annotation dependent depletion score, PolyPhen-2, SIFT, CentoMD, Ingenuity Knowledge Base, VISTA, OMIM, and Clinvar.

Results

Of 148 children less than 10 years of age admitted with ALF without an identifiable etiology between 2000 and 2018, targeted sequencing was carried out in 41. Exome sequencing was carried out in 4 children admitted in 2019 (**Figure 1**). The 45 children (26 male) from 45 families who were sequenced were primarily of European ancestry: United Kingdom (21 children), Middle East (7), Africa (5), Asian (6), and other (6). Consanguinity was defined by the parents being second cousins or closer and was reported in 9 but none had a family history of ALF in children. The median age at presentation for the full cohort was 23 months (range, 7 days to 9 years and 9 months).

Targeted sequencing in the 41 children achieved a read depth of > × 30 in >99.9% of regions. Variant annotation identified a total of 17 452 unfiltered variants, which was narrowed down to 69 variants in 40 genes in 29 children after the above filtering strategy was applied. Among them, 8 children were found to harbor compound heterozygous or homozygous variants including 1 child with a copy number gain: 3 children in *NBAS*; 1 each in *TWINK*, *CPT1A*, *MPV17*, and *DLD*; 1 child harbored compound heterozygous variants in both, *POLG* and *SUCLG1* (**Table I**). Sixty monoallelic

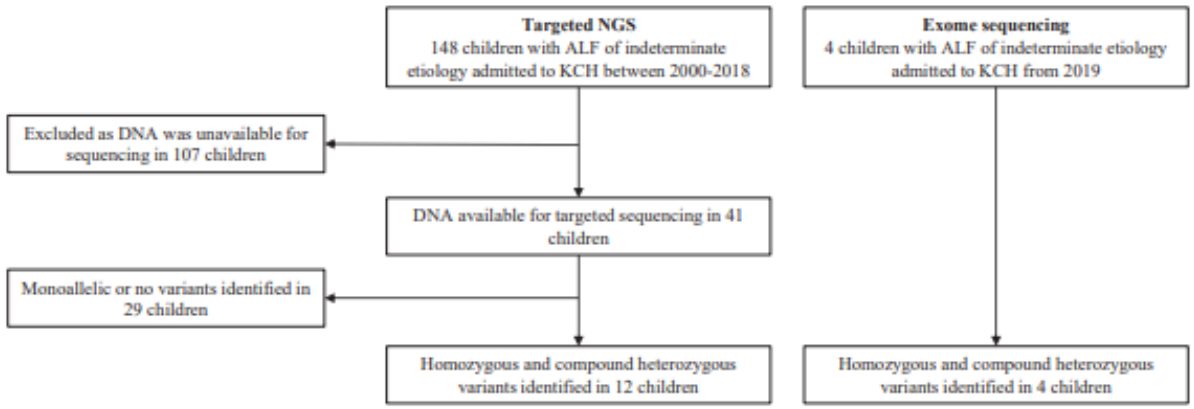

Figure 1. NGS in patients with ALF without etiology at King's College Hospital (*KCH*).

variants in 27 children were also identified: 48 missense (24 children), 2 deletion, 1 duplication, 1 nonsense, and 8 splice site (Figure 2). In addition, a monoallelic copy number gain was identified in 2 children. With this information, further interrogation seeking a second pathogenic variant was carried out but was unrevealing.

Exome sequencing achieved a read depth of >×20 in >95% of regions. All 4 children who had exome sequencing were identified with compound heterozygous or homozygous variants: 1 child each in *LARS1*, *FAH1*, *NPC1*, and *DLD* (Table I).

A comparison of the clinical characteristics between those who were identified with biallelic variants vs those who remained indeterminate identified that those with biallelic variants were younger at presentation and more likely to die ($P < .05$; Table II). There was no difference in the other clinical characteristics including biochemistry.

Overall, 3 children were found to harbor compound heterozygous or homozygous variants in *NBAS*. Patient 3 suffered from recurrent ALF associated with intercurrent infections before returning to the Middle East without liver transplantation. He was identified with the homozygous variant, c.4731_4733dup; p.Tyr1578dup. Patient 9 suffered from recurrent ALF and received microbead-encapsulated hepatocytes followed by liver transplantation and remains well on routine follow up. A copy number variant (CNV) ratio of 2 was identified in exon 17-19 in *NBAS*, which was confirmed by quantitative-polymerase chain reaction. Quantitative- polymerase chain reaction spanning the same region on the unaffected parents' DNA revealed a CNV ratio of 1.5 for each parent demonstrating their heterozygous status. A CNV in *NBAS* has not been observed in population databases nor reported previously in affected individuals. Patient 12 suffered from ALF at 3 years of age and recovered without liver transplantation. Twelve years later, he remains well without suffering from further episodes of ALF. He was found to harbor compound heterozygous missense variants in *NBAS*, c.191G>A, p.Arg64His; c.1702G>A, p.Val568Ile.

Four children were found to harbor compound heterozygous or homozygous variants in genes involved in mitochondrial DNA (mtDNA) maintenance: *MPV17*, *POLG*, *TWINK*, and *SUCLG1*. Patient 8 presented with ALF at 10 weeks of age. A mtDNA depletion syndrome (MDS) was clinically suspected but diagnostic NGS technology was not available at the time and he underwent liver transplantation 6 weeks after presentation. The child is now 7 years of age and attends mainstream school, although requires extra speech and language support. He was found to harbor compound heterozygous, missense variants in *TWINK*: c.1471C>G, p.Ser491Thr; c.1697A>G, p.Lys566Arg. Patient 18 presented at 17 months of age with ALF and underwent auxiliary liver transplantation. The patient is now 17 years old and is under follow-up for mild, cardiac left ventricular hypertrophy. Compound heterozygous missense variants were identified in 2 genes, *SUCLG1* and *POLG*. The variants in *SUCLG1* were c.601A>G, p.Arg201Gly; c.236G>A, p.Gly79Asp. The variants in *POLG* were c.153_158delGCAGCA, p.Gln54_Gln55del; and c.803G>C, p.Gly268Ala. Patient 17 presented with ALF at 18 months of age and received liver transplantation. He is now 19 years old and leads a semi-independent life with mild learning difficulties. Homozygous missense variants were found in *MPV17*: c.3338C>T, p.Pro98Leu.

In patient 43, urinary and plasma succinylacetone were negative at the time of ALF. This was later deemed a false-negative result for tyrosinemia type 1 following detection of succinylacetone by tandem mass spectrometry of the dried blood spot retrieved from day 5 of life.

Two children were identified with biallelic variants in *DLD* including a 1 child with the variants c.826A>T, p.Thr276Ser; and c.911T>C, p.Ile304Thr. She presented at 1 month of age with ALF and received liver transplantation and remains well at 15 years of age. To further interrogate the pathogenicity of this variant, pyruvate dehydrogenase activity was measured using the patient's skin fibroblasts. However, the result of 0.76 nmol/mg protein/minute (normal range 0.60-0.90) went against the possible diagnosis suggested from the genetics.

Table I. Clinical and genetic data on patients with homozygous and compound heterozygous variants after filtering

ID	Sex	Age at presentation	Clinical	Sequencing method	Gene	Genotype	Protein	MAF	CADD/pathogenicity	LT	Outcome	Age at last visit
Pat 1	F	1 mo	×1 ALF	Targeted NGS	*DLD*	c.826A>T	p.Thr276Ser	5.42E-04	25	Yes	Alive	15 y
						c.911T>C	p.Ile304Thr	1.57E-04	26			
Pat 3	M	6 mo	Recurrent ALF	Targeted NGS	*NBAS*	c.4731_4733dup	p.Tyr1578dup	Not reported	Pathogenicity likely	Yes	Lost to follow up	
Pat 8	M	2 mo	×ALF	Targeted NGS	*TWNK*	c.1471C>G	p.Ser491Thr	3.99E-06	24	Yes	Alive; NDD	7 y
						c.1697A>G	p.Lys566Arg	3.99E-04	22			
Pat 9	M	6 mo	Recurrent ALF	Targeted NGS	*NBAS*	c.exons 17-19 dup	p.?	Not reported	Pathogenicity likely	No	Alive	6 y
Pat 12	M	3 y	×ALF	Targeted NGS	*NBAS*	c.1702G>A	p.Val568Ile	0.0012	15	No	Alive	15 y
						c.1916>A	p.Arg64His	6.30E-05	19			
Pat 17	M	18 mo	×ALF	Targeted NGS	*MPV17*	c.338C>T	p.Pro98Leu	5.31E-05	25	Yes	Alive; NDD	19 y
Pat 18	M	17 mo	×ALF	Targeted NGS	*SUCLG1*	c.601A>G	p.Arg201Gly	1.99E-05	30	Yes	Alive; cardiomyopathy	17 y
						c.236G>A	p.Gly79Asp	0.0013	27			
					PDLG	c.153_158del6CAGCA	p.Gln54_Gln55del	0.0036	.			
						c.803G>C	p.Gly268Ala	0.0039	27			
Pat 19	M	2 y	×ALF	Targeted NGS	*CPT1A*	c.2198A>G	p.Asn733Ser	0.0018	16	No	Alive	6 y
Pat 42	M	1 wk	×ALF	Exome sequencing	*LARS1*	c.1292T>A	p.Val431Asp	3.47E-04	29	No	Dead	NA
						c.3126>T	p.Leu1042Phe	4.01E-06	26			
Pat 43	F	1 mo	×ALF	Exome sequencing	*FAH*	c.974C>T	p.Thr325Met	4.02E-06	26	No	Dead	NA
Pat 44	M	2 wk	×ALF	Exome sequencing	*NPC1*	c.3718G>A	p.Gly1240Arg	3.98E-06	25	No	Dead	NA
Pat 45	M	9 y	Recurrent ALF	Exome sequencing	*DLD*	c.685G>T	p.Gly229Cys	3.10E-04	35	No	Alive	17 y

CADD, combined annotation dependent depletion; *LT*, liver transplantation; *MAF*, minor allele frequency; *NA*, not applicable; *NDD*, neurodevelopmental delay; *Pat*, patient.
Homozygous and compound heterozygous variants were found in 8 out of 41 children (20%) and 4 out of 4 children (100%) in whom targeted and exome sequencing were carried out, respectively.
*Polyglutamine tract expansion.

Discussion

Acute liver failure is defined in children as a multisystem disorder in which there is severe impairment of liver function, with or without encephalopathy, with hepatocellular necrosis in a patient with no reported underlying chronic liver disease.[12] This in an inclusive description which inevitably covers numerous, underlying etiologies. Reaching a diagnosis can be difficult[13] and efforts to reduce the rate of indeterminate cases remain a challenge.[4] Monogenic disorders causing metabolic disease are thought to contribute to 10%-28% of these cases[2,14] and are thought to be more likely in younger children or infants.[9] Compound heterozygous or homozygous variants of varying pathogenicity were identified in 8 out of 41 (20%) and 4 out of 4 (100%) children in whom targeted and exome sequencing were carried out, respectively. Among these 12 children with compound heterozygous or homozygous variants, 10 were boys although this apparent discrepancy in sex compared against the group without biallelic variants did not amount to statistical significance (Table I). However, children in this group were younger at presentation and more likely to die. Subsequently, the genetic information was then compared against their disease phenotype and thought to provide the diagnosis with confidence in 9 (patients 3, 8, 9, 17, 18, and 42-45). These included disorders where diagnosis is primarily based on genetic sequencing (disease causing mutations in *NBAS* and *LARS1*) or those in which conventional diagnostic methods may take too long for children with ALF (filipin staining or pyruvate dehydrogenase activity measurement in cultured fibroblasts, for Niemann Pick C disease or dihydrolipoamide dehydrogenase [DLD] deficiency, respectively). In 1 infant (patient 43), exome sequencing uncovered a false negative result of a conventional diagnostic test, a rare but recognized case of succinylacetone negative tyrosinemia.[15,16] However, in others the significance of the genetic findings was less clear. In patient 1, DLD enzymology using skin fibroblasts demonstrated normal enzyme activity going against a diagnosis of DLD deficiency. Furthermore, in patient 19, repeat profiles of plasma acylcarnitine suggested that the carnitine transporter was not impaired. A possible interpretation of these results is that susceptibility to ALF was increased genetically, but the variants were not the cause of a monogenic disease.

These findings demonstrated that, although the genetic findings were helpful in reaching a diagnosis in some cases, in others it raised further questions. Challenges will remain in the future with regards to determining the pathogenicity and relevance of the genetic findings with enough confidence to influence therapeutic decision making.

Targeted, as well as exome, sequencing have been successful in providing diagnoses for children with rare diseases[17,18] both of which were employed in this study. However, whole genome sequencing using trio testing when possible is being used with superior diagnostic rates and cost-

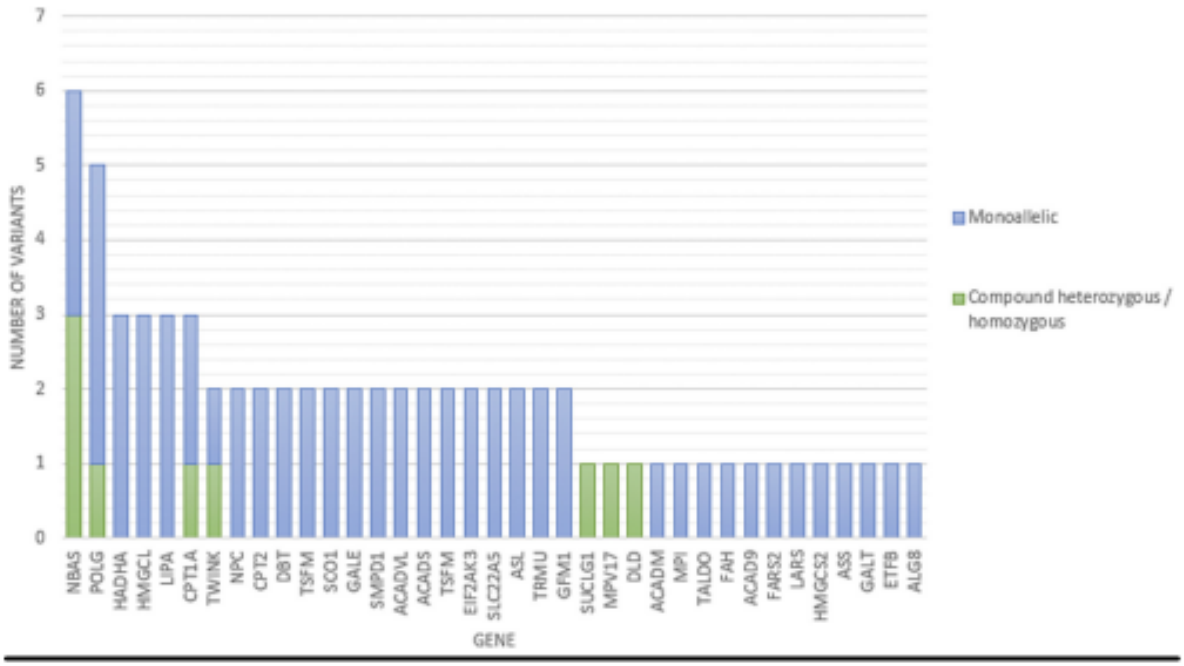

Figure 2. Targeted NGS in 41 children: genes in which variants of potential pathogenicity were identified after filtering. Eight children were found to harbor compound heterozygous or homozygous variants. Sixty monoallelic variants in 27 children were also identified. Without specific functional studies it is difficult to comment on the significance of monoallelic variants although it is possible that they contributed to the disease phenotype.

effectiveness.[19,20] Children with ALF pose specific challenges because of the short time frame between presentation to therapeutic decision making as they can lose hepatic function within days.[2,14] In this respect, whole genome sequencing has the added advantage of a shorter library preparation time than is required for targeted or exome sequencing. Efforts to develop rapid sequencing pipelines for critically ill children have demonstrated a turnaround time of 2-3 weeks.[19,20] Future efforts should concentrate around building the appropriate technology, infrastructure, and resources to reduce the turnaround time even further to maximize the clinical utility of NGS in children with ALF.

Table II. Clinical characteristics of 41 children who underwent targeted NGS

Patient characteristics		Biallelic (n = 12)	Indeterminate (n = 33)	*P* value
Demographics	Median age at presentation	3 mo (min, 7 d to max, 9 y and 9 mo)	30 m (min, 7 d to max, 8 y and 8 mo)	<.05*
	Male sex	3 (25%)	17 (41%)	ns†
Ethnicity	White	4 (33%)	18 (55%)	ns†
	Arab	3 (25%)	4 (12%)	ns†
	Pakistan	1 (8%)	3 (9%)	ns†
	Other	4 (33%)	8 (24%)	ns†
Clinical	History of consanguinity	4 (33%)	5 (15%)	ns†
	History of fever at presentation	4 (33%)	10 (24%)	ns†
	Max AST (IU/L)	2125 (range, 22 532)	2188 (range, 32 040)	ns*
	Max total bilirubin (mg/dL)	15.9 (range, 29.4)	13.3 (range, 31.2)	ns*
	Max INR	4.6 (range, 15)	4.8 (range, 11.7)	ns*
	Max ammonia (μmol/L)	98 (range, 201)	99 (range, 286)	ns*
Liver	Recurrent ALF	3 (25%)	0	ns†
	Resolution without LT	4 (33%)	11 (33%)	ns†
	Liver transplantation	5 (42%)	20 (60%)	ns†
Outcome	Alive	9 (75%)	32 (97%)	<.05†
	Neurodevelopmental delay	5 (42%)	7 (21%)	ns†

AST, aspartate aminotransferase; *ns*, not significant.
Children who were identified with biallelic variants were younger and more likely to die ($P < .05$). There were no other differences in the patient characteristics including biochemistry.
*Mann-Whitney U test.
†Fisher exact test.

Mitochondrial Hepatopathies and Liver Transplantation

MDS are caused by nuclear gene defects affecting genes responsible for the maintenance and replication of the mtDNA.[21] Liver transplantation for MDS is controversial because of the possibility of offering an organ transplant to a child with a multisystemic, life-limiting disorder. In this study, 3 children were found to have compound heterozygous or homozygous variants in mtDNA maintenance genes all of whom received liver transplantation and are alive at follow-up. In a series of 29 patients with *MPV17*-associated hepatocerebral MDS, liver transplantation was performed in about 40% in whom one-half died afterward.[22] It has been suggested that the degree of mtDNA depletion, in the most commonly identified p.R50Q variant, may give an indication of a milder severity of the disease whilst nonsense, splice site, and frameshift variants as well as deletions lead to death in infancy or early childhood.[22] In *POLG*-associated MDS, progressive neurologic deterioration ensues starting in the teens even if they were to survive with liver transplantation.[23,24] To our knowledge, there are no published reports of liver transplantation in *TWINK* or *SUCLG1* deficiency.

With the increasing use of NGS so too will there be an increase in the number of reported variants of potential pathogenicity. Nevertheless, genotyping is far from providing the phenotypic clarity that is required for therapeutic decision making in MDS; a risk is the possibility of overinterpreting genotypic information. Therefore, conventional biochemical and enzymatic tests should, for the time-being, continue to be carried out in parallel to help complement the genetic findings.

ALF and NBAS Deficiency

Over 100 cases of ALF and liver dysfunction secondary to NBAS deficiency have been described world-wide in children and adults. Typically, the onset of liver failure is in the first 2 years of life with fever as a triggering factor.[6,25-27] Notably, the biochemical derangement is hyperacute with significant elevations in aspartate aminotransferase and L-alanine aminotransferase.[28] In similar fashion, the INR elevates sharply, typically ranging between 4 and 20.[29] Affected children can suffer multiple episodes of liver failure although, with age, the occurrence of crises seems to diminish.[29] Treatment is dependent on the severity of the ALF: some children recover with supportive therapy whilst others undergo liver transplantation during the acute episode of ALF or as a preventative measure against future episodes.

In our study, 3 patients were found to have biallelic variants in *NBAS*. One patient (patient 9) received intraperitoneal transplantation of alginate-embedded human hepatocytes during an episode of ALF and recovered successfully.[30] The diagnosis was not known at the time and he did undergo liver transplantation 6 months later, after suffering from another episode of ALF. This case highlights the potential for hepatocyte transplantation as rescue therapy for ALF secondary to NBAS deficiency, thereby, gaining time until adulthood when affected children may grow out of these episodes; it also avoids conferring a child to the life-long risks associated with organ transplantation.

This study demonstrated the benefits of using NGS in improving diagnostic rates and how this can help clinicians make therapeutic decisions and support affected families. However, there will be challenges to its practical use given the speed in which ALF in children progresses and the wide range of possible etiologies. Future work should focus on close collaboration with laboratories using conventional, diagnostic methods to help interpret the genetic findings as well as developing rapid, NGS pipelines to meet the timeframe required for therapeutic decision making. ■

Submitted for publication Feb 10, 2021; last revision received May 14, 2021; accepted May 14, 2021.

Reprint requests: Robert Hegarty, MD, Pediatric Liver, GI and Nutrition Center and MowatLabs, Denmark Hill, King's College Hospital, SE5 9RS, UK. E-mail: roberthegarty@nhs.net

References

1. Rivera-Penera T, Moreno J, Skaff C, McDiarmid S, Vargas J, Ament ME. Delayed encephalopathy in fulminant hepatic failure in the pediatric population and the role of liver transplantation. J Pediatr Gastroenterol Nutr 1997;24:128-34.
2. Squires RH, Jr, Shneider BL, Bucuvalas J, Alonso E, Sokol RJ, Narkewicz MR, et al. Acute liver failure in children: the first 348 patients in the pediatric acute liver failure study group. J Pediatr 2006;148:652-8.
3. Psacharopoulos HT, Mowat AP, Davies M, Portmann B, Silk DB, Williams R. Fulminant hepatic failure in childhood: an analysis of 31 cases. Arch Dis Child 1980;55:252-8.
4. Alonso EM, Horslen SP, Behrens EM, Doo E. Pediatric acute liver failure of undetermined cause: a research workshop. Hepatology (Baltimore, Md) 2017;65:1026-37.
5. Narkewicz MR, Horslen S, Hardison RM, Shneider BL, Rodriguez-Baez N, Alonso EM, et al. A learning collaborative approach increases specificity of diagnosis of acute liver failure in pediatric patients. Clin Gastroenterol Hepatol 2018;16:1801-18010 e3.
6. Haack TB, Staufner C, Kopke MG, Straub BK, Kolker S, Thiel C, et al. Biallelic mutations in NBAS cause recurrent acute liver failure with onset in infancy. Am J Hum Genet 2015;97:163-9.
7. Lenz D, McClean P, Kansu A, Bonnen PE, Ranucci G, Thiel C, et al. SCYL1 variants cause a syndrome with low gamma-glutamyltransferase cholestasis, acute liver failure, and neurodegeneration (CALFAN). Genet Med 2018;20:1255-65.
8. Cousin MA, Conboy E, Wang JS, Lenz D, Schwab TL, Williams M, et al. RINT1 bi-allelic variations cause infantile-onset recurrent acute liver failure and skeletal abnormalities. Am J Hum Genet 2019;105:108-21.
9. Nicastro E, D'Antiga L. Next generation sequencing in pediatric hepatology and liver transplantation. Liver Transpl 2018;24:282-93.
10. Deans S, Chitty L, Ellard S, Jenkins L, Raymond L, Scott R, et al. Guidance document: rapid exome sequencing for acutely unwell children with a likely monogenic disorder United Kingdom2019 [updated June 12, 2020]. Accessed November 29, 2020. https://www.exeterlaboratory.com/wp-content/uploads/Guidance-Document-NICU-PICU-Referrals-v4.0-20200622.pdf
11. Ellard S, Kivuva E, Turnpenny P, Stals K, Johnson M, Xie W, et al. An exome sequencing strategy to diagnose lethal autosomal recessive disorders. Eur J Hum Genet 2015;23:401-4.
12. Bhaduri BR, Mieli-Vergani G. Fulminant hepatic failure: pediatric aspects. Semin Liver Dis 1996;16:349-55.
13. Narkewicz MR, Dell Olio D, Karpen SJ, Murray KF, Schwarz K, Yazigi N, et al. Pattern of diagnostic evaluation for the causes of pediatric acute

liver failure: an opportunity for quality improvement. J Pediatr 2009;155:801-806 e1.
14. Hegarty R, Hadzic N, Gissen P, Dhawan A. Inherited metabolic disorders presenting as acute liver failure in newborns and young children: King's College Hospital experience. Eur J Pediatr 2015;174:1387-92.
15. Cassiman D, Zeevaert R, Holme E, Kvittingen EA, Jaeken J. A novel mutation causing mild, atypical fumarylacetoacetase deficiency (Tyrosinemia type I): a case report. Orphanet J Rare Dis 2009;4:28.
16. Blackburn PR, Hickey RD, Nace RA, Giama NH, Kraft DL, Bordner AJ, et al. Silent tyrosinemia type I without elevated tyrosine or succinylacetone associated with liver cirrhosis and hepatocellular carcinoma. Hum Mutat 2016;37:1097-105.
17. Sawyer SL, Hartley T, Dyment DA, Beaulieu CL, Schwartzentruber J, Smith A, et al. Utility of whole-exome sequencing for those near the end of the diagnostic odyssey: time to address gaps in care. Clin Genet 2016;89:275-84.
18. Wright CF, Fitzgerald TW, Jones WD, Clayton S, McRae JF, van Kogelenberg M, et al. Genetic diagnosis of developmental disorders in the DDD study: a scalable analysis of genome-wide research data. Lancet 2015;385:1305-14.
19. French CE, Delon I, Dolling H, Sanchis-Juan A, Shamardina O, Megy K, et al. Whole genome sequencing reveals that genetic conditions are frequent in intensively ill children. Intensive Care Med 2019;45:627-36.
20. Mestek-Boukhibar L, Clement E, Jones WD, Drury S, Ocaka L, Gagunashvili A, et al. Rapid Paediatric Sequencing (RaPS): comprehensive real-life workflow for rapid diagnosis of critically ill children. J Med Genet 2018;55:721-8.
21. Davison JE, Rahman S. Recognition, investigation and management of mitochondrial disease. Arch Dis Child 2017;102:1082-90.
22. El-Hattab AW, Li FY, Schmitt E, Zhang S, Craigen WJ, Wong LJ. MPV17-associated hepatocerebral mitochondrial DNA depletion syndrome: new patients and novel mutations. Mol Genet Metab 2010;99:300-8.
23. Tzoulis C, Engelsen BA, Telstad W, Aasly J, Zeviani M, Winterthun S, et al. The spectrum of clinical disease caused by the A467T and W748S POLG mutations: a study of 26 cases. Brain 2006;129:1685-92.
24. Wong LJ, Naviaux RK, Brunetti-Pierri N, Zhang Q, Schmitt ES, Truong C, et al. Molecular and clinical genetics of mitochondrial diseases due to POLG mutations. Hum Mutat 2008;29:E150-72.
25. Staufner C, Haack TB, Kopke MG, Straub BK, Kolker S, Thiel C, et al. Recurrent acute liver failure due to NBAS deficiency: phenotypic spectrum, disease mechanisms, and therapeutic concepts. J Inherit Metab Dis 2016;39:3-16.
26. Staufner C, Peters B, Wagner M, Alameer S, Baric I, Broue P, et al. Defining clinical subgroups and genotype-phenotype correlations in NBAS-associated disease across 110 patients. Genet Med 2020;22:610-21.
27. Ricci S, Lodi L, Serranti D, Moroni M, Belli G, Mancano G, et al. Immunological features of neuroblastoma amplified sequence deficiency: report of the first case identified through newborn screening for primary immunodeficiency and review of the literature. Front Immunol 2019;10:1955.
28. Calvo PL, Tandoi F, Haak TB, Brunati A, Pinon M, Olio DD, et al. NBAS mutations cause acute liver failure: when acetaminophen is not a culprit. Ital J Pediatr 2017;43:88.
29. Chavany J, Cano A, Roquelaure B, Bourgeois P, Boubnova J, Gaignard P, et al. Mutations in NBAS and SCYL1, genetic causes of recurrent liver failure in children: three case reports and a literature review. Arch Pediatr 2020;27:155-9.
30. Dhawan A, Chaijitraruch N, Fitzpatrick E, Bansal S, Filippi C, Lehec SC, et al. Alginate microencapsulated human hepatocytes for the treatment of acute liver failure in children. J Hepatol 2020;72:877-84.

APPENDIX E Conference presentations

Oral presentations

Hegarty R, Sambrotta M, Gibson P, Strautnieks S, Foskett P, Grammatikopoulos T, Thompson RJ. Study of acute liver failure in children using next generation sequencing technology. *BSPGHAN Annual Meeting, January 2020, Brighton, UK.* Alex Mowat prize.

Hegarty R, Iansante V, Huang Z, Si T, Grammatikopoulos T, Thompson R. Acute liver failure in NBAS deficiency: characterisation of pathobiology using fibroblasts from affected patients. *BSPGHAN Annual Meeting, April 2022, Birmingham, UK*.

Poster presentations

Hegarty R, Sambrotta M, Gibson P, Strautnieks S, Foskett P, Grammatikopoulos T, Thompson RJ. Study of acute liver failure in children using next generation sequencing technology. *AASLD Annual Meeting, November 2019, Boston, USA.* Poster of distinction.

Hegarty R, Iansante V, Huang Z, Si T, Grammatikopoulos T, Thompson R. Acute liver failure in NBAS deficiency: characterisation of pathobiology using fibroblasts from affected patients. *ESPGHAN Annual Meeting, June 2022, Copenhagen, Denmark*. ePoster presentation.